Skin cells as a tool in genetic diagnosis of Duchenne muscular dystrophy

By

Lynn Tyers

(TYRLYN001)

SUBMITTED TO THE UNIVERSITY OF CAPE TOWN

In fulfilment of the requirements for the degree

MSc (Med) in Human Genetics

Faculty of Health Sciences

UNIVERSITY OF CAPE TOWN

24 August 2016

Supervisors:

Ms. Alina Esterhuizen, Department of Pathology, University of Cape Town

A/Prof Lester Davids, Department of Human Biology, University of Cape Town

Declaration

I, **Lynn Tyers**, hereby declare that the work on which this dissertation is based is my original work (except where acknowledgements indicate otherwise) and that neither the whole work nor any part of it has been, is being, or is to be submitted for another degree in this or any other university.

I empower the university to reproduce for the purpose of research either the whole or any portion of the contents in any manner whatsoever.

Signature: Signed by candidate

Date: 24/08/2016

The financial assistance of the National Research Fund and the German Academic Exchange service (NRF-DAAD) as well as the National Health Laboratory Service Research Trust (NHLS Research Trust) towards this research is hereby acknowledged. Opinions expressed and conclusions arrived at, are those of the author and are not necessarily attributed to the funders.

Acknowledgements

I would like to thank my supervisors, for their input in this study and their help and support during my Masters. I have grown tremendously since the start of this study and have learnt so much.

To the REDOX lab and the Division of Human Genetics, thank you for the assistance, it was a true pleasure working with everyone.

Thank you to our collaborator at Red Cross Children's War Memorial Hospital, Jo Wilmshurst, and the DMD patients and family members for consenting to this work. Without all of you this work would not have been possible.

I would also like to extend a special thank you to David Scott for his assistance with qPCR analysis and Western blotting and Fluery for his assistance with Western blotting.

To Jade and Julian thank you so much for being amazing friends, I would have gone insane if it wasn't for all the comic relief each of you brought me throughout these two years. To Hauwa, you were a pleasure to meet and I wish you the best with your future endeavours.

Thank you to my mom, grandparents and brother for all the support throughout my Masters.

Finally, to Alexander Kenneth John Robinson thank you for staying with me at campus when I had to work until the morning hours, for getting me to campus when the public transport system failed me, for your support while writing this dissertation, for reminding me to eat and take a break every once in a while and so much more. Your presence has made all the difference during these two years.

CONTENTS:

List of Figures

List of Tables

List of Abbreviations

%	Percent
°C	Degrees Celcius
2'OMePs	2' O-methylphosphorothionate
2°	Secondary
3'	Three prime
5'	Five prime
A	Adenine
A230	Absorbance at 230nm
A260	Absorbance at 260nm
A280	Absorbance at 280nm
addH_2O	Autoclaved double distilled water
adH_2O	Autoclave distilled water
AON	Antisense oligonucleotides
APS	Ammonium persulphate
bFGF	Basic fibroblast growth factor
BMD	Becker Muscular Dystrophy
Bp	Base pair
BSA	Bovine serum albumin
C	Cytosine
Cdc42	cell division cycle 42
cDNA	Complementary DNA
CGH	Comparative genomic hybridisation
Co_2	Carbon dioxide

CPIC	Complete protease inhibitor cocktail
CPK	Creatine phosphokinase
D/BMD	Duchenne/Becker Muscular Dystrophy
dbSNP	Single nucleotide polymorphism database
ddH_2O	Double distilled water
ddNTP	Dideoxynucleotide triphosphates
DEJ	Dermal-epidermal junction
del	Deletion
DEPC	Diethylpyrocarbonate
Dept.	Department
DGC	Dystrophin-glycoprotein complex
DMD	Duchenne Muscular Dystrophy
DMEM	Dulbecco's Modified Eagle Medium
DMEM++	DMEM supplemented with 10% (v/v) FCS and 1x pen/strep
DNA	Deoxyribonucleic acid
dNTP	Deoxynucleotide triphosphates
Dp116	Adult peripheral nerve isoform of dystrophin
Dp140	Central nervous system and kidney isoform of dystrophin
Dp260	Retinal isoform of dystrophin
Dp427C	Brain isoform of dystrophin
Dp427L	Lymphocyte isoform of dystrophin
Dp427M	Muscle isoform of dystrophin
Dp427P	Purkinje cell isoform of dystrophin
Dp71	Ubiquitous isoform of dystrophin

ECM	Extracellular matrix
EDTA	Ethylenediaminetetraacetic Acid
EJ	Exon junction
EMA	European Medicines Agency
EMLA	Eutectic mixture of local anaesthetics
Fb or F	Fibroblasts
FCS	Foetal calf serum
FDA	Food and drug Administration
FETI	Hams F10/Endothelin/ TPA/IBMX
FPKM	Fragments per Kilobase gene model and Million reads
g	grams
G	Guanine
GAPDH	Glyceraldehyde 3-phosphate dehydrogenase
Grb2	Growth factor receptor-bound protein 2
GTP	Guanosine triphosphate
GUSB	Glucuronidase Beta
h	Hours
HREC	Human Research Ethics Committee
HUGO	Human Genome Organisation
IBMX	3-isobutyl-1-methyl xanthine
ICC	Immunocytochemistry
IHC	Immunohistochemistry
JNK	c-Jun N-terminal kinases
Kb	Kilo bases

Kc	Keratinocytes
KCl	Potassium chloride
kDa	kilo Dalton
KH_2PO_4	Potassium dihydrogen phosphate
L	Litres
LOVD	Leiden Open Variation Database
M	Molar
MAPK	Mitogen-activated protein kinases
Mb	Mega bases
Mc or M	Melanocytes
MD	Muscular Dystrophy
mg	Milligrams
$MgCl_2$	Magnesium chloride
min	Minutes
mL	Millilitre
MLPA	Multiplex ligation dependant probe amplification
mm	Millimetre
mM	Millimolar
mPCR	Multiplex PCR
n	Number of biological repeats
N/A	Not applicable
Na_2HPO_4	Sodium hydrogen phosphate
NaCl	Sodium chloride
$NaHCO_3$	Sodium bicarbonate

ng	Nanograms
ng/µl	Nanograms per microlitre
NHLS	National Health Laboratory Service
nm	Nanometre
NRT	No reverse transcriptase
NT	No template
O_2	Oxygen
OCT	Optimum cutting temperature
OMIM	Online Mendelian Inheritance in Man
ORF	Open reading frame
p	Passage
PAK1	P21 activated kinase 1
PBS	Phosphate buffered saline
pen/strep	Penicillin and streptomycin
PFA	Paraformaldehyde
PMO	Phosphorodiamidate morpholino oligomer
PMSF	Phenylmethylsulfonylfluoride
PROVEAN	Protein Variation Effect Analyzer
PTC	Premature termination codon
PTT	Protein truncation test
qPCR	Quantitative PCR
Rac1	Ras-related C3 botulinum toxin substrate 1
RFLP	Restriction fragment length polymorphism
RFU	Relative fluorescent units

RhoA	Ras homolog gene family, member A
RIPA	Radioimmunoprecipitation assay
RNA	Ribonucleic acid
rpm	Revolutions per minute
rRNA	Ribosomal RNA
RT	Reverse transcriptase
RXH	Red Cross War Memorial Children's Hospital
s	Seconds
SA or RSA	South Africa/Republic of South Africa
SDS	Sodium dodecyl sulphate
SEM	Standard error of the mean
SNP	Single nucleotide polymorphism
snRNA	Small nuclear RNA
SOP	Standard operating procedure
Sos1	Son of sevenless homolog 1 protein complex
T	Thymine
TBE	Tris/Borate/EDTA
TBS	Tris-buffered saline
TBST	Tris-buffered saline containing tween-20
tcDNA	Trycyclo-DNA
TE	Trypsin/EDTA
TEMED	Tetramethylethylenediamine
TPA	12-O-tetradecanoylphorbol-13-acetate
TREAT-NMD	Translation Research in Europe – Assessment and Treatment of Neuromuscular Diseases

U	Uracil
U/mg	Units per milligram
u/µl	Units per microlitre
UCT	University of Cape Town
USA	United States of America
UV	Ultraviolet
v	Version
V	Volts
v/v	Volume per volume
w/v	Weight per volume
x	times
µg	Microgram
µl	Microlitre
µm	Micrometer
µM	Micromolar

Abstract

Duchenne muscular dystrophy (DMD) is the most common and severe of the dystrophies, with an incidence of 1 in 3500 live male births, worldwide. Becker Muscular dystrophy (BMD) has a lower incidence of approximately 1 in 17500 births, a milder progression and longer life expectancy. Many advancements have been made in the development of gene-based therapies for the treatment of D/BMD, however, these treatments require genetic confirmation of the disease which continues to present a significant diagnostic challenge. The current standard for RNA-based analysis requires obtaining an invasive, often distressing, muscle biopsy. This dissertation investigated the utility of human autologous epidermal melanocyte and dermal fibroblast cell cultures for use as a tool for genetic confirmation of D/BMD from a much less invasive shave skin biopsy. Methodologies included immunohistochemical, immunocytochemical, Western blot, qPCR analysis and cDNA sequencing. The results suggest that melanocytes and fibroblasts express the full length muscle isoform of dystrophin, although at differing levels, and that melanocytes could potentially be used as an alternative for the genetic confirmation of D/BMD.

Chapter 1: Introduction

The muscular dystrophies are a large group of heterogeneous neuromuscular disorders, characterised by progressive weakness and wasting of muscle[1–3]. Over 30 types of muscular dystrophies has been identified thus far[2,3], mainly distinguished from one another on the basis of the predominantly affected muscle groups. According to this method of classification, the muscular dystrophies including congenital muscular dystrophies, can be divided into six major groups: Duchenne/Becker (D/BMD), Emery-Dreifuss, distal, facioscapulohumeral, oculopharyngeal and limb-girdle muscular dystrophies (Fig. 1.1)[1,2,4]. Muscular dystrophies are caused by diverse defects in numerous genes, each with a different mode of inheritance, degree of severity and age of onset[3].

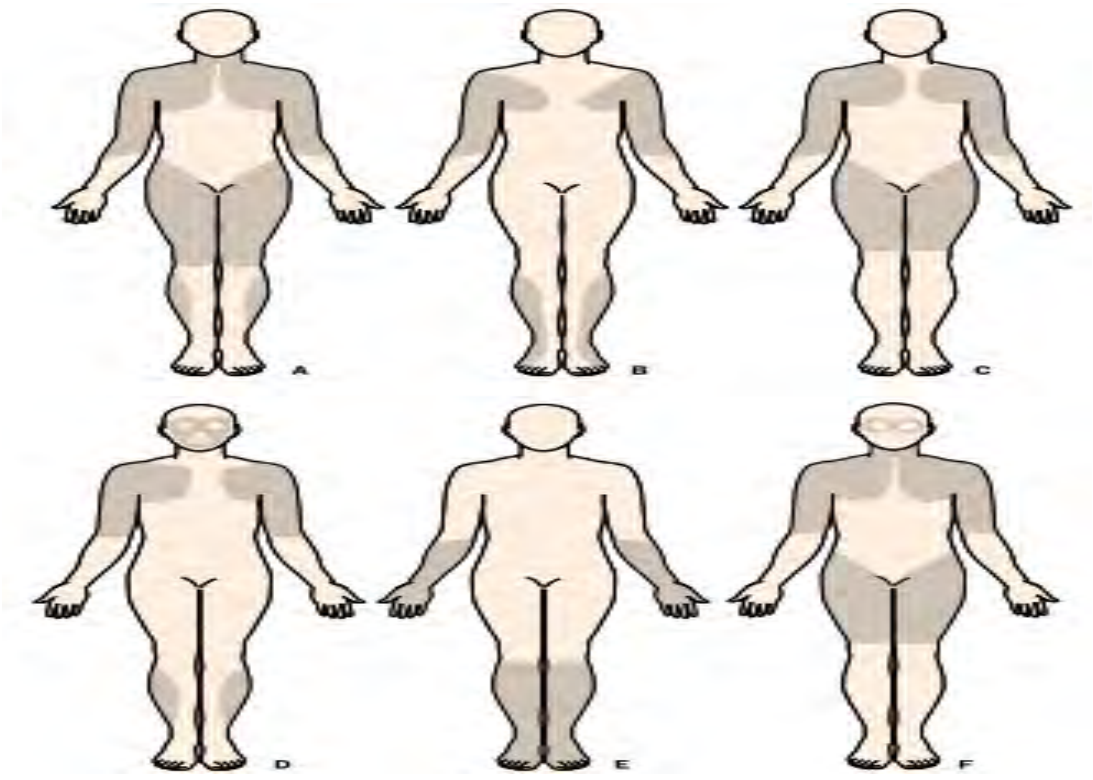

Figure 1.1 Subdivision of muscular dystrophies based on the observation of muscle groups predominantly affected by weakness. Affected areas indicated in grey. A- Duchenne/Becker, B- Emery-Dreifus, C- limb- girdle, D- facioscapulohumeral, E-distal, F-oculopharyngeal[3] (adapted from Emery, A.E.H., 2002[2]).

Duchenne muscular dystrophy (DMD) is the most common and severe of the inherited dystrophies[2]. Since the discovery of its causal gene (*DMD*) in 1986, much progress has been made in the understanding of DMD as a disease and insights gained into its genetic aetiology [5]. Recent developments in the field of gene-based therapy have placed increased emphasis on the importance of identification of the disease-causing mutation in every DMD

patient, as a basis for determining eligibility for therapy[6]. The majority of the currently employed diagnostic testing methods for D/BMD are based on mutation detection in DNA from blood lymphocytes. However, the downstream effect of DNA mutation on the transcript and the resulting protein can only be seen with RNA-based analysis, traditionally involving a muscle biopsy. This procedure is inherently traumatic and risky to the D/BMD patient, as depending on the stage of the disease, the patient can present with a potentially fatal malignant hyperthermia-like reaction when exposed to suxamethonium or a halogenated inhaled anaesthetic for a surgical procedure[7]. The focus of this research project was the development of a potential alternative diagnostic tool for RNA-based diagnosis of D/BMD using skin biopsy samples.

1.1 Duchenne/Becker muscular dystrophy (D/BMD)

Duchenne muscular dystrophy (DMD, OMIM #310200) and its milder allelic form Becker muscular dystrophy (BMD, OMIM #300376) are X-linked recessive disorders where males are generally affected, while females, in most instances, are unaffected carriers of the disease[2]. DMD has a prevalence of 1 in 3500 live male births worldwide, whereas BMD has a much lower prevalence of approximately 1 in 17500 affected males, a later onset, milder progression and a longer life expectancy[2,5].

1.1.1. Clinical presentation and progression

DMD generally starts to manifest between the ages of 2-4 years and is diagnosed by the age of 5. The affected boys suffer from progressive weakness of the proximal muscles and consequently delayed motor milestones such as sitting, standing and walking[3,8]. The disease progression can be divided into five stages: pre-symptomatic, early ambulatory, late ambulatory, early non-ambulatory and late non-ambulatory[9].

During the pre-symptomatic stage raised levels of creatine phosphokinase (CPK), an enzyme involved in muscle cell ATP production, can be detected in the blood of affected individuals[9,10]. Serum CPK is a non-specific biomarker of muscle damage and increased levels are often observed after e.g. strenuous exercise. However, in a DMD patient CPK is massively elevated 10 to 100 times that of a healthy individual[11]. Serum CPK levels are also a good indicator of DMD carrier status, as levels are raised in approximately 66% of carrier females[12]. Developmental delay and calf enlargement (pseudohypertrophy, due to the muscle being replaced by fat and connective tissue) is also observed in the pre-symptomatic stage. Although the diagnosis of DMD could be made at this stage, patients are usually only diagnosed during the early ambulatory stage.

Decreased physical ability is first noted during the early ambulatory stage. Patients tend to have a waddling gait and may display the use of Gower's manoeuvre (Fig. 1.2). The Gower's manoeuvre is a manner of getting up from a prone position, whereby the patient places his hands on the ground and shifts his body weight onto his hands and feet. He then places his hands on his knees and slowly moves them along his thighs in order to help himself rise up[3,9].

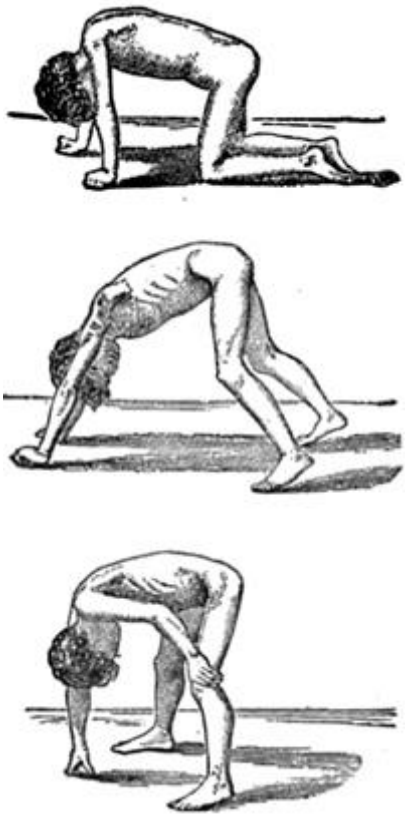

Figure 1.2. Illustration of Gower's manoeuvre[3].

In the late ambulatory stage an increasingly laboured gait is observed, along with contractures of the Achilles tendon, resulting in toe-walking. This stage is also marked by the inability to rise from a supine position or climb stairs[3].

Patients are usually confined to a wheelchair during the early non-ambulatory stage, but are generally still able to maintain their posture and propel themselves. During this stage patients suffer from nocturnal hypoventilation, an increased risk of developing scoliosis and may develop cardiomyopathy. DMD patients typically reach this stage by the age of 12 years whereas BMD can maintain ambulation well past 16 years of age, depending on the severity[9,13].

The late non-ambulatory stage of DMD is the final stage of the disease, during which patients develop scoliosis and require ventilators to assist with breathing. A considerably weakened

heart and a loss of most of the upper limb function is also associated with this stage. Without any clinical intervention, most patients die by the age of 20 years due to respiratory or cardiac complications[2,9,13,14].

Approximately 20% to 30% of DMD boys suffer from some form of mental impairment[2,14]. This mental impairment is, however, not very common in BMD and in both cases it is not progressive[3]. The visual function of some DMD patients may also be impaired and is usually accompanied by non-progressive red-green colour blindness. It is important to note that in both DMD and BMD the carriers of the disease are generally unaffected with only 5-10% displaying some of the D/BMD phenotype[2].

1.2. Clinical Management of D/BMD

D/BMD affects multiple body systems and a multidisciplinary team is required for the ideal management of patients. Different treatments and interventions are available, involving a combination of glucocorticoids, splints, physiotherapy, surgery, regular monitoring of heart function, monitoring of lung function, use of assisted ventilation and maintenance of a well-balanced diet[3,9]. These are mainly aimed at prolonging ambulation and sustaining a good quality of life, allowing many DMD patients today to live well into their third decade[15].

1.3. The *DMD* gene and its protein

The *DMD* gene was first mapped to the middle of the short-arm of X-chromosome (Xp21) in 1982 by Davies et al[16]. This was shortly followed by the isolation of the *DMD* gene in 1986[17,18].

DMD is one of the largest known human genes approximately 2.2Mb in size, with a transcript size of 14kb[6,19]. The gene consists of 79 exons, 7 promoters as well as various alternative transcripts (Fig. 1.3)[20,21]. The first three promoters, indicated in figure 1.3, drive the expression of three 14kb, full-length transcripts of dystrophin, specifically Dp427C (C), Dp427M (M) and Dp427P (P). Dp427C is primarily expressed in the cortical neurons and hippocampus of the brain. Dp427M is primarily expressed in skeletal and smooth muscle, with minor expression in the glial cells of the brain and Dp427P is primarily expressed in the Purkinje cells, with minor expression in the skeletal muscle[20]. A fourth lymphocyte promoter (Dp427L) was identified in 1994[22]. However, in 2003 the promoter was concluded to not be biologically relevant due to the large size of the transcript (7 Mb), the estimated time for transcription (2 days) and the negligible level of the Dp427L transcript in lymphocytes versus the Dp427M transcript in the same cells[23].

Dp260, Dp140, Dp116 and Dp71 are all shorter transcripts which code for smaller isoforms of the dystrophin protein. Dp260 is primarily expressed in the retina, with minor expression in the brain and heart. Dp140 is expressed in the central nervous system and kidney, while Dp116 is only expressed in adult peripheral nerves. Finally Dp71 is a ubiquitously expressed transcript found in most tissues including the heart, brain, kidney, liver, lung and retina, but not in skeletal muscle[20].

Figure 1.3. A schematic representation of the DMD gene and promoters. Black vertical lines on the linear representation of the gene indicate exons Arrows indicate the locations of the various promoters: namely the brain (C), muscle (M), Purkinje (P), retinal (Dp260), central nervous system and kidney (Dp140) Schwann cells (Dp116) and ubiquitous (Dp71) promoters (adapted from Muntoni et.al., 2003[20]).

1.4. Dystrophin

Dystrophin is a large, rod-shaped cytoskeletal protein that was first described in 1987 by Hoffman et al[14,24]. The full length protein is 427kDa in size and is associated with the sarcolemma or plasma membrane of cardiac and skeletal muscle and its primary function is to maintain the integrity of the muscle cell membrane.

Dystrophin comprises of 4 domains, namely the N-terminal domain, central rod domain, cysteine-rich domain and the C-terminal domain. The N-terminal domain has homology with α-actinin and associates with cytoskeletal actin. The central rod domain consists of a succession of 25 triple-helical repeats similar to spectrin and also associates with actin[24]. The cysteine-rich domain as well as C-terminal domain contains various binding motifs. The cysteine-rich domain allows dystrophin to bind to β-dystroglycan via WW domains; while the C-terminal domain allows dystrophin to interact with the dystrobrevins via the coiled-coil motif and with syntrophins by means of unique binding sequences[24].

1.4.1. The Dystrophin-Glycoprotein Complex (DGC)

DGC is an integral structural component of the muscle cell wall. It forms a bridge across the sarcolemma and connects the basal lamina of the extracellular matrix to the inner cytoskeleton[14,24]. The complex is an assembly of important membrane proteins namely dystroglycans, dystrobrevin, sarcoglycan and syntrophin (Fig. 1.4). The main role of the DGC is to stabilise the sarcolemma and to protect muscle fibres from long-term contraction induced damage and necrosis. In addition to its mechanical function, the DGC is also suggested to have a role in cellular communication by acting as a transmembrane signalling

complex. This is supported by the fact that the main mechanisms of cell death due to mutations of the DGC components might be related to the disruption of survival pathways and cellular defence mechanisms that are regulated by signalling cascades[24].

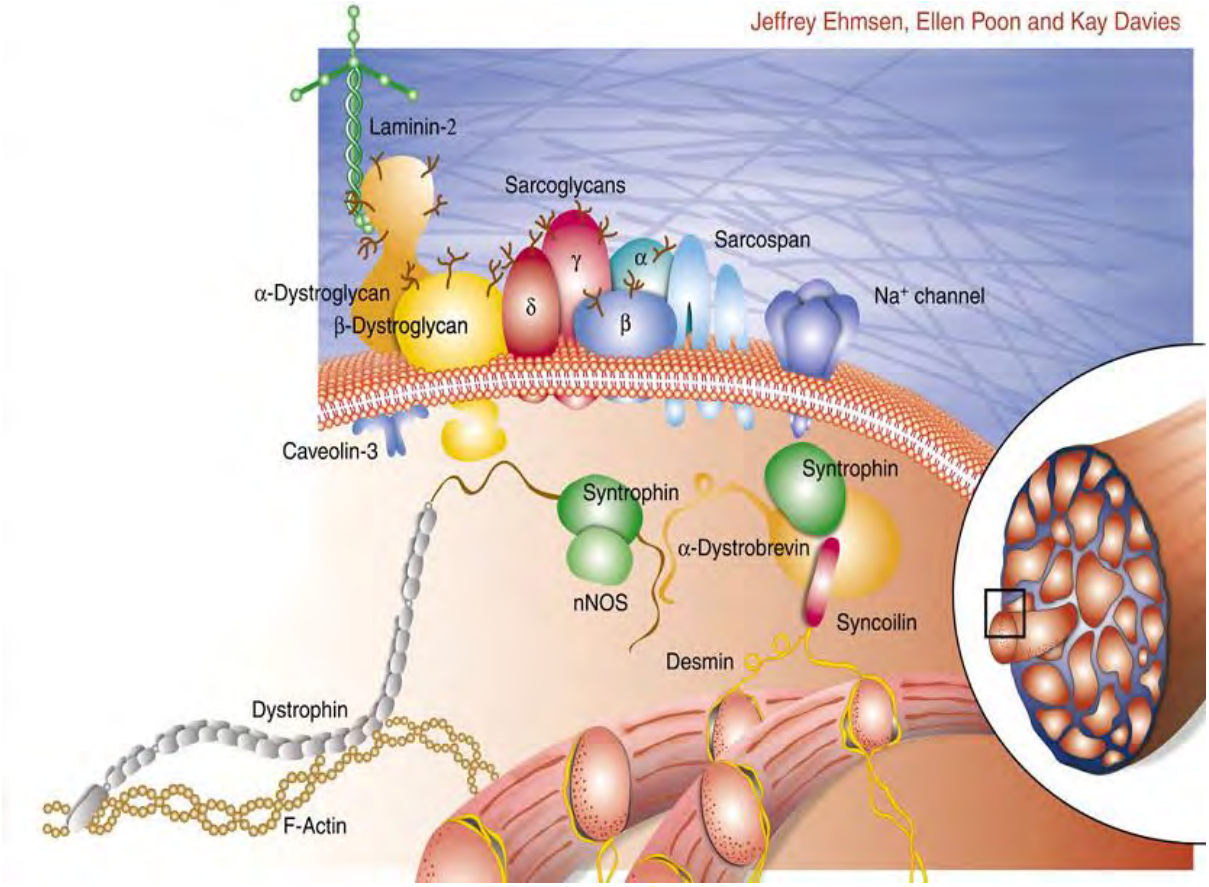

Figure 1.4. Illustration of the dystrophin-glycoprotein complex (adapted from Ehmsen et al., 2002[25]).

1.5. Genetic aetiology of D/BMD

D/BMD is a monogenic disorder, with mutations in the *DMD* gene as the only known underlying cause. Approximately a third of all *DMD* cases are a result of *de novo* changes. This high mutation rate of the *DMD* gene is speculated to be mostly due to its large size and positioning within meiotic recombination hot-spots on the X chromosome[13,21,26,27].

Exonic deletions and duplications account for approximately 70-80% of the disease-causing mutations and tend to cluster within two hot spots, located at exons 2-20 (5' hotspot) and 44-53 (3' hotspot)[6,20,28]. The remaining cases are caused by small mutations and deep intronic changes[6]. Small mutations include a variety of mutation types such as nonsense, frame-shift, splice site, small insertions/deletions and missense[6]. The frequencies of small mutations in relation to the total number of mutations in the Translational Research in Europe –

Assessment & Treatment of Neuromuscular Diseases (TREAT-NMD) global database is seen in Table 1[29]. Unlike deletions and duplications, small mutations do not display clustering.

The location of the mutations in the *dystrophin* gene plays an important role in the phenotypic presentation of the disease. For example, mutations such as a deletion downstream of exon 30 may result in decreased visual function and red-green colour blindness, possibly due to the mutation affecting Dp260[30,31]. It has also been found that mutations affecting the function of Dp140 are associated with mild mental retardation, whereas mutations in Dp71 are associated with severe intellectual disability[32,33]. This indicates that the effect of the mutation on the smaller dystrophin isoforms impacts the disease phenotype.

Table 1.1. Type of small/point mutation and frequency in the TREAT-NMD DMD global database. (adapted from Bladen et al., 2015[29])

Mutation type	% of total mutations
Small deletions (<1 exon)	5
Small insertions (<1 exon)	2
Nonsense	10
Missense	0.4
Splice-site	3
Deep intronic	0.3

1.5.1. Reading-frame rule

Studies have shown that the severity of the disease is not determined by mutation size, but rather the effect of the mutation on the translational reading frame[20,34,35]. Mutations which do not disrupt the open reading frame (ORF), allow for the production of a truncated dystrophin which may be partially functional[20,34]. However, frameshift and nonsense mutations result in premature termination of translation[20]. The production of the unstable, truncated mRNA triggers the cellular process of nonsense-mediated decay, which degrades the mRNA and protein[34]. Therefore individuals with the DMD phenotype typically have mutations which disrupt the ORF, whereas, those with the less severe BMD phenotype are likely to have mutations that maintain the ORF. This observation is known as the reading-frame rule/hypothesis or the frame-shift hypothesis and holds true for approximately 90% of all cases[20,34].

1.5.2. Exceptions to reading-frame rule

It is estimated that approximately 10% of DMD cases do not conform to the reading-frame rule and have in-frame mutations. The exception rate is much higher in BMD, with approximately 30% of BMD cases having out of frame mutations which can be partly

explained through the use of alternative translation initiation sites or exon-skipping events[36,37]. Some of the more frequent exceptions to the reading-frame rule are discussed below. It is important to note that certain mutations have been shown to underlie both DMD and BMD, thus disease severity can vary for the same mutations, sometimes within the same family, as previously reported by Ginjaar et al., where three males with BMD within the same family displayed three different phenotypes[38]. It is hypothesised that epigenetic factors may play a role in the manifestation of phenotype severity[6].

One of the factors that accounts for some of the exceptions to the reading-frame rule is the location of the mutation. For example, mutations that abolish the actin binding domain in the 5' region of the gene or the domains interacting with the extracellular matrix result in a severe phenotype regardless of whether the mutations are in-frame or not[6,20]. This is seen in the intermediate/severe BMD cases, where the disease progression is similar to that of DMD, as these individuals generally have mutations close to the 5' end of the gene (Fig. 1.5)[2,20]. Similarly it is observed that large deletions that extend into the middle of the rod domain (deletions of exons 3-31, 3-25, 4-41 or 4-18), despite being in-frame result in a DMD phenotype[20].

An exception to the reading-frame rule can also occur due to activation of an alternative translation initiation site. One such example is the development of a BMD phenotype with frame-shifting or nonsense mutations before exon 8. This has been linked to the presence of an alternative translation initiation site at exon 6 or 8, which can be activated by certain frame-shifting mutations such as the deletion of exon 2 or deletions of exons 3-7[6,36].

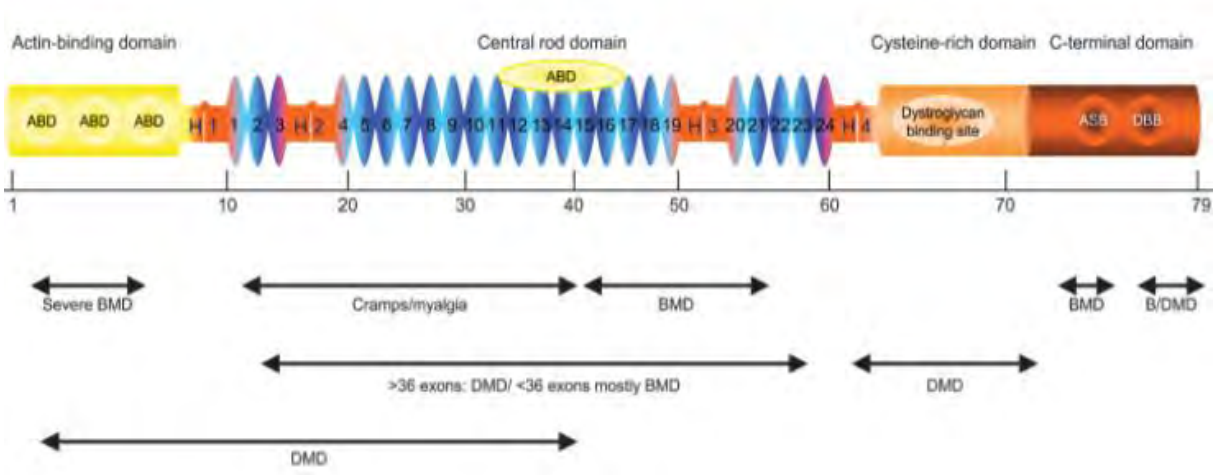

Figure 1.5. Schematic of the dystrophin protein structure with domains and the relationship between in-frame deletions and phenotypic severity. ABD – Actin binding domains (yellow). The central rod domain consisting of 24 spectrin-like repeats (1-24; blue), with an actin binding domain between repeats 11-17. H1, 2, 3 and 4 – Hinge regions (red). Cysteine-rich domain/Dystroglycan binding site (orange). C-terminal domain (dark red) consisting of α-syntrophin (ASB) and dystrobrevin binding domains (DBB). The location of different exons is shown by the numbered line bellow the schematic (adapted from Aartsma-rus et al., 2006[36]).

Cases have been described of nonsense mutations in BMD patients, where the mutation was shown to disrupt an exon recognition site resulting in skipping of the exon whilst maintaining the open reading frame[6].

1.6. Gene-based therapies

In recent years, research in the field of genetic therapies has shown much promise, specifically with regards to DMD.

Genetic therapy for DMD can be divided roughly into two groups, namely gene replacement and gene modification[39]. Gene replacement strategies involve replacement of the mutated gene with a functional copy by using a viral vector (viral gene therapy) or increasing the expression of a functionally compensatory dystrophin homologue utrophin (utrophin upregulation)[40]. Transplantation of cells containing a functional gene copy has also been investigated and could be classified as a gene replacement therapy (myoblast and stem cell transplantation)[41,42].

Multiple proof-of-concept studies of these strategies have been performed using the *mdx* mouse model, demonstrating variable efficiency at restoring dystrophin expression[40]. Although the results are promising, more work is required to overcome the issues of restoring dystrophin expression in all muscles in the body, decreasing the cost of treatment and overcoming problems related to the immune response. Nonetheless, these studies are promising and further refinement of the techniques are being performed[40].

The strategy group of gene modification is currently closest to clinical application, with a number of clinical trials in various phases and applications for approval[43–46]. It involves the 'fooling' of the cellular machinery into either bypassing stop codons (stop codon read-through therapy) or skipping the exons containing the disease causing mutations (exon skipping therapy). These treatments are of particular interest to this study as they require knowledge of the exact disease-causing mutations in patients[39,40].

Stop codon read-through therapy is specifically designed for use on patients with nonsense mutations. This therapy is applicable for approximately 15% of patients with DMD as nonsense mutations, which lead to the production of a premature stop codon, only occurs in approximately 15% of patients[40]. The introduction of a premature stop codon results in early termination of translation[45].

All stop codons, regardless of whether they are premature or not, undergo some level of read-through which is dependent on various factors including the use of certain drugs[45]. The use of drugs that can bypass these mutations is an alluring prospect for the treatment of

DMD, where the underlying defect is a premature stop codon introduced by a nonsense mutation. One such group of drugs is the aminoglycosides, which are antibiotics that function by targeting the 16S rRNA subunit of the bacterial ribosome, to inhibit protein synthesis[45]. It has been shown that these compounds also interact with the A-site of human ribosomal complexes, which results in high rates of stop codon read-through. In studies involving the *mdx* mouse (a dystrophin deficient mouse, with a nonsense mutation in exon 23) it was demonstrated that gentamicin induced expression of full-length dystrophin in the mouse. Gentamicin was tested in clinical trials, but never convincingly showed restoration of dystrophin. In addition, high levels of gentamicin were required and its long-term has known nephron- and ototoxic side effects[43,45].

Ataluren also known as Translarna (PTC Therapeutics, USA), is a read-through therapy and has completed a confirmatory phase 3 clinical trial in North and South America, Australia, Asia and Europe and has been granted conditional marketing authorisation by the European Commission in 2014. Translarna is approved for use in ambulant DMD patients older than 5 years whose condition is caused by a nonsense mutation in the *DMD* gene, in European Medicines Agency (EMA) countries[43]. PTC Therapeutics filed for accelerated approval with the Food and Drug Administration (FDA; USA) in January 2016, but the FDA refused to file for the accelerated approval on the grounds that the current data available was not sufficient for an FDA review[43].

Another intensively investigated mutation-based therapy is ”exon-skipping”. This approach uses antisense oligonucleotides (AONs), which are small RNA or DNA molecules that are able to hybridise to complementary sequences in or adjacent to the exon targeted for skipping. This binding alters the splicing of the pre-mRNA by essentially concealing the exon from the splicing machinery, resulting in the skipping of the exon containing the mutation. This produces a truncated, functional protein thereby converting the severe DMD phenotype to the less severe BMD phenotype[44–46]. Approximately 83% of all DMD mutations are amenable to correction using this therapy, with the skipping of some exons being applicable to more patients than others, for example the skipping of exon 51[43,47].

There are a number of AON chemistries under investigation namely 2’O-methylphosphorothionate (2’OMePS), phosphorodiamidate morpholino oligomers (PMOs), non-spliceosome small nuclear RNA (SnRNA), peptide-PMOs and trycyclo-DNA (tcDNA)[48]. Eteplirsen (Sarepta Therapeutics, USA) and Drisapersen (Prosensa Therapeautics/BioMarin Pharmaceutical, USA) for skipping of exon 51 are currently undergoing clinical trials and are examples of PMO and 2’OMEPS chemistries, respectively.

A phase 3 trial to evaluate the safety and efficacy Eteplirsen is currently on-going[43,48]. The results to date indicate that the drug is well tolerated and has a slowed disease progression based on the six minute walk test. Accelerated approval with the FDA in the USA was filed for by Sarepta Therapeutics for Eteplirsen and the decision by the FDA was due on 16 May 2016, but has been delayed[43].

A trial to study the safety, tolerability and efficacy of long term administration of Drisapersen is currently underway[43]. Results to date indicate that the drug is well tolerated and that there is slower disease progression based on the six minute walk test, which is improved with continuous treatment for 25 weeks[48]. Accelerated approval with the FDA and marketing authorisation with the EMA was applied for in 2015 for Drisapersen. Unfortunately in January 2016 the FDA stated that the drug was not yet ready for approval and on 31 May 2016 BioMarin Pharmaceutical withdrew their application with EMA[43].

Both Eteplirsen and Drisapersen showed a variable increase in sarcolemmal dystrophin of <20%. These first generation exon-skipping therapies (PMOs and 2'OMePS) have been limited by the low efficacy in cardiac muscle, poor cellular uptake and rapid clearance from circulation, therefore repeated administration of the drugs is necessary and development of new chemistries and delivery methods are still under investigation[48].

One of these new chemistries is a SnRNA such as U7snRNA, which shuttles the AONS after vectorisation into adeno-associated virus to induce exon skipping. This chemistry was found to induce efficient exon-skipping *in vitro* and *in vivo*[48,49]. A study testing the therapy on the *mdx* mouse displayed near normal expression of dystrophin in all muscle, including cardiac, as well as an increase in the *mdx* mouse muscle function after a single dose[49]. Nonetheless this strategy requires further study and faces immunological and delivery challenges specific to adeno-associated viral vectors[48,49].

Currently the two most promising AON chemistries are peptide-PMOs and tcDNA. Peptide-PMOs utilise cell penetrating peptides that are conjugated to the AONs, in order to increase potency and delivery of the drug. Recent reports indicated that a single intravenous dose of peptides known as PMO internalising peptides (Pip) resulted in high levels of dystrophin restoration in both skeletal and cardiac muscle of *mdx* mice[48].

TcDNA is the other chemistry in development that has shown improved distribution of dystrophin expression in skeletal muscle, heart and brain[44]. It was also shown to be more effective than PMOs and 2'OMePS chemistries in studies involving the *mdx* mouse. Although these newer exon-skipping therapies show promise, further study into the toxic effects of chronic treatment with these drugs needs to be performed before being tested in humans[48].

One of the major limitations of the exon-skipping therapy is that the dystrophin protein is truncated, meaning that the best clinical outcome is the conversion from a DMD phenotype to a BMD phenotype. Also, the AONs are mutation/exon specific, which means that a range of AONS must be developed for a number of mutations. It also means that some patients will remain untreated[45].

Nevertheless, the treatment is viewed as an improvement on the currently available interventions, as the treatment could potentially add years onto some patient's lives.

Both strategies, however, (stop codon read-through and exon-skipping) are dependent on the knowledge of the underlying genetic defect in each patient. This requires an effective method of quickly and accurately determining the disease causing mutation in every DMD patient.

1.7. Laboratory diagnosis of D/BMD

The diagnosis of D/BMD should be prompt and accurate, to enable commencement of the appropriate treatment and interventions which may prolong ambulation and increase life expectancy. Diagnosis should initially be performed by a neuromuscular specialist, who can interpret the clinical presentation and request laboratory testing to confirm the diagnosis and refer the family for genetic counselling. Carrier testing of the mother and other at-risk female relatives may also be recommended to assist with family planning.

Initial screening in a child suspected to have D/BMD involves a thorough clinical examination and determination of the blood CPK levels. If consistent with a clinical diagnosis of B/DMD genetic testing for detection of mutations in the *DMD* gene will be undertaken. If no mutation is found, the patient will be required to undergo a muscle biopsy with subsequent staining for dystrophin[2,9].

1.7.1. Genetic confirmation of DMD

Exonic deletions and duplications account for the majority of DMD patients (approximately 70%)[12] and the diagnostic protocols generally focus on the detection of exonic rearrangement as a first tier test. The current preferred method is the multiplex ligation-dependent probe amplification (MLPA) assay (MRC-Holland, Netherlands). In patients who test negative for exonic deletions or duplications, testing for small/point mutations may be pursued. While genomic DNA from blood lymphocytes is the most commonly used template in the diagnostic protocols for sequencing, RNA-based analysis from muscle tissue may be more informative in terms of the downstream effects of a sequence alteration in DNA[13,36,37].

Currently, there are no recommendations for RNA-based analysis for D/BMD, mostly due to the expense associated with sequencing of the 79 exons in the *DMD* transcript[12]. However, this may change with a wider application of gene-based therapies and the need to determine eligibility. Figure 1.6 indicates the ideal workflow for the genetic diagnosis of D/BMD based on currently available methodologies.

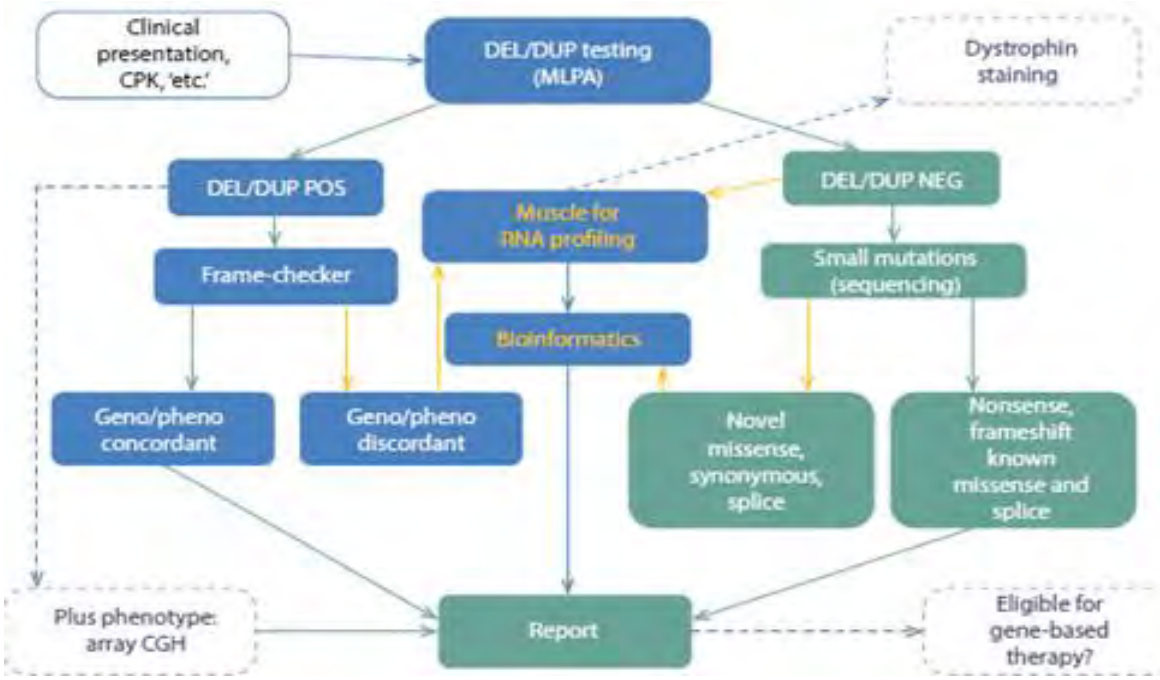

Figure 1.6. General procedure for genetic diagnosis of D/BMD (used with permission from from Esterhuizen et al., 2016[50]). CPK = creatine phosphokinase, DEL/DUP = deletion or duplication, CGH = comparative genomic hybridisation, Geno/pheno = genotype-phenotype correlation.

1.7.2. Immunohistochemical confirmation of D/BMD

In patients with uninformative genetic test results, laboratory confirmation of the diagnosis is achieved through immunohistochemical (IHC) analysis of muscle biopsy material. This process involves microscopic examination of frozen tissue sections, stained with dystrophin-binding antibodies (Fig. 1.7). A positive test for DMD displays a complete lack of binding by the antibodies due to the absence of dystrophin in the tissues, whereas, BMD displays non-uniform binding of the antibodies due to discontinuous, low level expression of the protein[20]. Other features, that may also be noted from the muscle biopsy include: split muscle fibres, fibrosis, necrosis, variation in muscle fibre size as well as signs of muscle regeneration. Although immunohistochemical analysis can confirm the diagnosis D/BMD, it does not reveal the specific disease-causing mutation[5].

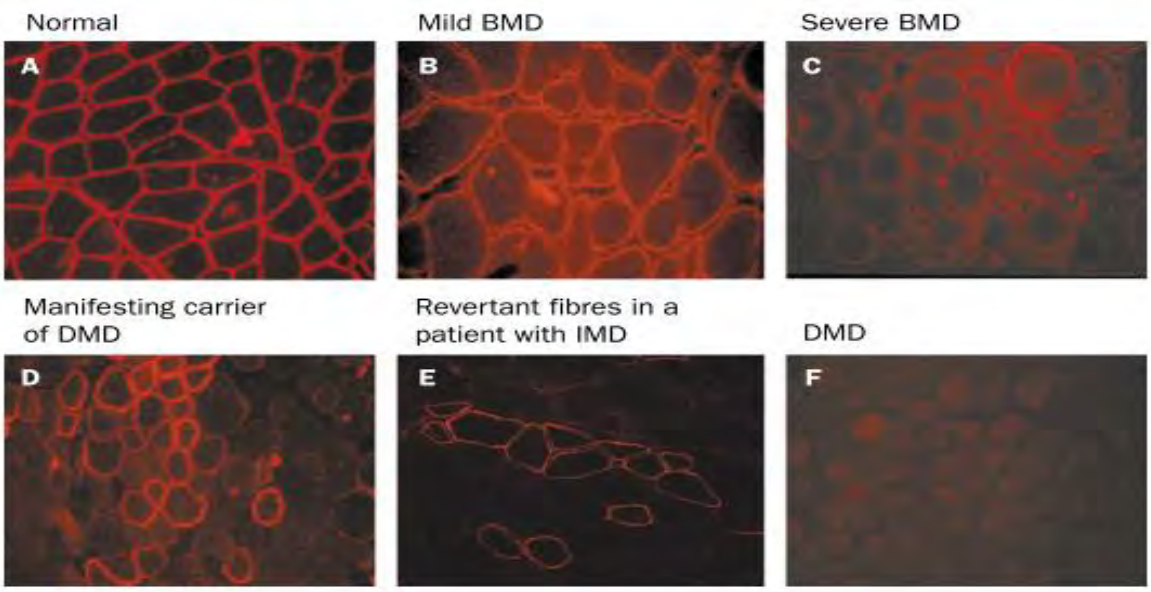

Figure 1.7. Immunohistochemical staining of muscle sections for dystrophin. A - Normal muscle displaying positive staining of the muscle membrane for dystrophin. B and C – BMD patients displaying low level dystrophin expression. D – Carrier displaying mosaic staining. E – Patient with intermediate phenotype displaying mosaic staining with relatively abundant reverent muscle fibres. F – DMD patient displaying complete absence of dystrophin. (adapted from Muntoni et al., 2003[20]).

More recent investigations of dystrophin expression in various tissues, using RNA sequencing, have also shown moderate expression of dystrophin in skin (Fig. 1.8). Furthermore, studies investigating dystrophin expression in the various skin cells revealed expression in fibroblasts and melanocytes, which is the main focus of this project.

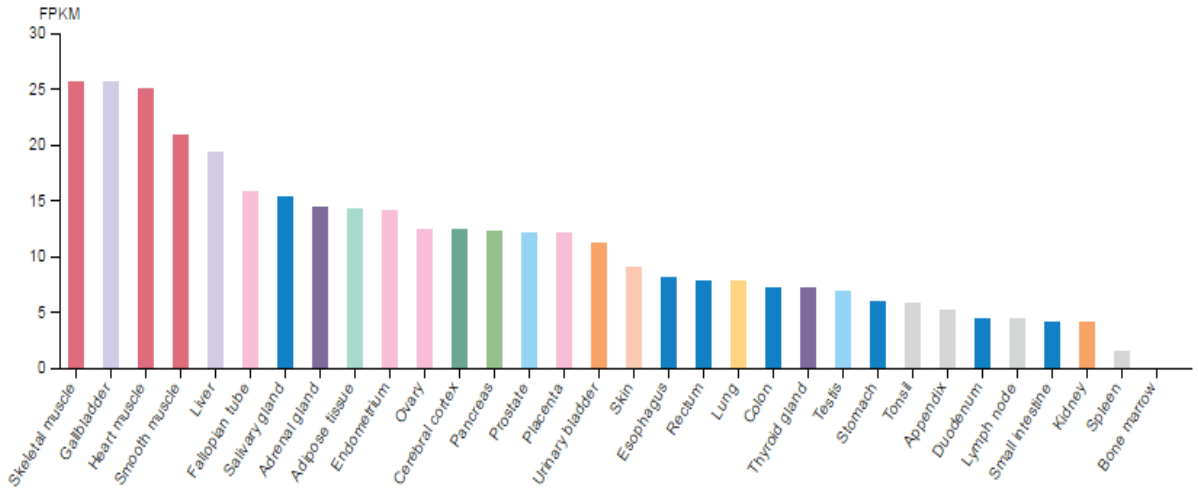

Figure 1.8. *Dystrophin* RNA expression in different tissues based on RNA sequencing data of 32 tissue types. FPKM = Fragments Per Kilobase gene model and Million reads. (http://www.proteinatlas.org/ENSG00000198947-DMD/tissue).

1.8. The skin and D/BMD

The skin is considered the largest organ of the body and plays an important role in temperature regulation, sensation and as a protective barrier[51,52]. It comprises three layers namely the epidermis, dermis and hypodermis (Fig. 1.9). The epidermis is the outermost layer of the skin and is mostly comprised of keratinocytes, keratin producing cells that differentiate from the basal layer of the epidermis and migrate to the upper layers of the epidermis[53]. Melanocytes, which produce the pigment melanin, are also located in the epidermis, close to the basement membrane[53]. Other cell types found in the epidermis include the Langerhans cells for immunity and the Merkel cells for sensory input[52,53].

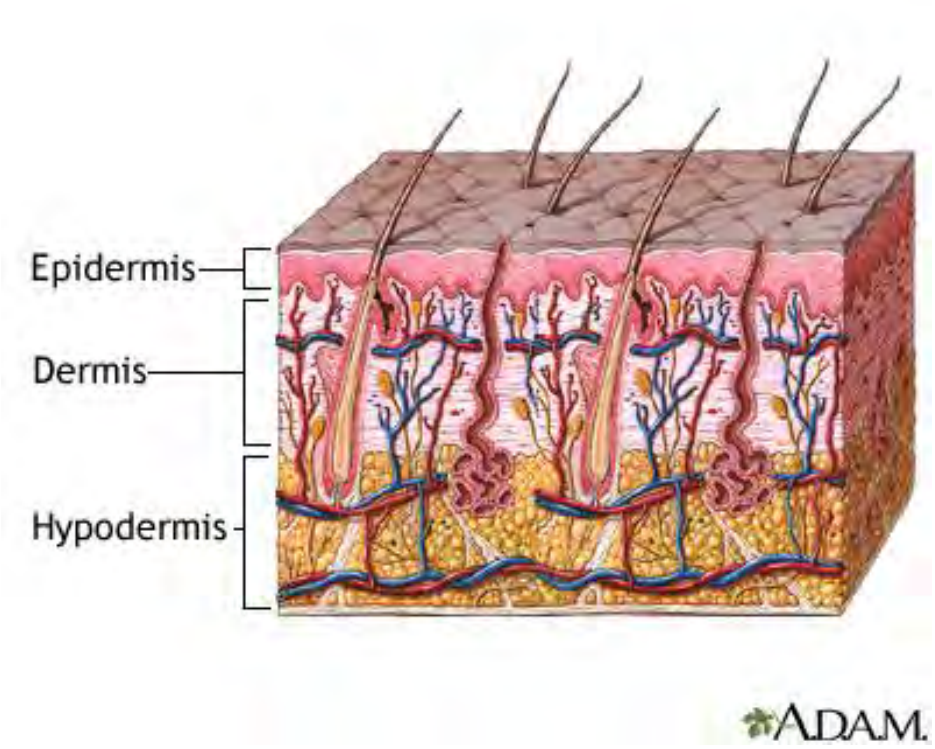

Figure 1.9. Diagrammatic representation of the layers of the skin.
(https://www.nlm.nih.gov/medlineplus/ency/imagepages/8912.htm).

The dermis is located below the epidermis and mostly consists of fibroblasts in a dense, unstructured extracellular matrix (ECM), mostly made up of collagen[51–53]. Other structures also found within the dermis of the skin include blood vessels, hair follicles, subcutaneous glands, sweat glands, nerve endings and arrector pili muscle. The hypodermis, which is located below the dermis, is the final layer of the skin and incorporates fat, blood vessels and nerves[52,53]. The skin is therefore a complex, multifunctional organ comprising of many different tissues, structures and cell types; the three main cell types being keratinocytes, melanocytes and fibroblasts.

1.8.1. Fibroblasts

Fibroblasts are the most abundant cell type in the body's connective tissue and have a spindle-shaped morphology. One of their main functions is to secrete components of the ECM such as collagen, elastin and fibronectin[51,53,54]. Fibroblasts also play a very important role in the embryo by directing skin morphogenesis and are involved in various processes such as wound healing, skin cancer, aging and fibrosis[54].

Fibroblasts have also been used in the study of various genetic disorders. This includes studies of Parkinson's disease, where fibroblasts were used to investigate abnormalities in mitochondrial function and morphology and as a cellular disease model[55,56]. Fibroblasts have also been used for gene expression analysis in bipolar disorder as well as gene expression profiling using microarray analysis for inherited metabolic disorders[57,58]. Finally as fibroblasts play an important role in fibrosis and fibrosis is a hallmark of many myopathies, it is not surprising to find that fibroblasts have been studied intently with regards to DMD. Various studies have found that fibroblasts obtained from DMD patients differed from fibroblasts obtained from healthy individuals. These differences included increased adhesion of muscle fibroblasts[59], decreased adhesion of dermal fibroblasts[60] and altered collagen metabolism[61]. Expression of dystrophin in fibroblasts has also been reported though these reports are contradictory. One study described low amounts of expression which correlated to illegitimate transcription while another reported high levels of expression in dermal fibroblasts[62,63]. However, no further work on the utility of fibroblasts in the investigation of DMD was pursued due to the perceived low levels of dystrophin expression in these cells.

1.8.2. Melanocytes

Melanocytes are pigment-producing cells that can be found in various areas of the body, such as the brain, heart, eye, lungs, ear, adipose tissues and skin[64]. There are two types of melanocytes, namely, differentiated melanocytes derived from the neural crest and the melanocytes that form the retinal pigment epithelium of the eye which develop from the optic cup of the brain[64].

Morphologically, the cells are dendritic in shape and can appear as bipolar or multipolar in culture with dendrites either originating from the cell body or from another dendrite. These dendrites are used to transport vesicles containing the pigment melanin (melanosomes) to keratinocytes. Melanin plays an important role in the protection of the skin against ultraviolet light. Melanocytes are terminally differentiated (they no longer divide under normal circumstances) and comprise approximately 5-10% of the cells found in the epidermis. In human skin, melanocytes are localized at the dermal–epidermal junction (DEJ) in a

characteristic regularly dispersed pattern[65]. Attachment of melanocytes to the DEJ is crucial for their role in the signalling between the epidermis and the dermis and involves laminin-binding receptors such as integrins and dystroglycans[66,67].

Interestingly, two studies recently reported the expression of the full-length muscle isoform of dystrophin in primary melanocyte cultures[68,69]. Both studies revealed relatively robust levels of expression of the Dp427M dystrophin isoform as well as expression of the Dp260, Dp116 and Dp71 isoforms in melanocytes[68,69].

As RNA-based diagnosis of D/BMD is traditionally performed using muscle biopsies which are inherently traumatic and risky to the patients, this study focuses on the use of skin cells as an alternate tool for RNA-based diagnosis of D/BMD. Driven by the need to provide DMD patients with a genetic diagnosis and determine their potential eligibility for gene-based therapy.

1.9. D/BMD in South Africa

The testing service for D/BMD in South Africa (SA) was first initiated in 1987, in Cape Town, by Professor Peter Beighton and colleagues, in conjunction with the Red Cross War Memorial Children's Hospital (RXH)[50,70]. This service initially offered Southern blotting as the first molecular test, which was followed by restriction enzyme length polymorphism analysis (RFLP) for D/BMD carrier testing and multiplex PCR (mPCR)[50]. In 2007 MLPA was introduced as the preferred method for genetic testing for D/BMD and has successfully increased the mutation detection rate from approximately 30% to 45%, replacing mPCR.

Currently the genetic testing service for D/BMD is housed by the National Health Laboratory Service (NHLS) in Cape Town and Johannesburg, and is available to the public and private sector in and outside of South Africa[50]. A dedicated neuromuscular clinic at RXH, provides access to genetic counselling and support from the Muscular dystrophy foundation of South Africa. This clinic assures that patients are managed according to international guidelines, within the capacity of the facility[50].

1.10. Aims and objectives

Aims:

1) To culture epidermal melanocytes and dermal fibroblasts to determine expression of the full length dystrophin isoform, and to quantify the expression thereof.

2) To demonstrate whether total RNA extracted from epidermal melanocytes and/or dermal fibroblasts can be used in the genetic diagnosis of D/BMD.

1.10.1. Objectives:

- To recruit D/BMD patients for skin biopsy samples and culture primary melanocyte and fibroblast cells therefrom.
- To optimise immunocytochemical staining (ICC) for detection of dystrophin expression in cultured human melanocytes, fibroblasts and C2C12 mouse myoblasts.
- To extract RNA and synthesise cDNA from cultured patient and wild type melanocytes and fibroblasts.
- To extract protein from patient and wildtype melanocytes and fibroblasts, for use in Western blotting.
- To extract protein from C2C12 mouse myoblasts, as a positive control for dystrophin, for use in Western blotting.
- To quantify the expression of dystrophin transcripts and protein, present in the melanocytes and fibroblasts using qPCR and Western blotting.
- To sequence the coding region of the *DMD* gene in the patients' cDNA to identify the disease causing mutations.
- To devise a protocol for potential introduction of melanocyte/fibroblast culture and cDNA analysis into the diagnostic environment.

1.10.2. Hypothesis:

Melanocytes and fibroblasts express varying levels of the full length muscle isoform of dystrophin and can be used for the genetic diagnosis of D/BMD.

Chapter 2: Materials and Methods

2.1. Ethics approval and consent for participation

Ethical approval for the study was granted by the University of Cape Town (UCT) Faculty of Health Sciences Human Research Ethics Committee (HREC REF 311/2014), in accordance with the tenets of the Declaration of Helsinki 2013 (Appendix 1.1). Written parental consent or child assent for participation was obtained prior to the shave biopsy procedure (Appendix 1.2).

2.2. Cohort Recruitment and sample collection

Five patients with a molecular diagnosis of DMD were recruited from the Muscle Clinic at the Red Cross War Memorial Children's Hospital (RXH) (Table 2.1). Each patient was given a unique patient code using the date that the sample was collected with a letter A or B if more than one patient provided a sample on the same day.

Skin biopsy samples were taken using eutectic mixture of local anaesthetics (EMLA) cream (APP pharmaceuticals, USA), a sterile needle and surgical blade. The forearm of the patients was disinfected and EMLA cream was applied and left for 30 min to numb the area. The needle was shallowly inserted under the skin, to lift the skin. The lifted section of skin was cut using a surgical blade to obtain a small biopsy of approximately 4mm by 4mm in size. All biopsies were performed by a doctor from the Muscle Clinic at RXH. The samples were transported in tubes containing Dulbecco's Modified Eagle medium (DMEM) (Highveld Biological, RSA or Sigma-Aldrich, USA; appendix 2.1) supplemented with antibiotics penicillin and streptomycin (100x pen/strep) (100U/mL penicillin and 100µg/mL streptomycin; appendix 2.1).

Table 2.1. Patient identification codes and genetic diagnosis.

Patient Code	Disease-causing mutation	Molecular Diagnostic Method*
151006A	Deletion at 5' region (Dp427M promoter – exon 6)	Host-spot Multiplex PCR
151006B	Duplication of exons 12-18	MLPA
151013A	c.968_981del;p.Glu323Fr (frameshift) (Exon 10)	MLPA, sequencing of exon 10
151013B	Duplication of exon 19	MLPA
151020	Deletion of entire gene (contiguous gene deletion syndrome)	MLPA

*Diagnostic performed by the National Health Laboratory Service (NHLS), Western Cape.

2.2.1. Control cell lines and primary cell cultures

C2C12 mouse myoblasts (Dr. Gaurang Deshpande, Cardiology, UCT) were used as a positive control for dystrophin in immunocytochemistry and Western blotting. Laboratory cell stocks (courtesy of Ms T Wiggins, Division of Cell Biology, UCT) of primary foreskin-derived melanocytes and foreskin-derived fibroblasts from healthy individuals were used as wild type skin cell controls in this study.

2.3. Cell Culture

2.3.1. Isolation and culture of melanocytes

Primary melanocytes were aseptically isolated from patient shave skin biopsies, using a modified method described by Aasen et al[71]. The samples were washed with phosphate buffered saline (PBS, appendix 2.1) containing pen/strep and cut finely using a scalpel (KIMIX, RSA) before being transferred to a tube containing a 0.25% trypsin, 0.05% EDTA solution (pH 7.5; appendix 2.1) at 37°C. The tube was agitated every 5 min and after 15 min the contents were triturated in order to obtain a cell suspension. The trypsin was inactivated using 10% foetal calf serum (FCS; GIBCO, USA). The cell suspension was then filtered using a 70µm cell strainer (BD Biosciences, USA) which was pre-wet with melanocyte specific growth medium. The suspension was strained to remove any large pieces of tissue that did not dissociate into a cell suspension. The suspension was centrifuged at 500rpm for 10 min, the supernatant was aspirated and the cell pellet was resuspended in 1mL melanocyte growth medium. The cells were plated into 35mm culture dishes and incubated at 37°C with 5% CO_2/95% O_2 (O_2/CO_2 incubator; Sanyo, Japan) overnight. Fresh medium was added to the cells after they adhered overnight and these cells were denoted as passage 0 (p0).

Melanocytes were cultured in the melanocyte specific growth medium, FETI (Table 2.2). Medium was changed every 3-4 days. The cells were regularly monitored using the Olympus CK2 brightfield microscope (Olympus, Japan) and tested for *Mycoplasma spp*. Images of cells in culture were taken using the Evos XL Care microscope (Life Technologies, USA).

Table 2.2. List of melanocyte growth medium components.

Medium	Component	Final Concentration	Supplier
FETI	Hams F10	9.86g/L with 1.2g/L sodium bicarbonate	Highveld Biological /Sigma-Aldrich
	Endothelin 1	2ng/mL	Sigma-Aldrich
	12-O-tetradecanoylphorbol-13-acetate (TPA)	16nM	Sigma-Aldrich
	3-isobutyl-1-methyl xanthine (IBMX)	0.05mM	Sigma-Aldrich
	Ultroser G	1%	PALL Life Sciences, USA
	Basic fibroblast growth factor (bFGF)	2ng/mL	Miltenyi Biotech, Germany
	Foetal Calf Serum (FCS)	2%	GIBCO
	Penicillin/streptomycin (pen/strep)	1x	Sigma-Aldrich,

Cells were routinely checked for *Mycoplasma spp.* contamination using the Hoechst nuclear stain (Ms Susan Cooper, Dept. of Human Biology, University of Cape Town; Appendix 2.1). Upon reaching 80%-100% confluency the cells were trypsinised or passaged. This was performed using Trypsin/EDTA solution (0.025% trypsin and 0.01% EDTA in PBS; GIBCO) for 2 min at 37°C, followed by the addition of FETI to inactivate the trypsin. The cells were triturated and centrifuged at 2000rpm for 2min. The cell pellet was resuspended in FETI, placed into new sterile tissue culture dishes and incubated at 37°C with 5% CO_2/95% O_2. None of the melanocytes used in this project exceeded passage 9 (p9).

2.3.2. Isolation and culture of fibroblasts

Primary fibroblasts were also isolated from the dermis of shave biopsies obtained from patients. Each sample was finely cut in DMEM (Highveld Biological/Sigma) supplemented with 10% (v/v) heat inactivated FCS and 1x pen/strep (DMEM++), using a scalpel (KIMIX). The pieces were placed into 35mm culture dish, in a drop of DMEM++ and covered with a sterile coverslip. The coverslip was held down using a sterile pipette tip (Greiner Bio-One, Austria) and covered with 2mL DMEM++. Once the fibroblasts were growing well the coverslip was transferred to a sterile 35mm culture dish and cultured in DMEM++ prior to trypsinisation and expansion in a larger culture dish. Cells were monitored using brightfield microscopy and regularly tested for *Mycoplasma spp*. Images of the cells in culture were taken using the Evos XL Care microscope (Life Technologies) and the cells were passaged upon reaching 80%-100% confluency using trypsin/EDTA (0.25% trypsin, 0.05% EDTA solution in PBS).

2.3.3. C2C12 culture

C2C12 mouse myoblast cells were cultured in DMEM++. Similarly to the melanocytes, the cells were monitored using brightfield microscopy and regularly tested for *Mycoplasma spp.* contamination. Images of the cells in culture were taken using the Evos XL Care microscope (Life Technologies) and the cells were passaged upon reaching 80%-100% confluency using trypsin/EDTA. C2C12 cells were cultured for use as a positive control for dystrophin Western blots and immunocytochemistry.

2.4. Immunohistochemistry (IHC)

Fluorescent immunohistochemistry was performed on wild type frozen rat muscle sections (Dr. Tertius Kohn, Dept. of Human Biology, University of Cape Town), in order to confirm the functionality of the dystrophin antibodies, and wildtype adult human foreskin sections. Frozen rat muscle and frozen foreskin were embedded in optimum cutting temperature medium (OCT; Thermo Fisher Scientific, USA) and 0.5µm sections were cut using the Leica CM1850 cryostat (Leica Biosystems, Germany). The sections were then placed onto Superfrost® Plus microscope slides (Thermo Fisher Scientific) and the slides left for 5 min to allow the sections to reach room temperature. An outline of the section was drawn on the slide using a diamond tipped pencil and approximately 50µL of each primary antibody (Table 2.3) was applied respectively to each of the sections. Tris-buffered saline (TBS; appendix 2.2) was applied to the negative control. The slides were incubated in a humidity chamber for 1h at room temperature after which they were washed in TBS for 5-8 min with mild agitation using a platform shaker (Stovall Life Science, USA). The areas around the sections were dried using

paper towel and 50µL of the secondary antibody was applied (Table 2.3). The slides were incubated in a dark humidity chamber at room temperature for 30min, before rinsing for 5min in TBS with mild agitation. Coverslips were mounted onto the slides using mowiol mounting fluid (Ms Susan Cooper) containing n-propyl gallate (Sigma-Aldrich). Sections were allowed to dry overnight in the dark at room temperature before images were captured with the Axiovert 200M fluorescence microscope (Carl Zeiss Microscopy, Germany), AxioCam HRm camera (Carl Zeiss Microscopy) and the AxioVision version 4.8 software (Carl Zeiss Microscopy).

Table 2.3. List of primary and secondary antibodies and their dilutions.

Antibody	**Dilution**	**Supplier**
NCL-DYS1 (Dys1; Rod domain)	Undiluted	
NCL-DYS2 (Dys2; C-terminus)	1:10	Leica Biosystems
NCL-DYS3 (Dys3; N-terminus)	Undiluted	
Secondary Antibody		Ms Susan Cooper, Dept. of Human Biology, University of Cape Town
Donkey anti-mouse CY3	1:500	

2.5. Immunocytochemistry (ICC)

The immunocytochemistry (ICC; Appendix 3.1) staining protocol was optimised using the C2C12 myoblast cells and the human melanocytes in order to determine the optimal dilutions for the dystrophin antibodies. A comparison between two wash buffers, TBS and PBS, as well as two methods of fixation was carried out (Fig. 2.1) to determine the source of the crystal-like artefacts and the cell damage observed in melanocytes during the first staining attempt.

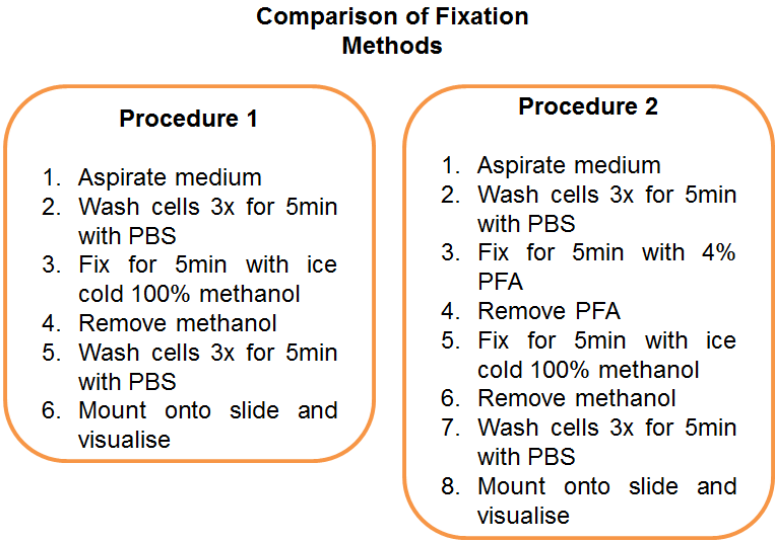

Figure 2.1. Methodology for the comparison between fixation methods.

Staining of wildtype fibroblasts and melanocytes was then performed, using the wash buffer and fixation methods in procedure 2 (Fig. 2.1).

Briefly, $3x10^4$ cells were seeded onto a sterile coverslip in a 35mm culture dish and cultured. After three days the medium was removed and the cells were washed using PBS. The cells were then fixed to the coverslip using 4% paraformaldehyde (PFA; Appendix 2.2) and 100% ice cold methanol (United laboratories, Philippines). The coverslips were washed again before blocking with 5% bovine serum albumin (BSA; Sigma-Aldrich) containing 0.1% Triton-X (Sigma-Aldrich). Immediately after blocking the coverslips were incubated with the undiluted primary antibodies in table 3.2 for 1h at room temperature. The cells were then washed again with PBS and incubated using the Donkey anti-mouse CY3 secondary (1:1000; Ms Susan Cooper) for 2h.

After incubation using the secondary antibody the coverslips were washed, stained with Hoechst nuclear stain and washed again before being mounted onto a microscope slide. The slides were viewed and images were captured with the Axiovert 200M fluorescence microscope (Carl Zeiss Microscopy, Germany), AxioCam HRm camera (Carl Zeiss Microscopy) and the AxioVision version 4.8 software (Carl Zeiss Microscopy). Image fluorescence was quantified using ImageJ version 1.74 (National Institute of Health, USA)[72].

2.6. Protein extraction and Western blotting

Protein was extracted from patient and control cells using the radioimmunoprecipitation assay (RIPA) buffer extraction method (Appendix 3.2). Briefly, the cells were lysed and transferred to a 1.5mL microfuge tube; the cell lysate is centrifuged at 10000rpm at 4°C for 10min to pellet debris. The supernatant was transferred to a new 1.5mL microfuge tube and

stored at -80°C for future experiments. The protein concentration of each sample was determined using the Pierce BCA Protein Assay Kit (Thermo Fisher Scientific) according to the manufacturer's instructions.

The full length dystrophin is 427kDa in size and as such the Western blot technique required optimisation with respect to the protein transfer to the nitrocellulose membrane and visualisation of the protein. The optimal concentration of protein to use to obtain the best signal for the 427kDa full length dystrophin protein was also determined.

The results obtained indicated that the optimal conditions for the Western blot technique was to boil 100µg of protein with 5x loading dye (Appendix 2.3) at 90°C in a heating block (AccuBlock Digital Dry Bath; Labnet International, USA) for 5 min. The samples were separated onto a 6% polyacrylamide gel and transferred to a nitrocellulose membrane at 35V overnight at 4°C using the Mini-PROTEAN Tetra Cell system (Bio-Rad Laboratories, USA).

The membrane was washed with Tris-buffered saline containing tween-20 (TBST) and blocked using 10% (w/v) BSA (Sigma-Aldrich) in TBST for 1h at room temperature, followed by an overnight incubation with DYS2 (1:40; Leica Biosystems) and p38 (1:5000; Cell Signalling Technology) primary antibody, diluted in 5% (w/v) BSA in TBST, at 4°C. The following day the membrane was washed and incubated with the goat anti-mouse and goat anti-rabbit secondary antibodies (Bio-Rad), conjugated to horseradish peroxidase, for 1h at room temperature on a shaker. Membranes were visualised using the SuperSignal® West Pico chemiluminescent substrate (Thermo Fisher Scientific).

2.7. RNA isolation and cDNA synthesis

RNA was isolated from control and patient's cultured melanocytes and fibroblasts, at successive passages (p3-p8). RNA was extracted using the Roche HighPure RNA Isolation Kit (Roche Diagnostics, Switzerland), according to the manufacturer's instructions (Appendix 3.3). RNA quantity and quality was assessed using the ND-1000 NanoDrop Spectrophotometer (Thermo Fisher Scientific) and the ND-1000 software version 3.5.2 (Thermo Fisher Scientific). The integrity of the RNA samples was checked using agarose gel electrophoresis. Non-degraded RNA with a A260:280 ratio of 1.8-2.0 and a A260:230 ratio of 1.7-2.0 was used in complementary DNA (cDNA) synthesis.

cDNA synthesis was performed using the M-MLV reverse transcriptase (RT) (Promega, USA) according to a previously defined protocol (Appendix 3.4). Briefly, 1µg of total RNA and 61µM random oligonucleotides (University of Cape Town DNA Synthesis Service, South Africa) was combined with sterile distilled water, to a total volume of 10.5µL and incubated at 70°C for 5min. This is followed by the addition of the master mix (Table 2.4) and 1µL M-MLV

RT, to all tubes except the no RT control, to a total volume of 20µL. Total reaction is incubated at 42°C for 1h and stored at -20°C for future experiments.

Table 2.4. Composition of cDNA master mix.

Reagent	Final Concentration	Volume per reaction	Supplier
10mM dNTP	1mM	2µL	Promega
25mM $MgCl_2$	2.5mM	2µL	
5x RT Buffer	1x	4µL	
RNase inhibitor (40u/µL)	1u/µL	0.5µL	

To demonstrate that cDNA synthesis occurred PCR amplification of *GAPDH* (reference gene) was performed on all samples. The PCR was performed using the *GAPDH* primers used for quantitative PCR (qPCR).

2.8. Quantitative PCR

qPCR analysis of dystrophin gene expression in control melanocytes and fibroblasts was investigated in order to determine which dystrophin isoforms were expressed by each cell type, and whether a difference existed in expression across passages and between primary cell cultures. Analysis of expression was performed using the Applied Biosystems StepOne Plus Real-time PCR system (Life Technologies) and the PowerUp™ SYBR® Green Master Mix (Thermo Fisher Scientific).

DMD qPCR primer sequences (Appendix 4.1) were obtained from Zatti et al and synthesised by Integrated DNA Technologies (IDT, USA). The primers target various isoforms of the *DMD* gene namely the full length muscle isoform (Dp427M), the retinal isoform (Dp260) and the ubiquitous isoform (Dp71) of dystrophin. Primers which amplify fragments corresponding to the full length *DMD* transcript were also included as a control and amplified exon junctions 9 to 10, 25 to 26 and 34 to 35.

Tyrosinase expression in melanocytes was quantified to determine whether there was a link between the differentiation status of melanocytes and their dystrophin expression. Tyrosinase, the rate-limiting enzyme for melanin synthesis, was chosen as there is a close relationship between melanin production and the differentiation status of the cells[73].

Gene expression analysis was performed using the standard curve method, which provides the relative quantities of the target mRNAs. Standard curves were prepared for each primer pair, using serial dilutions of pooled sample cDNA (Fig. 2.2).

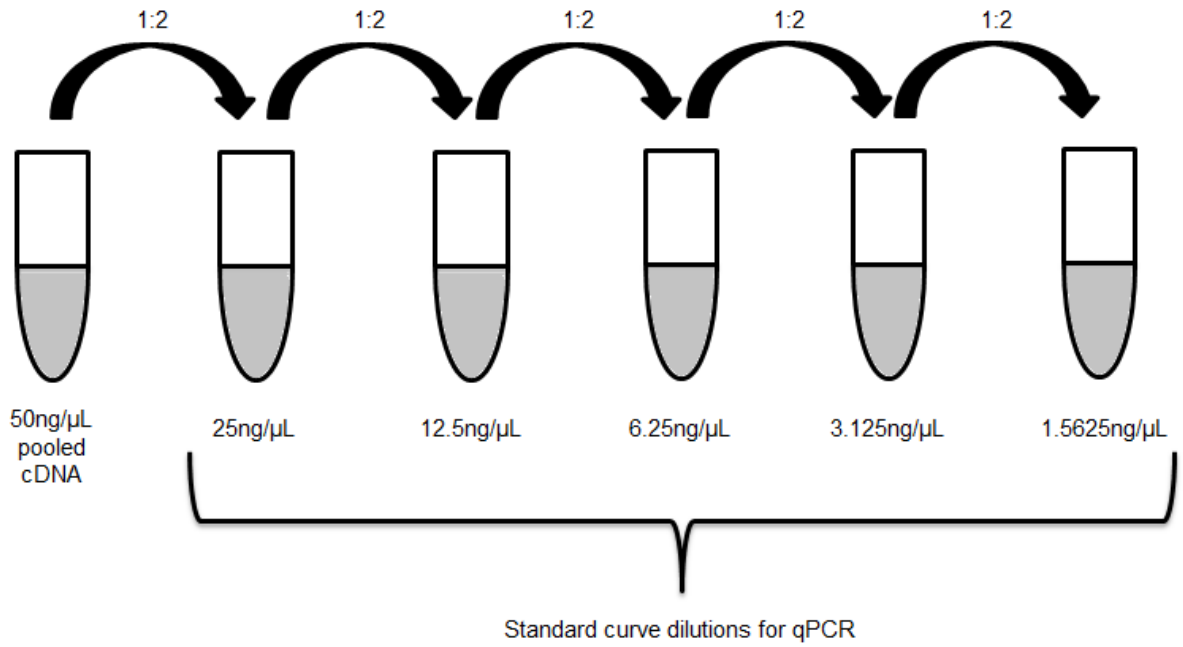

Figure 2.2. Preparation of standard curve for standard curve method. cDNA was diluted 1:2, using sterile distilled water. Initial concentration of cDNA samples = 50ng/µL.

PCR cycling conditions for all primer pairs, excluding dystrophin exon junction 9-10 (EJ9-10), were as follows: an initial denaturation step of 95°C for 10min, followed by 40 cycles of 95°C for 15 seconds and 60°C for 1min. For the EJ9-10 primer pair the annealing temperature was changed to 65°C for 1min. QPCR reactions were performed in technical triplicate on at least three biological replicates and the genes of interest expression was normalised to *GAPDH* (Appendix 4.1; IDT, USA) and *GUSB* (Qiagen, Germany), as these reference genes were found to be stably expressed in melanocyte and fibroblasts using the bioinformatics tool BestKeeper version 1 (www.gene-quantification.com/bestkeeper.html)[74]. The components of the qPCR reaction can be found in table 2.5.

Table 2.5. qPCR reaction composition.

Component	Final Concentration	Volume per reaction	Volume per reaction*
2x PowerUp™ SYBR® Green Master Mix	1x	5µL	5µL
Forward Primer (10µM)	0.2µM	0.1µL	1µL
Reverse Primer (10µM)	0.2µM	0.1µL	-
adH_2O	-	3.8µL	3µL
cDNA (10ng/µL)	1ng/µL	1µL	1µL
Total Volume		10µL	10µL

*Composition of qPCR reaction for *GUSB,* as forward and reverse primers are combined.

2.9. cDNA sequencing and Mutation analysis

2.9.1. Nested-PCR of *DMD* gene

Nested-PCR was performed on the patient and control individual cDNA from both cell types. Due to the large size of the *DMD* transcript, the cDNA was amplified in ten overlapping fragments (Fig 2.3) using the Leiden PTT primer sets (Appendix 4.2, www.dmd.nl). The second primer set targeted a region within the product of the primary PCR reaction, thereby increasing the specificity of primer binding to the target gene and increasing product yield (Fig. 2.4).

As the nested-PCR was designed for use on muscle cDNA, amplification of cDNA from cultured melanocytes and fibroblasts required optimisation, owing to the difference in *dystrophin* expression levels. The PCR was optimised on cDNA from cultured control melanocytes. The original protocol, for muscle biopsy samples, utilised no $MgCl_2$ in the reaction and was performed using 20 cycles. The original PCR reaction was compared to reactions containing $MgCl_2$ performed using 20 cycles and 40 cycles as well as a 40 cycle reaction containing no $MgCl_2$. The decision to test 40 cycles was made based on a previous qPCR finding that theDp427M isoform of dystrophin only amplified after 30 cycles in fibroblast samples. Only the reaction which contained $MgCl_2$ and was performed using 40 cycles successfully amplified the products. These conditions were chosen for all future PCR reactions and all reactions were prepared as shown in Table 2.6.

The following cycling conditions were used for both the primary and secondary PCR reactions: activation of polymerase at 95°C for 5 min; initial denaturation at 94°C for 5 min, followed by 40 cycles of 94°C for 40s, 60°C for 40s, 72°C for 2 min; and a final elongation step at 72°C for 5 min.

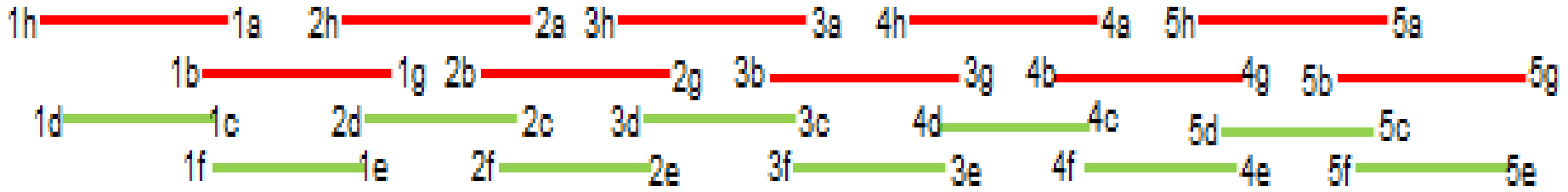

Figure 2.3. Illustration of primer combination for the amplification of the *DMD* transcript. The black line represents the *DMD* transcript. The red lines represent the fragments generated during the primary PCR reaction, whereas the green lines represent the fragments generated from the secondary PCR reaction. Primer sets h-a and b-g (red) represent the outer primer sets, while d-c and f-e represent the nested primer sets (green). The d-c primer set binds to the h-a PCR products while the f-e primer sets bind to the b-g PCR products.

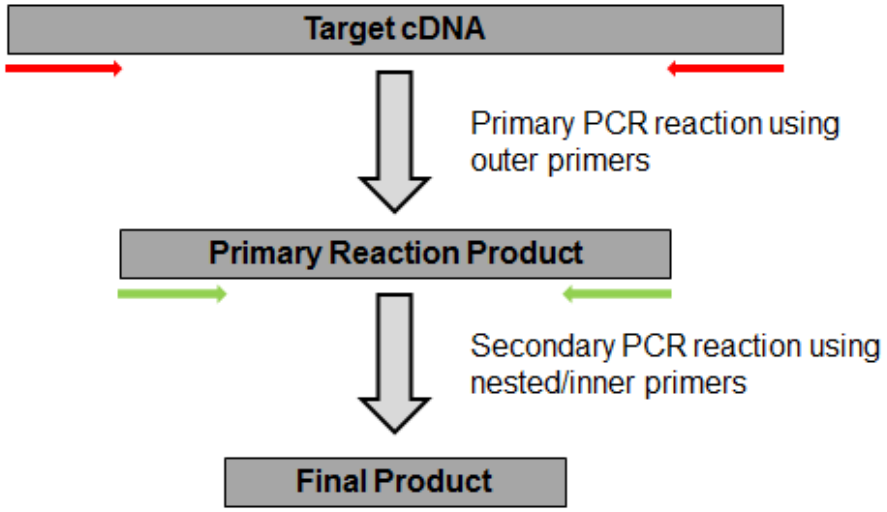

Figure 2.4. Illustration of the Nested-PCR. Red Arrows indicate the outer primer set used in the first PCR and green arrows indicate the nested primer set used for the second PCR.

Secondary PCR products were electrophoresed on a 1% agarose gel at 80V for 45min and visualised using SYBR® Safe DNA stain (Invitrogen, USA) on the TS-302 Transilluminator (Spectroline, USA). Images of the agarose gels were taken using the EOS 1200D Camera (Canon) and the EOS Utility 2 software, version 2.14.0.0 (Canon).

Table 2.6. Nested-PCR reaction composition.

Component	Manufacturer	Final Concentration	Primary PCR reaction volume	Secondary PCR reaction volume
5x GoTaq Buffer	Promega	1x	5µL	5µL
10mM dNTP mix	Promega	0.2mM	0.5µL	0.5µL
GoTaq Hotstart polymerase (5U/µL)	Promega	0.04U/ µL	0.2µL	0.2µL
25mM $MgCl_2$	Promega	1.9mM	2µL	2µL
Forward Primer (10µM)	IDT	0.4µM	1µL	1µL
Reverse Primer (10µM)	IDT	0.4µM	1µL	1µL
adH_2O	-	-	14.5µL	15.3µL
Template	-	-	1.8µL [a]	1µL [b]
Total volume			26µL	26µL

[a] Template used in primary PCR is total cDNA. [b] Template used in secondary PCR is PCR product of the primary PCR reaction.

Post-PCR clean-up was done using the NucleoFast® 96 PCR clean-up kit (Macherey-Nagel, Germany) according to manufacturer's instructions. Cycle sequencing was performed using the BigDye Terminator v3.1 cycle sequencing kit (Thermo Fisher Scientific) according to standard methodologies. After cycle sequencing the samples were treated with SDS, transferred to Sephadex columns (Princeton Scientific, USA) and centrifuged to remove unincorporated fluorescently labelled dideoxynucleotides (ddNTPs). The cleaned sequencing reaction products were dried and resuspended in Hi-Di (Thermo Fisher Scientific). Prior to electrophoresis on the 3130xl Genetic Analyser (Thermo Fisher Scientific), the samples were denatured for 2 min at 95°C and cooled to 4°C. Electrophoresis was performed on the Applied Biosystems 3130xl genetic analyser (Thermo Fisher Scientific) using the 50cm capillary array and POP7^{TM} polymer run module.

2.9.2. Mutation identification and bioinformatic analysis

Cycle sequencing output files were compared to the Dp427M coding sequence reference for dystrophin, GenBank Reference Sequence file NM_004006.2. The sequences were aligned to form one contiguous sequence using the MEGA5 sequence alignment software version 5.02 (www.megasoftware.net)[75], in order to detect the disease-causing mutations.

Point/small mutations were identified using novoSNP (www.molgen.ua.ac.be/bioinfo/novosnp)[76]. The novelty of the identified point/small mutations was determined based on a literature search, the Leiden Open Variation Database (LOVD, http://www.dmd.nl)[36], the single nucleotide polymorphism database (dbSNP) and Ensembl Variant Effect Predictor (www.ensembl.org)[77]. The predicted pathogenicity of the novel point/small mutations found was determined *in silico* using MutationTaster (www.mutationtaster.org/)[78] and Protein Variation Effect Analyzer (PROVEAN; http://provean.jcvi.org/)[79].

2.10. Statistical Analysis

GraphPad Prism v5.0 (GraphPad Software, San Diego, California, United States) was employed to analyse the data obtained.

The fluorescent quantification data was analysed by the Two-way Analysis of Variance (ANOVA) and Bonferroni post-test algorithm to determine whether there was a significant difference in fluorescence across passages for melanocytes and fibroblast, respectively and to determine whether there was a significant difference in fluorescence between melanocytes and fibroblasts at matched passages.

Similarly, the qPCR data was analysed by two-way ANOVA and Bonferroni post-test algorithm to determine whether there was a significant difference in *dystrophin* expression across passages for melanocytes and fibroblast, respectively, and to determine whether there was a significant difference in expression between melanocytes and fibroblasts at matched passages.

Expression of the Dp260 isoform of dystrophin and *tyrosinase* was analysed by means of the one-way ANOVA and Bonferroni post-test algorithm.

Chapter 3: Results

3.1. Culture and characterisation of melanocyte and fibroblast primary cultures

The outline of the generation of the matched melanocyte and fibroblast primary cultures isolated from the different individuals used for this study can be found in figure 3.1. The earliest passage used in this study was passage 3, for melanocytes and fibroblasts.

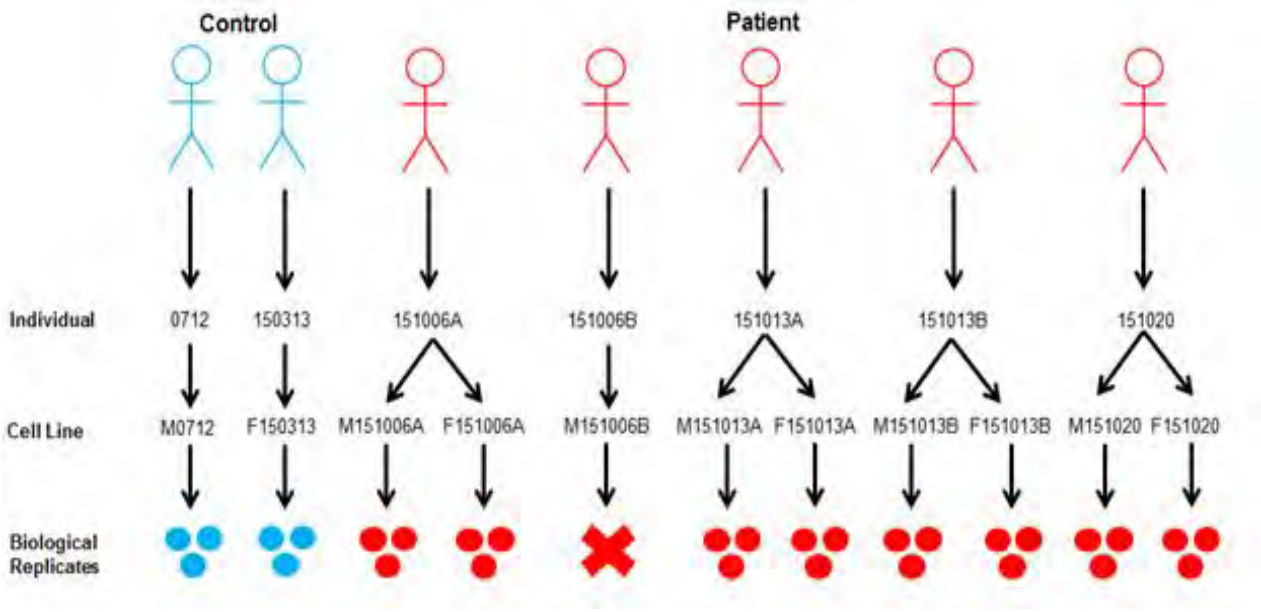

Figure 3.1. Outline of melanocyte and fibroblast cell line generation. The number of biological replicates from each primary culture is represented by the number of dots. The 'X' represents a primary culture that was lost due to a recurring bacterial infection. Biological replicate refers to cells obtained from the same initial culture, passaged and split into replicates which were then cultured separately. Individuals were named according to the date the samples were collected, with an identifier A or B if more than one patient provided a sample the same day. The letter M prior to the individual name denotes a melanocyte culture, while F denotes a fibroblast culture.

3.1.1. Morphology of primary human skin cells and C2C12 mouse myoblasts

Primary cells were initially isolated and cultured from neonatal foreskin samples, in order to become acquainted with the different cell types (melanocytes and fibroblasts) and cell culture methodology (HREC REF 493/2009). The method of cell isolation and propagation differs between melanocytes and fibroblasts due to their respective localisation in the epidermal and dermal layers of the skin. Initial processing of the epidermis (see Methods section 2.3.1) to isolate the melanocytes, denoted p0, yielded a mixed culture containing melanocytes and keratinocytes with accompanying fibroblast contamination (Fig. 3.2A). Pure melanocyte cultures were obtained and maintained for the duration of the study, after passaging the cells over a course of 10 days (Fig. 3.2B). Isolation of fibroblasts from the dermis yielded pure cultures, denoted as p0 (Fig. 3.2C). Morphologically the two cell types were quite distinct. The majority of melanocytes exhibited a bipolar, dendritic phenotype, although some

multipolar cells were observed (Fig. 3.2B). Fibroblasts appeared elongated and spindle-shaped in culture (Fig. 3.2C). Interestingly, the patient melanocytes were multipolar and highly dendritic (Fig. 3.3A) compared to the foreskin-derived control melanocytes which were bipolar in culture (Fig. 3.3B). Images were taken using the Axiovert 200M inverted fluorescence microscope (Carl Zeiss Microscopy), AxioCAm HRm camera (Carl Zeiss Microscopy) and the AxioVision 4.8 software (Carl Zeiss Microscopy) or the Evos XL Care microscope (Life Technologies).

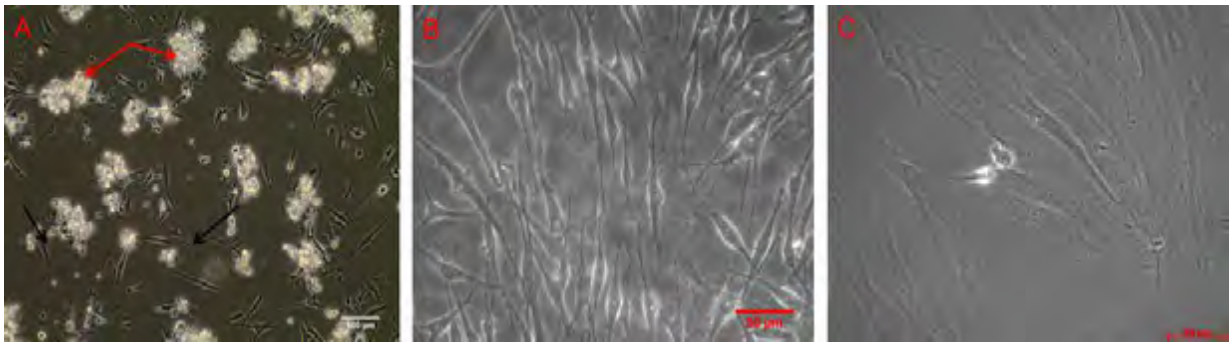

Figure 3.2. Morphology of primary melanocytes and fibroblasts. A – Melanocyte culture at p0. Red arrows indicate clusters of keratinocytes and black arrows indicate fibroblasts. B – Pure culture of melanocytes displaying both multipolar and bipolar growth. C – Pure culture of fibroblasts. Image A was taken at 200x magnification, images B and C were aquired at 400x magnification. Scale bar of image A = 100µm, scale bars of images B and C = 50µm.

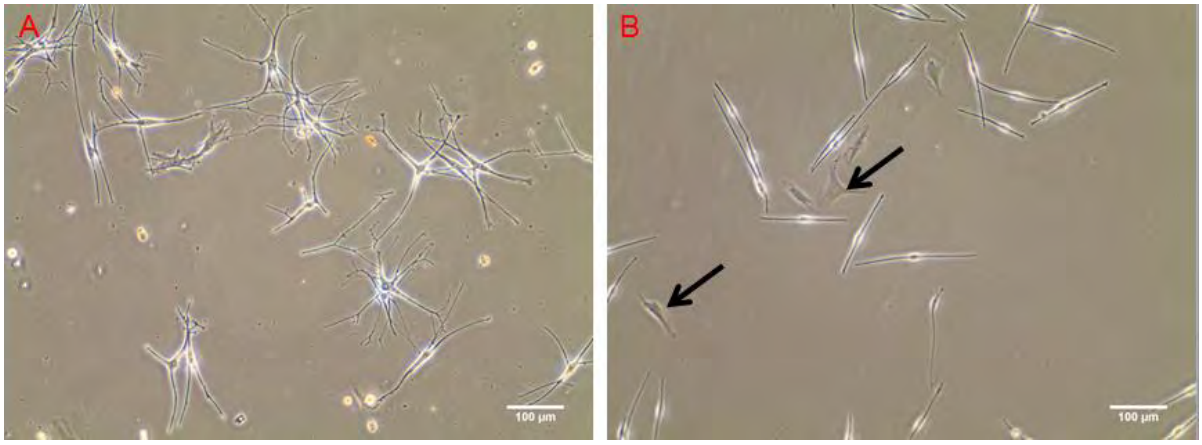

Figure 3.3. Morphological differences between patient and control melanocytes. A – Phase contrast image of primary patient melanocytes (p1) displaying multipolar and dendritic growth. B – Phase contrast image of foreskin-derived control melanocytes (p2) displaying regular bipolar growth. Arrows indicate the presence of fibroblasts. Images were aquired at 200x magnification. Scale bars = 100µm.

C2C12 mouse myoblasts were cultured as a positive control for use in immunocytochemical and Western blotting analysis of dystrophin. The C2C12 myoblasts, similarly to fibroblasts appear spindle-shaped (Fig. 3.4A); however, once grown to confluency the cells begin to form multinucleated myotubes in culture (Fig. 3.4B). Differentiation of the myotubes was enhanced by culturing the cells in DMEM supplemented with 2% FCS instead of the usual 10% FCS. Images were taken using the Evos XL Care microscope (Life Technologies).

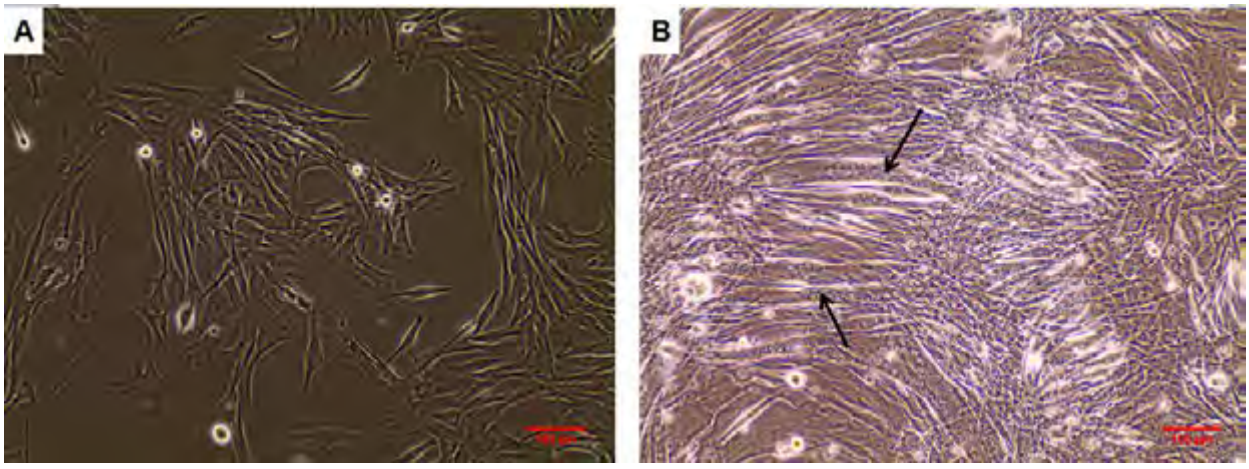

Figure 3.4. Morphology of C2C12 cells, pre- and post-differentiation. A – C2C12 cells prior to differentiation displaying a spindle shaped morphology. B – Differentiated C2C12 cells, with arrows indicating myotube formation. Images were aquired at 200x magnification. Scale bars = 100µm.

3.2. Immunological confirmation of dystrophin protein expression in skin

3.2.1. Immunohistochemistry (IHC)

To determine the functionality and optimal working concentrations of the dystrophin antibodies, IHC was performed on frozen rat muscle sections, expected to express the full length dystrophin protein. A no-primary only control, which omits the primary antibody, was included in order to ensure that the signal observed was not due to non-specific binding of the secondary antibody. No reactivity on the periphery of the muscle fibres was observed, indicating absence of non-specific binding of the secondary antibody (Fig. 3.5D). Positive staining for dystrophin, seen as bright red signal on the periphery of the muscle fibres, was observed for the muscle sections. It was also noted that the DYS1 (Leica Biosystems) and DYS2 (Leica Biosystems) antibodies produced better staining of the muscle sections than the DYS3 antibody (Leica Biosystems; Fig. 3.5).

After optimisation using rat muscle, frozen human foreskin sections were stained to determine whether dystrophin expression could be detected in skin sections. As the DYS1 antibody was discontinued by the suppliers and the DYS3 antibody was previously shown to display weak staining on muscle tissue, all subsequent immunohistochemistry was conducted using the DYS2 antibody.

Sections displayed some reactivity to the DYS2 dystrophin antibody in the dermis of the skin (Fig. 3.6A), however, this signal appeared to be due to non-specific binding of the secondary antibody, as the control samples (with primary antibody omitted) displayed a similar staining pattern (Fig. 3.6B).

All images were taken using the Axiovert 200M inverted fluorescence microscope (Carl Zeiss Microscopy), AxioCAm HRm camera (Carl Zeiss Microscopy) and the AxioVision 4.8 software (Carl Zeiss Microscopy).

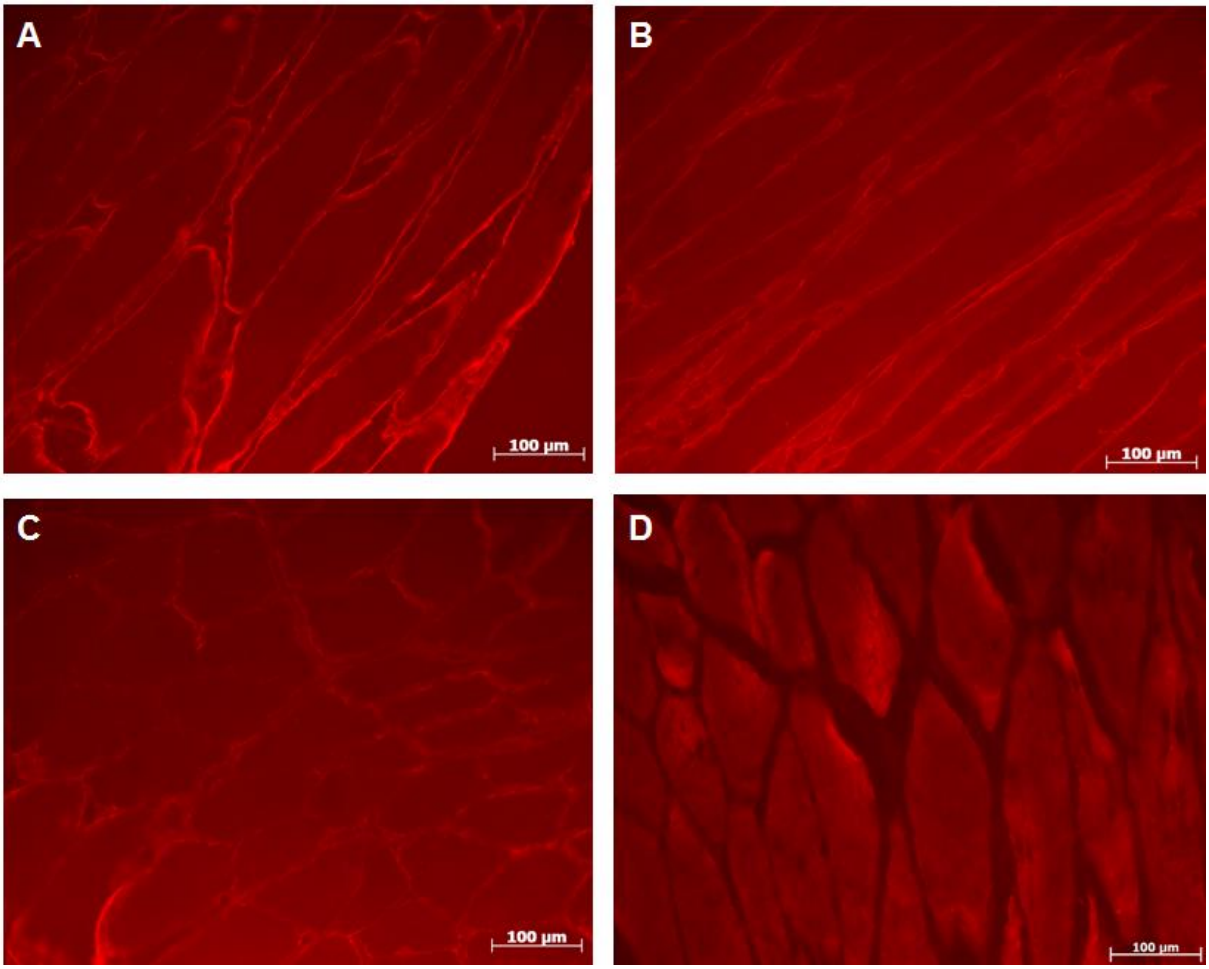

Figure 3.5. Staining of wildtype rat muscle for the presence of dystrophin. A-C – Muscle stained using DYS1, DYS2 and DYS3 antibodies, respectively, each displaying positive staining for dystrophin. D – Antibody control (primary antibody omitted). Images taken at 200x magnification. Scale bars = 100µm.

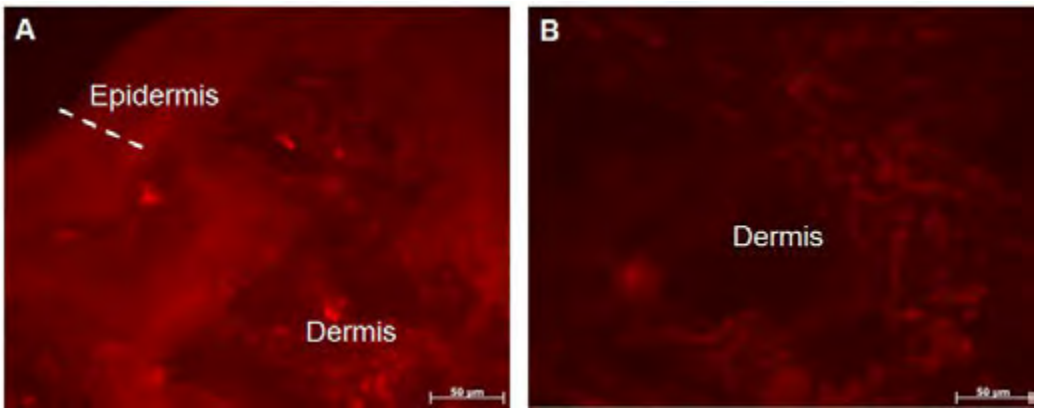

Figure 3.6. Staining of wild type foreskin sections for the presence of dystrophin. A – Skin stained using DYS2 antibody. The dotted line demarcates the epidermis. B – No primary antibody control. The entire field of view consists of the dermis. Images taken at 400x magnification. Scale bars = 50µm.

3.2.2. Immunocytochemistry (ICC)

The staining protocol for immunocytochemistry was optimised using the C2C12 myoblast cells and cultured human foreskin-derived melanocytes. Optimisation of the staining procedure was performed to determine the optimal dilutions for the dystrophin antibodies and to determine what was causing the formation of crystal-like artefacts on the slide as well as the damage to the cells.

A comparison between TBS and PBS wash buffers was performed in order to ascertain whether this affected the staining procedure. In brief, the cells were washed using either TBS or PBS, fixed using ice cold 100% methanol and washed again using the same wash buffer. The cells were then stained with Hoechst, mounted onto slides and viewed using the Axiovert 200M inverted fluorescence microscope (Carl Zeiss Microscopy). It was found that the TBS wash buffer resulted in the formation of the crystal-like artefacts, whereas PBS produced a clear image of the cells (Fig. 3.7A).

Next, the fixatives were compared to one another to find out whether the fixatives were the source of the cell damage. Fixation using ice cold 100% methanol for 5 minutes was compared to fixation using 4% PFA for 5 minutes followed by ice cold 100% methanol for 5 minutes. It was observed that the methanol alone resulted in the cells shrivelling (Fig. 3.7B); whereas the PFA and methanol combination produced healthy-looking cells (Fig. 3.7C).

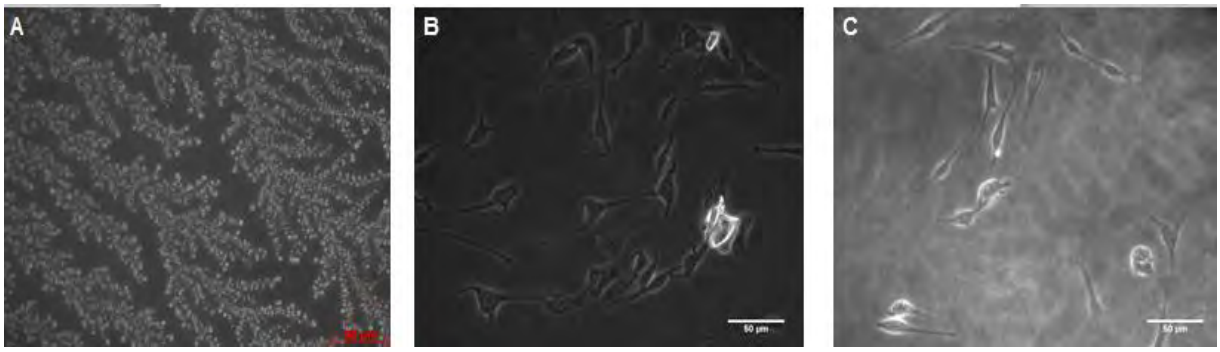

Figure 3.7. Optimisation of dystrophin immunocytochemistry. A – Crystal-like artefact seen on slides after washing cells with TBS. B – Melanocytes fixed using ice cold 100% methanol. C- Melanocytes fixed using PFA and methanol. Images taken at 200x magnification. Scale bars = 50µm.

C2C12 cells were stained as a positive control for dystrophin expression. Similar to the immunohistochemistry results on muscle tissue, the cells displayed strong reactivity with the DYS1 and DYS2 antibodies, but not the DYS3 antibodies (Fig. 3.8). As the DYS2 antibody appeared to produce the best signal, it was confirmed as the antibody of choice for future staining. Melanocytes and fibroblasts were then stained across a range of successive passages (p3-p8) in order to confirm dystrophin expression as well as to determine whether this expression varied across passages.

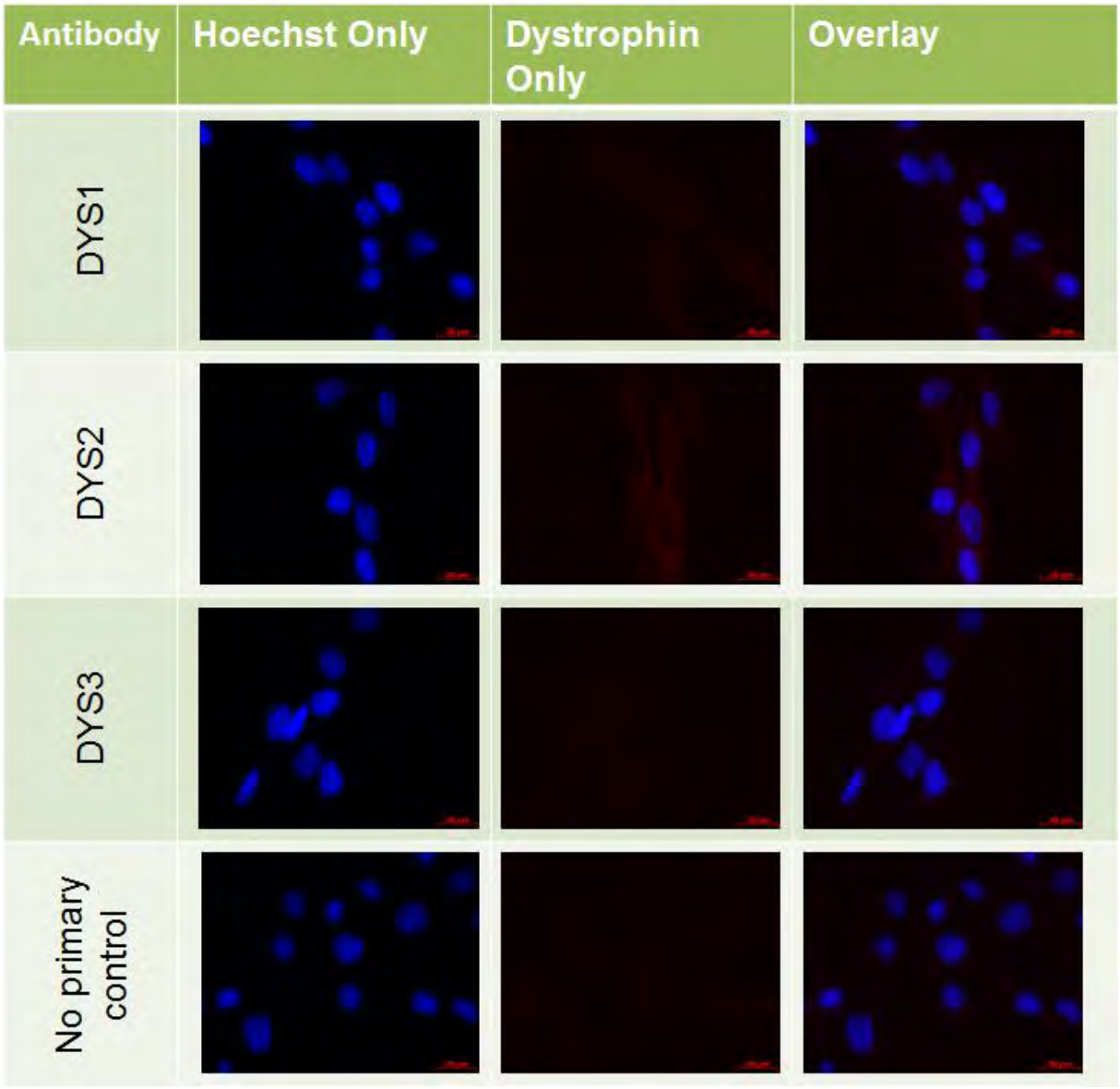

Figure 3.8. Staining of C2C12 cells for dystrophin. Antibody column - Cells stained with the primary antibodies DYS1, DYS2, DYS3 respectively and secondary antibody only (no primary control). Images taken at 1000x magnification. Scale bars = 20µm. Nucleus = blue and dystrophin = red.

The staining of the control melanocyte (Fig. 3.9) and fibroblast (Fig. 3.10) cultures revealed differential expression of dystrophin across passages for both cell types. In melanocytes the fluorescent staining suggested a passage dependent increase in expression of dystrophin from p3 to p5 (Fig. 3.9). Subsequently the expression seemed to decrease dependently from p6 to p8, with p7 and p8 appearing to have almost no expression.

Fibroblasts displayed a very different staining pattern of dystrophin expression compared to melanocytes. Dystrophin appeared to be present in fibroblasts at passages 4, 6, 7 and 8 and absent in p3 and p5, with the strongest expression present at p4.

Fluorescent quantification of the dystrophin expression observed for both the melanocytes and fibroblasts (Fig. 3.11 and Table 3.1) confirmed that dystrophin was expressed across all

passages for both cell lines. Interestingly, the fluorescence for melanocytes also displayed a significant increase in fluorescence up to p5 followed by a decrease to p8. Melanocytes at p5 were found to have significantly higher fluorescence than the melanocytes at p3 and p6 to p8 (Fig. 3.11A). No significant difference was observed between p4 and p5, which displayed the highest level of dystrophin expression (Table 3.1 and Fig. 3.11A).

Table 3.1. Quantification of fluorescence in melanocytes and fibroblasts measured in RFU*.

Passage Number	Melanocytes*	Fibroblasts*
3	1.775	0.125
4	2.342	6.224
5	4.367	0.539
6	1.455	3.854
7	0.638	2.993
8	0.580	0.680

*Quantification provided as relative fluorescent units (RFU), using the average fluorescence of 3 cells.

Quantification of fibroblast fluorescence indicated a more sporadic pattern of expression with an increase in fluorescence from p3 to p4, followed by a decrease at p5, followed by an increase at p6 and a further decrease from p7 to p8. Statistically, fibroblasts at p4 displayed significantly higher fluorescence compared to fibroblasts at p3, p5, p7 and p8. No significant difference was observed between p4 and p6 fluorescence levels although p4 had higher levels of fluorescence, confirming that dystrophin protein expression was highest in fibroblasts at p4 or p6.

A comparison of expression between melanocytes and fibroblasts indicated that fibroblasts exhibit peak fluorescence, and hence dystrophin expression, at p4. In turn, melanocytes reach their peak expression at p5 (Fig. 3.11B).

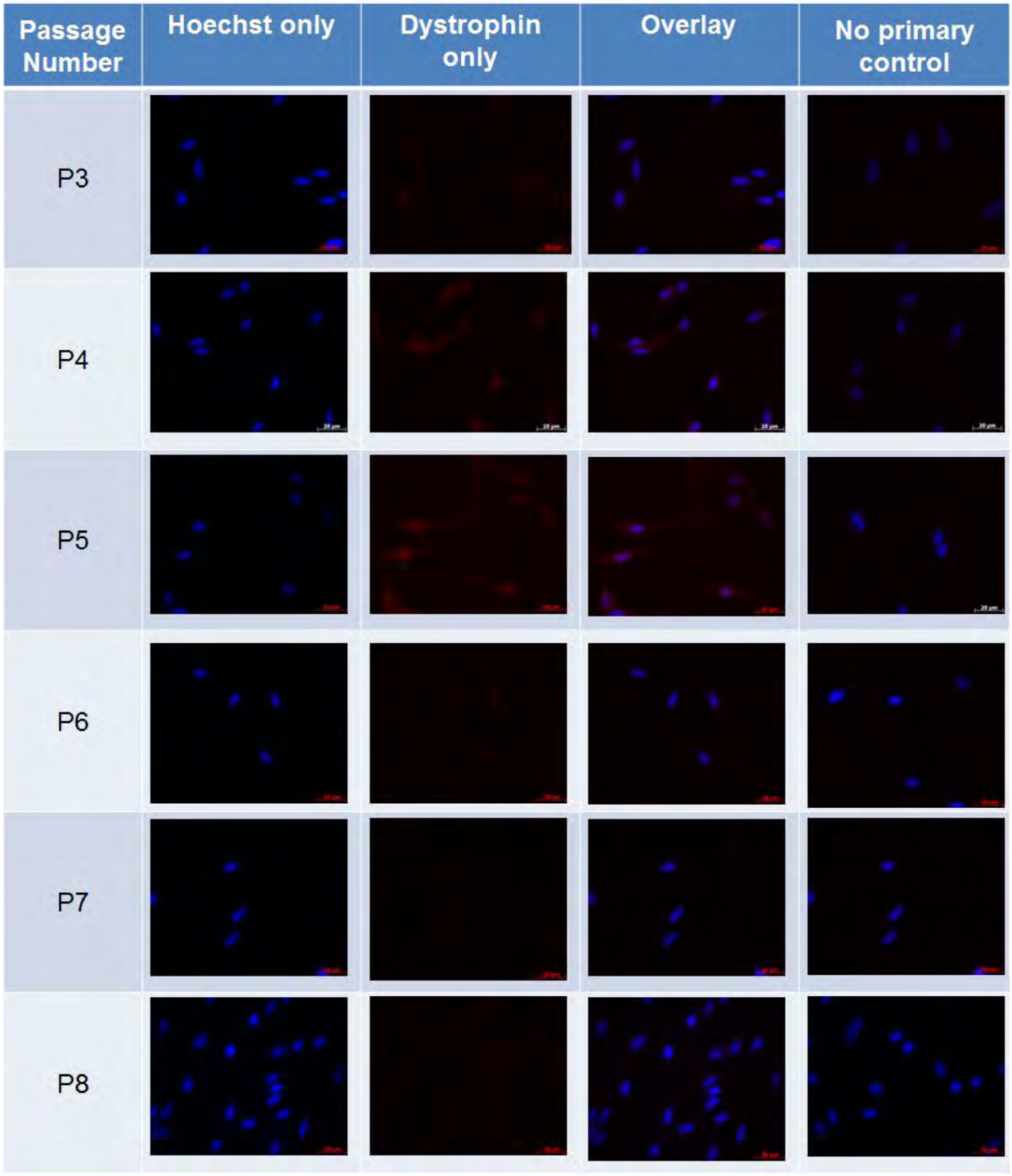

Figure 3.9. Positive staining of control melanocytes for dystrophin across successive passages. All cells were stained with the primary antibody DYS2 as well as secondary antibody. Rows p3-p8 represents the passage numbers at which the image was taken. The no primary control column represents the cells stained only using the secondary antibody. Images taken at 1000x magnification. Scale bars = 20μm. Nucleus = blue and Dystrophin = red.

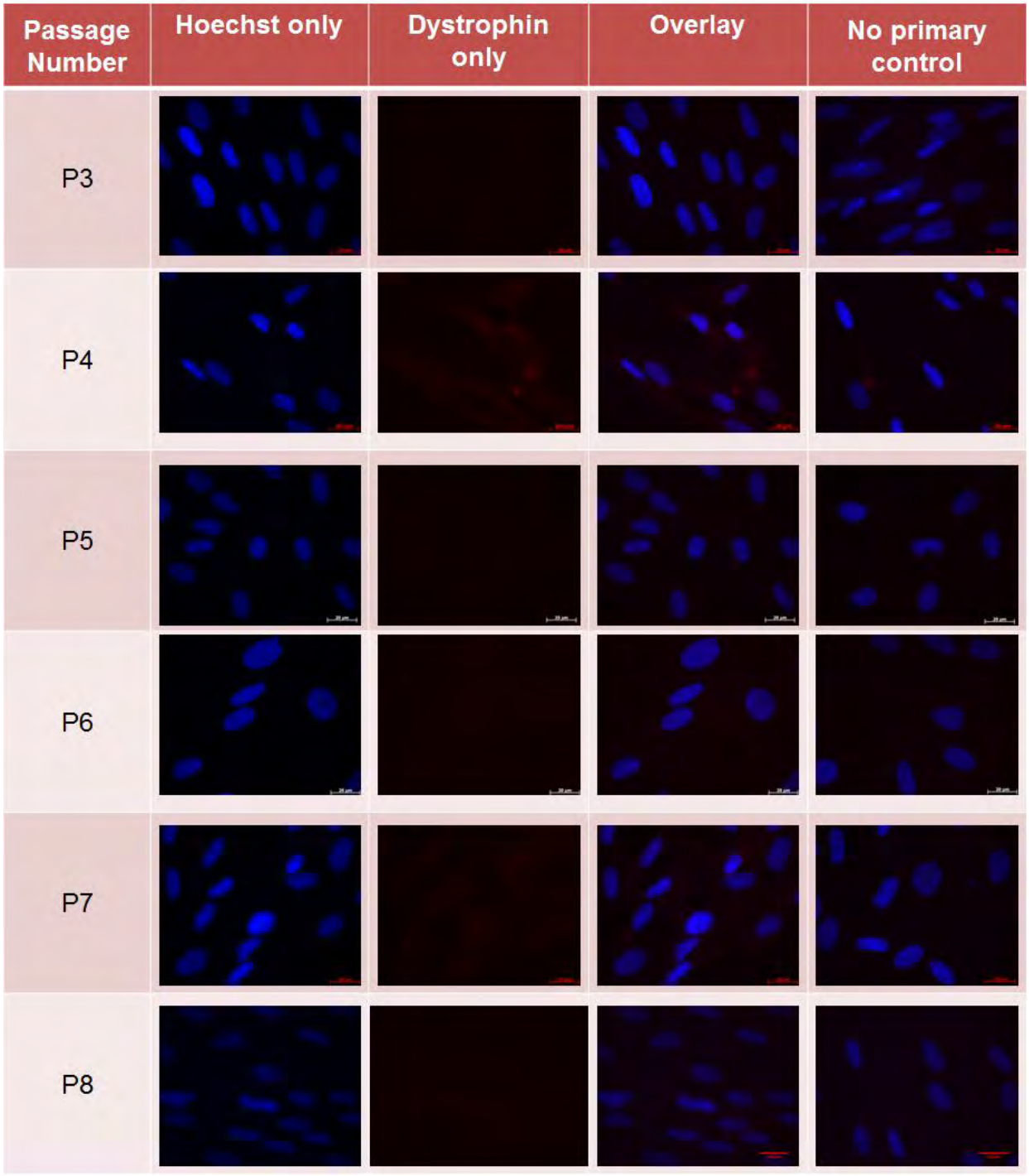

Figure 3.10. Positive staining of control fibroblasts for dystrophin across successive passages. All cells were stained with the primary antibody DYS2 as well as secondary antibody. Rows p3-p8 represents the passage numbers at which the image was taken. The no primary control column represents the cells stained only using the secondary antibody. Images taken at 1000x magnification. Scale bars = 20µm. Nucleus = blue and Dystrophin = red.

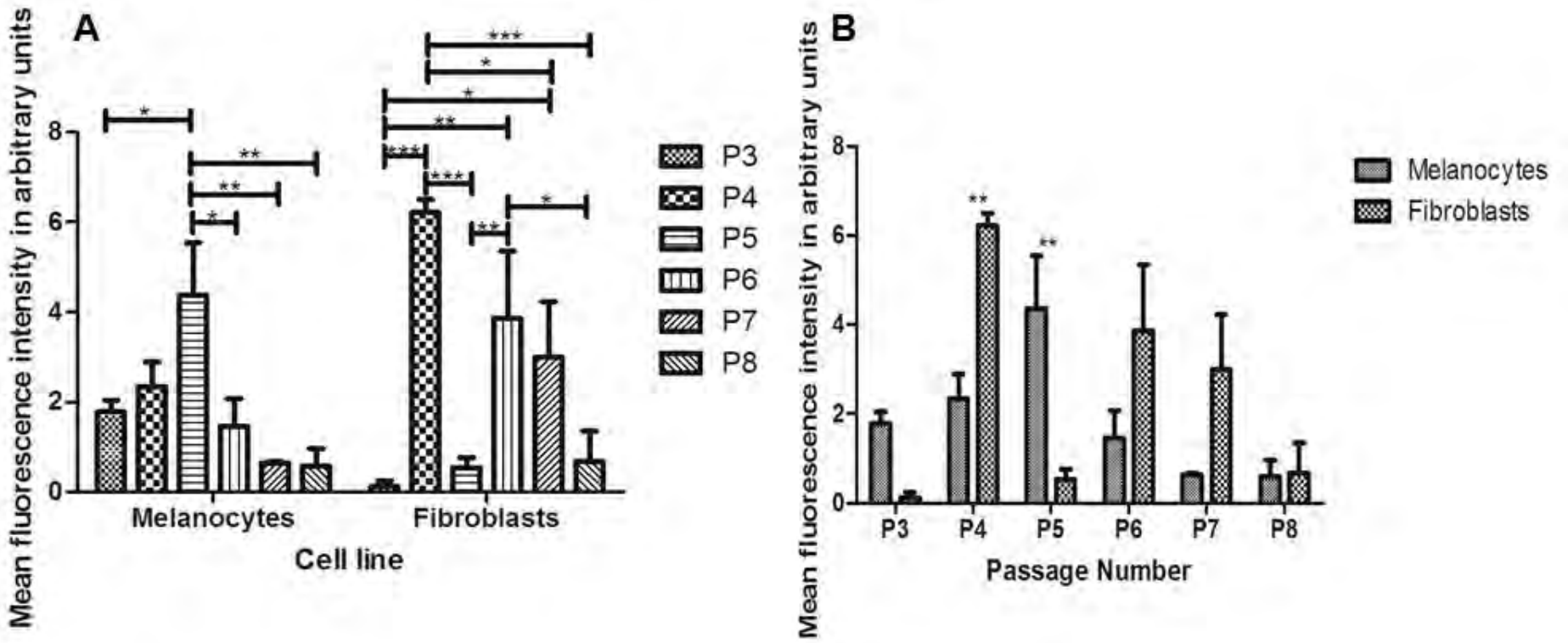

Figure 3.11. Quantification of immunofluorescence of melanocytes and fibroblasts. A – Comparison of fluorescence across passages for each cell line. B – Comparison of fluorescence between melanocytes and fibroblasts at matched passage numbers. * = $p \leq 0.05$, ** = $p \leq 0.01$, *** = $p \leq 0.001$. Error bars represents the standard error of the mean (SEM). n=3.

3.2.3. Dystrophin Western Blot analysis

The full length dystrophin is 427kDa in size, which presented a challenge in optimising the Western blot technique with respect to protein transfer from the gel to the nitrocellulose membrane to and visualise of the protein.

Transfer times of 6h, 8h and 16h (overnight) were attempted, using protein extracted from the C2C12 mouse myoblasts (positive control). It was observed that the shorter transfer times of 6 and 8h did not transfer proteins larger than 270kDa. Larger proteins of up to 460kDa were only successfully transferred after 16h as seen by the Ponceau S stained membrane (Fig. 3.12).

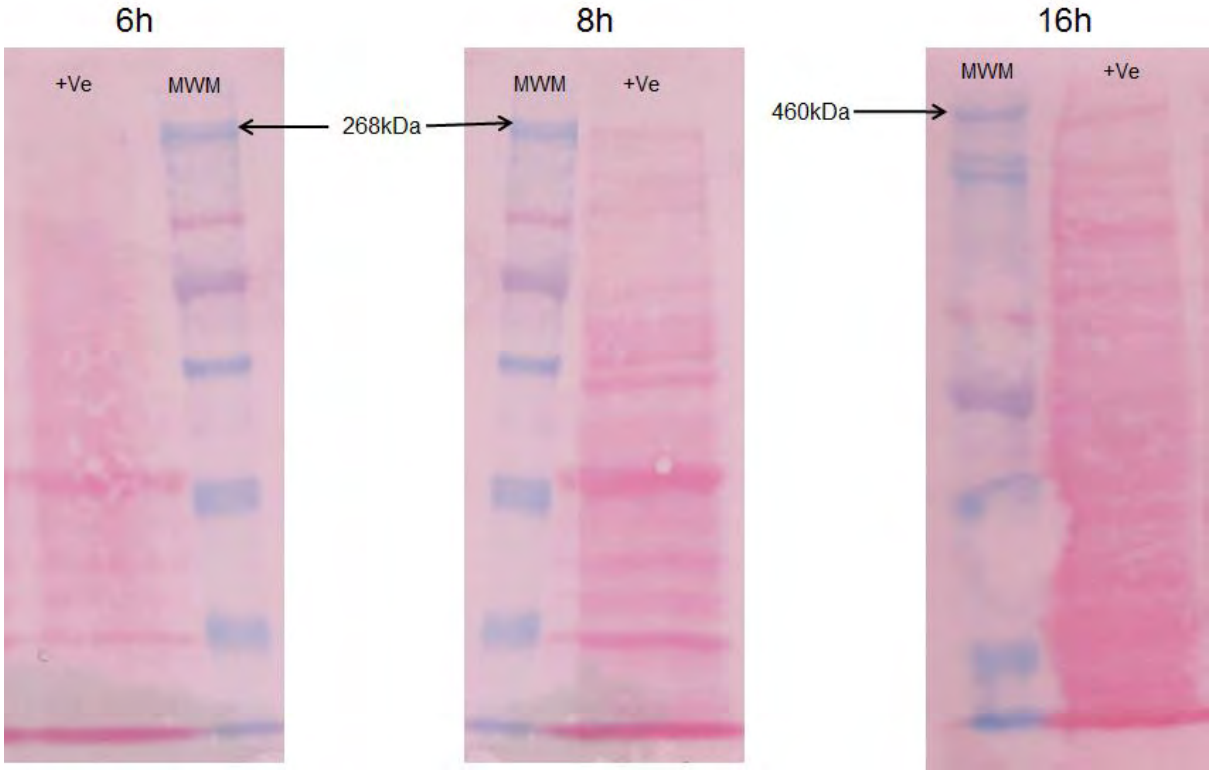

Figure 3.12. Ponceau S stained nitrocellulose membranes after 6, 8 and 16h transfers. MWM = molecular weight marker. +Ve = protein extracts from C2C12 myoblast cells; positive control.

Protein extracted from the C2C12 myoblast cells was used to perform a protein concentration gradient ranging from 100µg to 20µg in order to determine which concentration yielded the best signal for the 427kDa muscle isoform of dystrophin. One hundred micrograms of protein produced the best signal, while 20µg proved to be too low for detection (Fig. 3.13B), after 1h 30min exposure of the blot to the x-ray film.

Based on this, it was decided to use a protein concentration of 100µg for all future experiments despite the high level of background signal present on the blot for 100µg, 80µg

and 50µg (Fig. 3.13A). In an attempt to reduce this background signal, a comparison between BSA and fat free UHT milk (Parmalat, Italy) blocking solutions was performed.

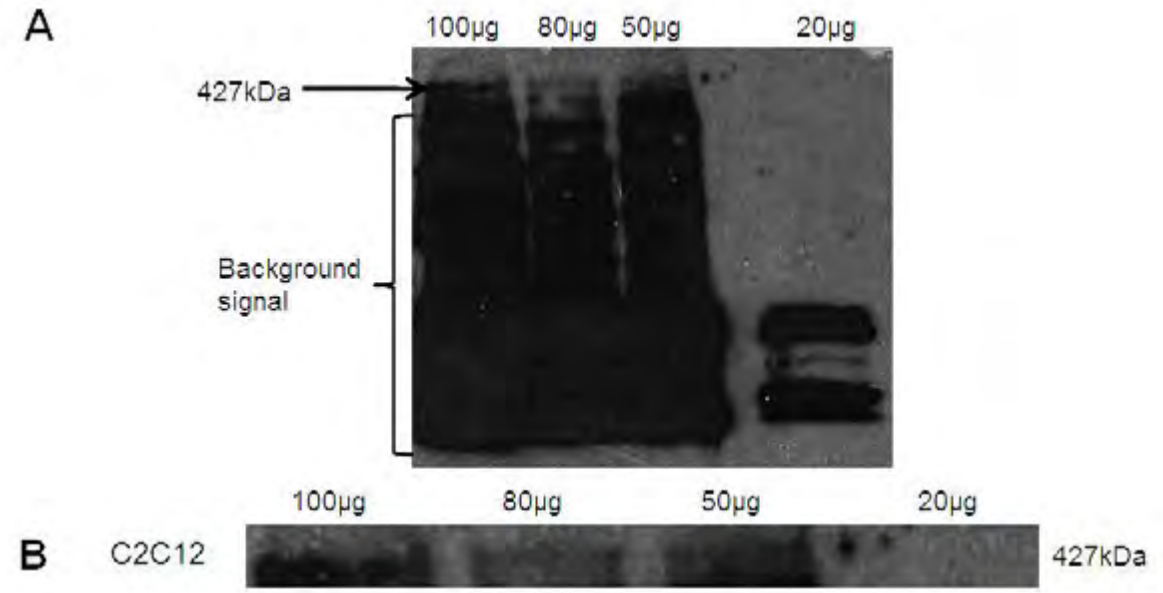

Figure 3.13. Western blot protein gradient using protein extracted from C2C12 cells. A – Image of entire blot with arrow indicating where the 427kDa dystrophin protein should be located and bracket indicating the background signal. B – Enlarged image of the area indicated by the arrow in A.

Briefly, blocking solutions of 15% BSA in TBST as well as 5% milk in TBST and 100% milk were utilised to determine whether changing the blocking solution could remove the background signal in the blots. A comparison between the blocking solutions displayed a marked decrease in the background signal, although bands between 71kDa and 55kDa were observed for all of the blocking solutions. The 427kDa isoform of dystrophin could not be detected on the blots (Fig. 3.14)

The absence of the 427kDa protein isoform in the positive control was thought to be due to over blocking of the membrane. Therefore all future Western blot experiments included 10% BSA in TBST blocking solution, as per the original method. However, subsequent attempts at detection of the full length 427kDa dystrophin isoform were not highly reproducible. It was hypothesised that the inadequate or absent signal was likely a result of incomplete transfer of the protein due to its large size.

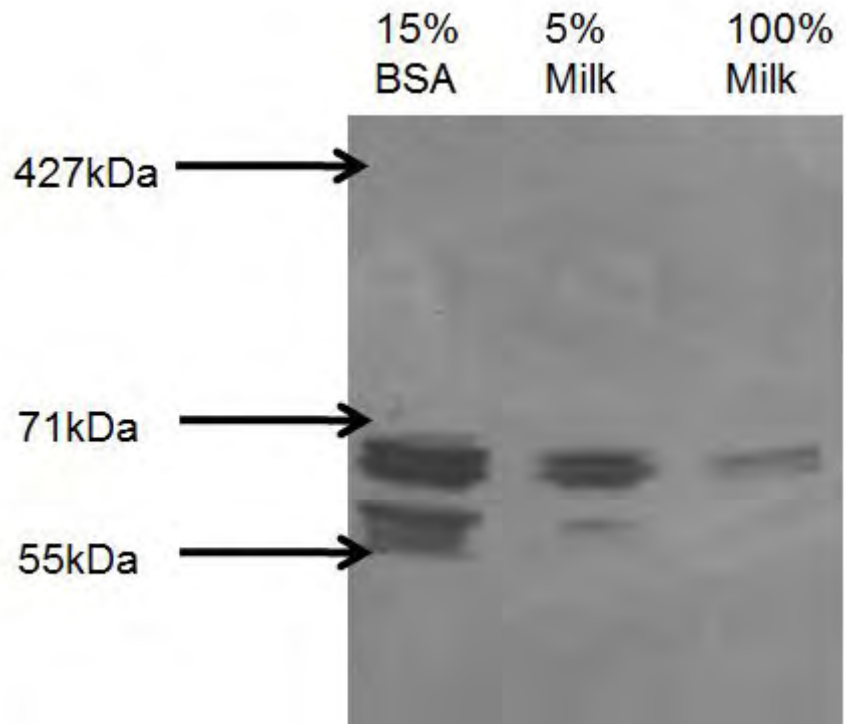

Figure 3.14. Comparison of three different blocking solutions.

To overcome this, a longer transfer time of 21h was applied and the polyacrylamide gel percentage was lowered from 6% to 5% to facilitate protein transfer. A no-primary (secondary-only) control was included, to account for the background signal observed on the blots when using the 10% BSA in TBST blocking solution (Fig. 3.15). Cultured melanocyte and fibroblast protein extracts were included to determine whether the 427kDa dystrophin protein isoform could be detected in these cells. This was of limited success, yielding a weak positive signal at 437kDa for the C2C12 myoblasts (positive control) and for control fibroblasts at p4. No signal was observed for fibroblasts at p6 or melanocytes at p5 (Fig. 3.15). The absence of the 427kDa band in the secondary-only control was perceived as an indication of a true positive signal in those samples which the 427kDa band displayed in. However, the validity of these findings could not be confirmed due to financial and time constraints of the project.

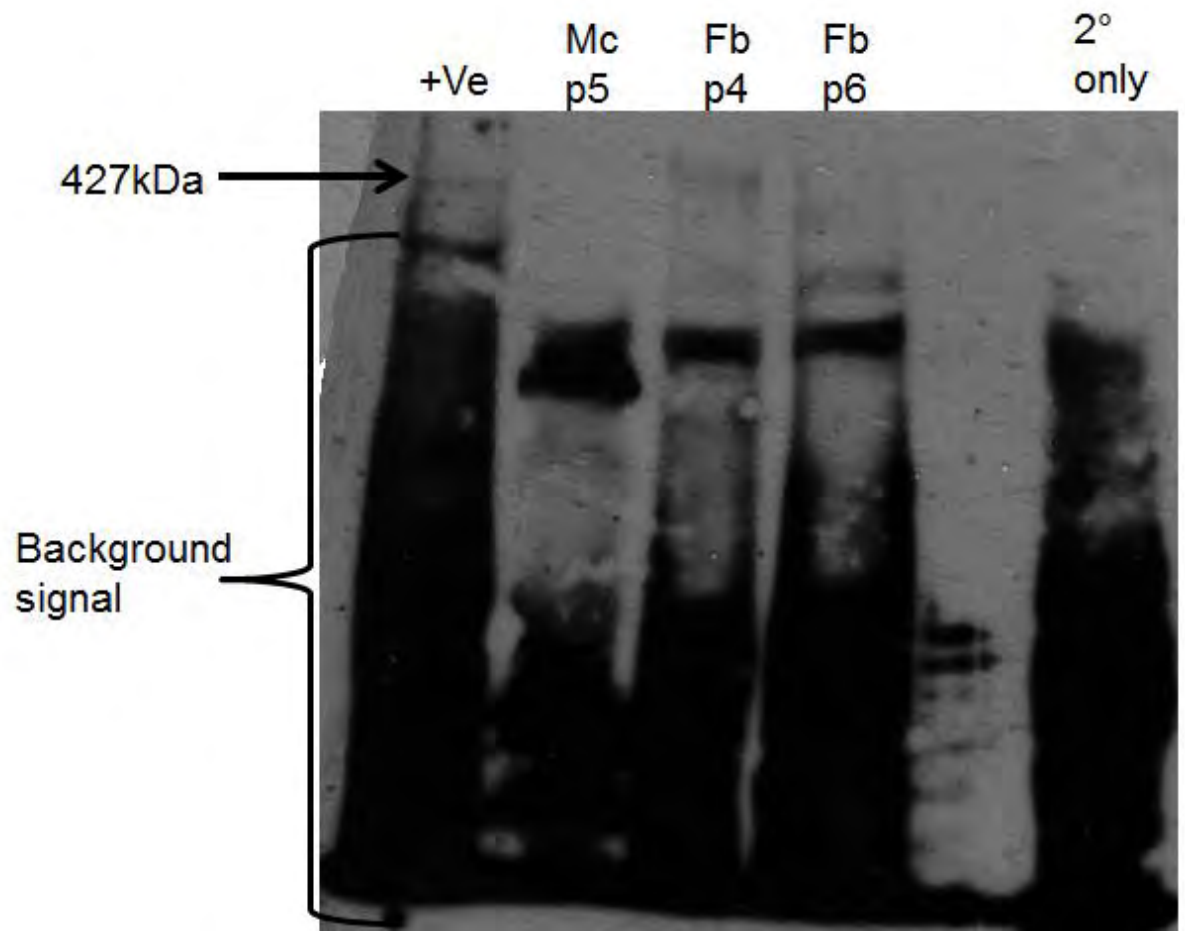

Figure 3.15. Dystrophin Western blot. Mc = melanocytes, Fb = fibroblasts, 2° only = secondary only control, +ve = C2C12 myoblast cells.

3.3. Dystrophin gene expression in melanocytes and fibroblasts

3.3.1. RNA isolation and integrity analysis

Total RNA was isolated from control and patient melanocytes and fibroblasts at successive passages. The purity and concentration of the isolated RNA from the primary cell cultures was assessed spectrophotometrically, using the ND-1000 NanoDrop Spectrophotometer (Thermo Fisher Scientific), with an A260/A230 ratio of 1.8 to 2 indicating a sample free of organic solvents and an A260/A280 ratio of 2 indicating a sample is free of protein contamination. All samples had ratios within the given ranges.

The integrity of the RNA samples was determined by agarose gel electrophoresis. RNA from control melanocytes at p3 and p4 was electrophoresed as a representative of the integrity of the RNA obtained from the isolations (Fig. 3.16). The RNA samples appeared as two defined 28S and 18S ribosomal RNA bands. The RNA was therefore of good integrity, not degraded and fit for use.

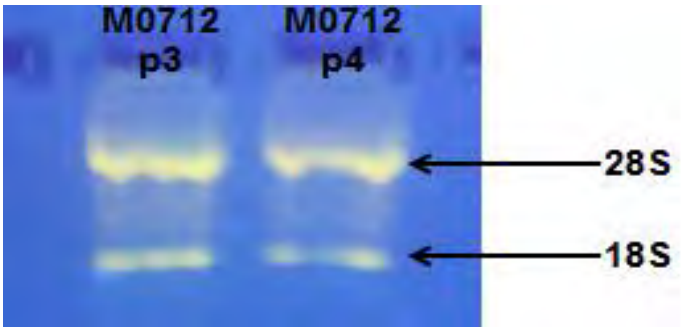

Figure 3.16. Agarose gel electrophoresis of RNA isolated from melanocytes. The 28S and 18S bands are indicated by the arrows. RNA samples were electrophoresed through a 2% agarose gel, stained with 1X SYBR® Safe (Invitrogen), at 80V for 30min and visualized under UV light.

3.3.2. Molecular analysis of dystrophin gene expression in control cells across successive passages

Quantitative PCR (qPCR) analysis of dystrophin gene expression in control melanocytes and fibroblasts was investigated in order to determine which dystrophin isoforms were expressed by each cell type, and whether a difference existed in expression across passages and between primary cell cultures (Fig. 3.17 to Fig. 3.19). Gene expression was represented as the relative expression of the individual gene normalised to the reference genes *GAPDH* and *GUSB*.

The expression of the full length dystrophin isoform (Dp427M) was significantly higher in the melanocytes than fibroblasts, peaking at p8 (Fig. 3.17A1). The fibroblasts exhibited very low or no expression across all passages (Fig. 3.17A2). These expression levels do not correlate with the results of the immunocytochemical staining, where melanocytes showed a passage-dependant increase peaking at p5 followed by a decrease from p6 to p8, and fibroblasts displayed expression of dystrophin across all passages with a peak in expression at p4. However, the absence of a direct correlation between gene expression levels and protein expression levels is not uncommon[80].

Similar levels of expression were observed for the ubiquitous isoform of dystrophin (Dp71), for both melanocytes and fibroblasts (Fig. 3.17B1), except at p4 which showed a significantly higher expression in melanocytes. Melanocytes showed significantly higher expression of Dp71 at p3 compared to p6 as well as at p4 compared to p6. No difference in expression of Dp71 was observed in fibroblasts across all passages (Fig. 3.17B2).

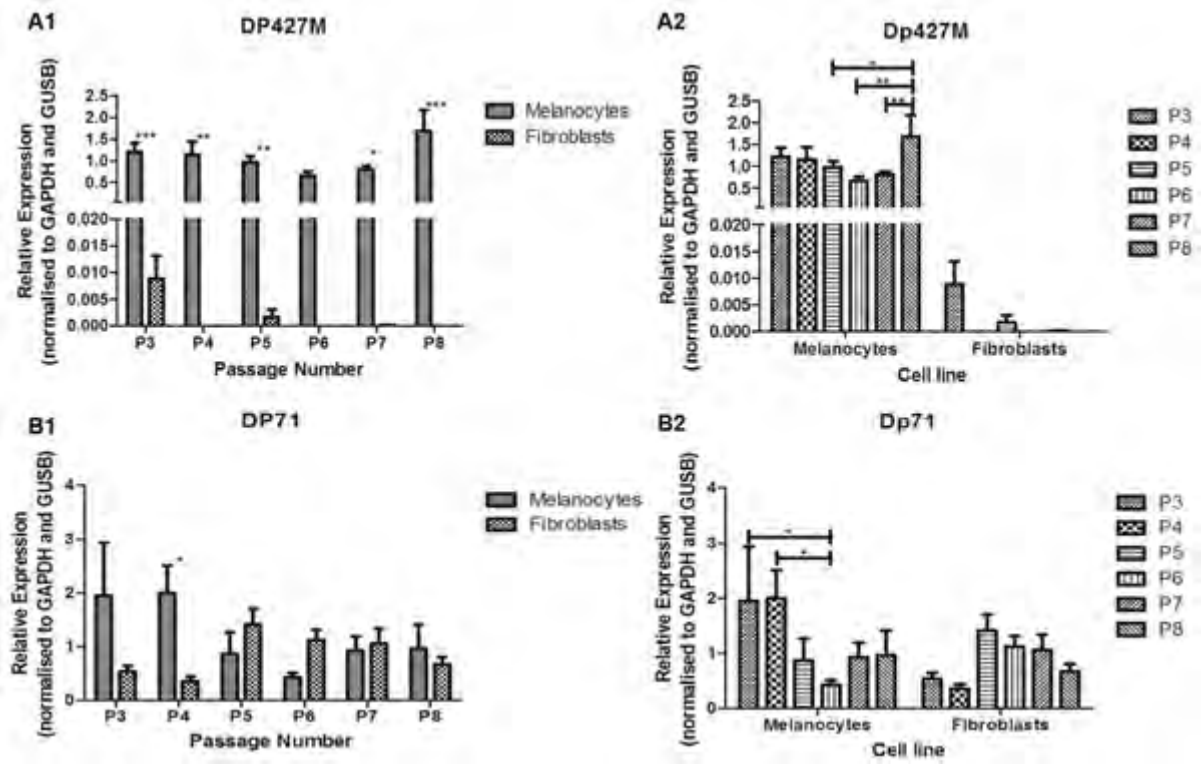

Figure 3.17. Quantification of Dp427M and Dp71 expression for melanocytes and fibroblasts. A1 and B1 compare gene expression between melanocytes and fibroblasts at matched passages. A2 and B2 compare gene expression of melanocytes and fibroblasts across successive passages. Error bars represents the standard error of the mean (SEM). * = $p \leq 0.05$, ** = $p \leq 0.01$, *** = $p \leq 0.001$. n=3.

Fragments spanning exons 9 to 10, 25 to 26 and 34 to 35 were quantified in order to verify the expression of the Dp427M isoform. Amplification of these fragments was robust and consistent in melanocytes and low and variable in fibroblasts. This was consistent with the expression of the full-length dystrophin isoform (Dp427M) in these cells.

In melanocytes, expression of these fragments across passages was found to be similar to that observed for Dp427M expression. The fragments spanning exons 9 and 10, 25 and 26 and 34-35 displayed significantly higher expression at p8 when compared to p7 and p6 (Fig. 3.18A1, B1 and C1). Expression of the fragment spanning exons 34 to 35 was also found to have a significantly high expression at p8 compared to p5 (Fig. 3.18C1), which correlates to that observed for Dp427M (Fig. 3.17C2). Although p8 was not found to be significantly higher than p5 for the fragments spanning exons 9 to 10 and 25 to 26 (Fig. 3.18A1 and B1), overall the trend observed in the expression profile of these fragments were quite similar to that of Dp427M. A significant difference was observed between melanocytes and fibroblasts at passages 3, 4, and 8 for fragments spanning exons 9 to 10 and 25 to 26 (Fig. 3.18 A2 and B2) and at passages 3 to 5, 7 and 8 for the fragment spanning exons 34 to 35 (Fig. 3.18C2).

Fibroblast expression of these regions was interesting as expression of dystrophin was observed at p3, p5, p7 and p8 for exon junction 9-10 (Fig. 3.18A1) and p3-p6 and p8 for

exon junction 25-26 and 34-35 (Fig. 3.18B1 and C1); whereas expression of the full length isoform Dp427M was only observed in p3, p5 and p7. This difference in expression pattern may indicate that the longer isoforms of dystrophin containing these regions were present in lower abundance than the smaller isoforms fibroblast samples, which supports the trends observed for the expression of Dp427M and Dp71 in fibroblasts.

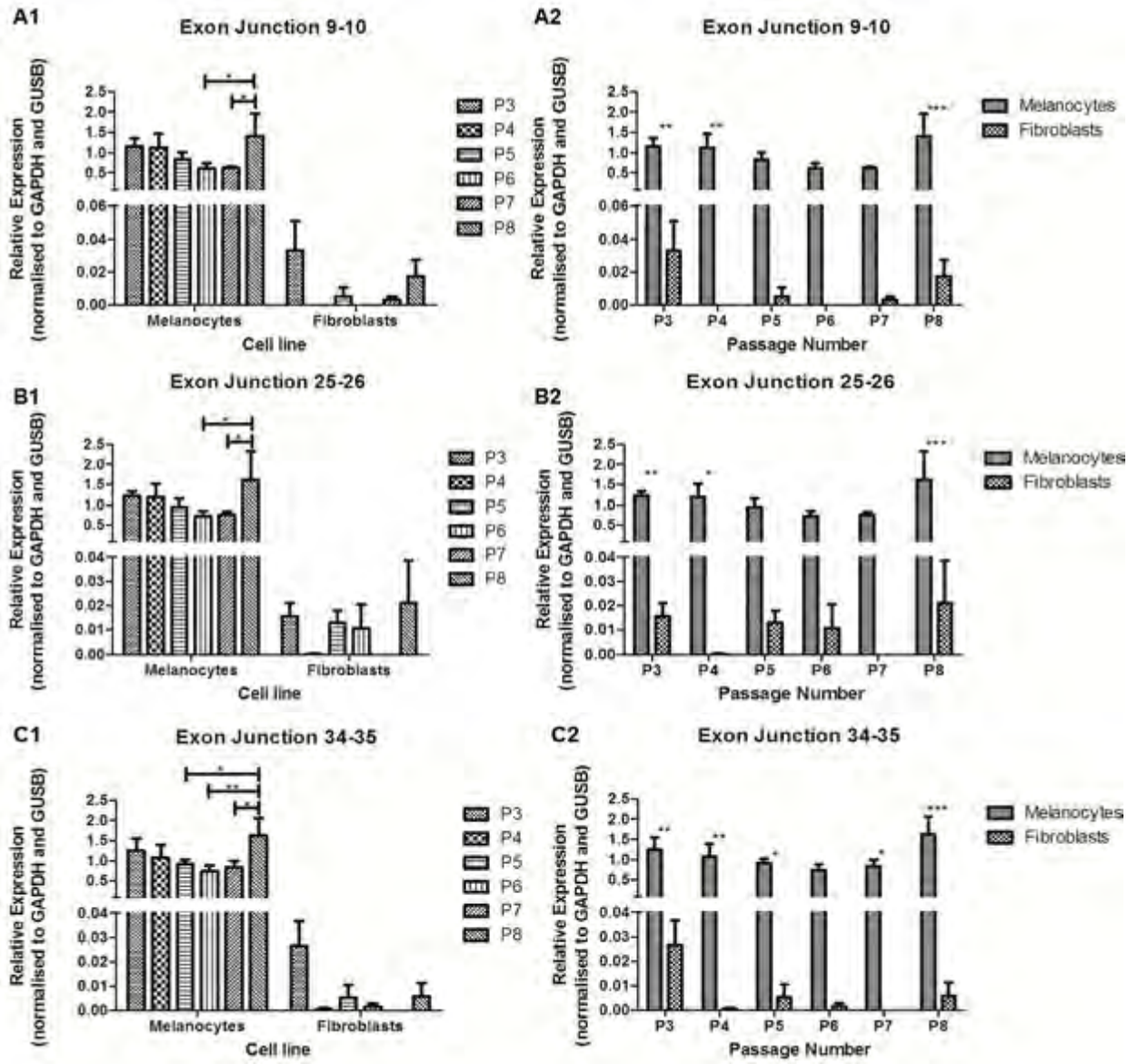

Figure 3.18. Quantification of the fragments spanning exon junctions 9 to 10, 25 to 26 and 34 to 35 of the *dystrophin* gene for melanocytes and fibroblasts. Left column (A1, B1 and C1) compares gene expression of melanocytes and fibroblasts across successive passages. Right column (A2, B2 and C2) compares gene expression between melanocytes and fibroblasts at matched passages. Error bars represent the standard error of the mean (SEM). * = $p \leq 0.05$, ** = $p \leq 0.01$, *** = $p \leq 0.001$. n=3.

Expression of the retinal isoform of dystrophin (Dp260) was quantified for melanocytes and fibroblast and was found to only be expressed in melanocytes. This expression did not appear to be influenced by passage number (Fig. 3.19).

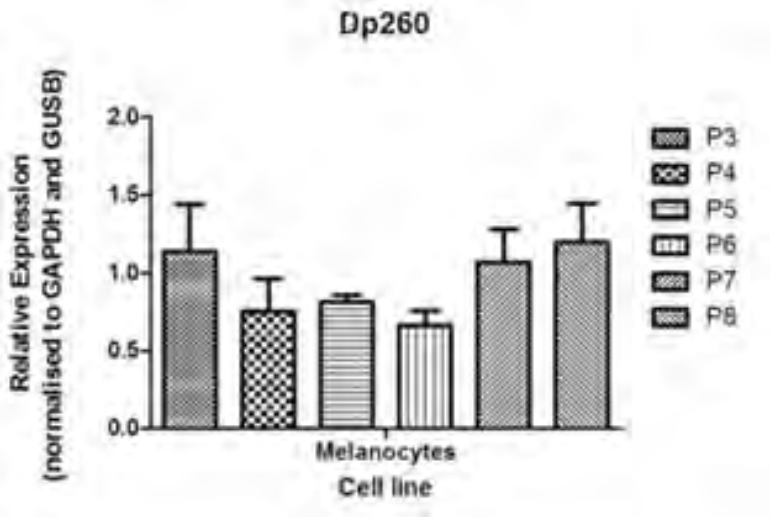

Figure 3.19. Quantification of Dp260 in melanocytes. Error bars represent the standard error of the mean (SEM). n = 3.

Primary cultured melanocytes are suspected of dedifferentiating in culture at higher passage numbers. Tyrosinase expression was used as a proxy to determine if the differentiation status of the cells in culture affects expression of dystrophin[81]. More highly differentiated cells produce increased levels of tyrosinase, which results in higher levels of melanin[65]. No significant differences were observed in the expression of *tyrosinase* for all of the passages analysed (Fig. 3.20), thus no dedifferentiation is inferred for the passages analysed.

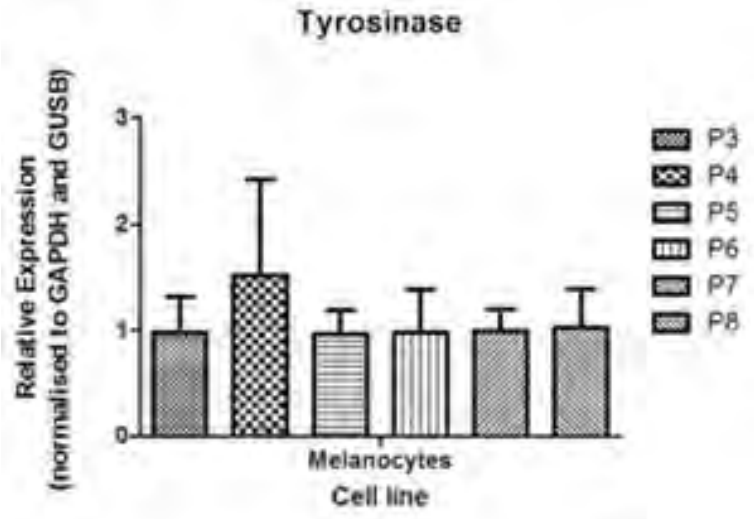

Figure 3.20. Quantification of tyrosinase expression in melanocytes. Error bars represent the standard error of the mean (SEM). n = 3.

Statistical analysis of the data indicated that passage number did not significantly affect the expression of the dystrophin isoforms or tyrosinase. However, expression of the dystrophin isoforms, except Dp71, was found to be significantly linked to the cell type. Dystrophin expression overall was found to be more robust in melanocytes compared to fibroblasts.

3.4. Identification of *DMD* gene mutations using skin cells

3.4.1. Nested-PCR

A *GAPDH* (reference gene) PCR was performed on the cDNA samples from each patient for both melanocytes and fibroblasts, to confirm that cDNA synthesis had occurred (Fig. 3.21). Amplification was observed in all patient samples and no amplification was seen in the no-template control (NT) nor the no-reverse transcriptase control (NRT). This confirmed the absence of contamination in the PCR set up and absence of DNA contamination in the RNA used for cDNA synthesis. It was therefore concluded that the cDNA synthesis was successful and the samples could be used for the nested-PCR.

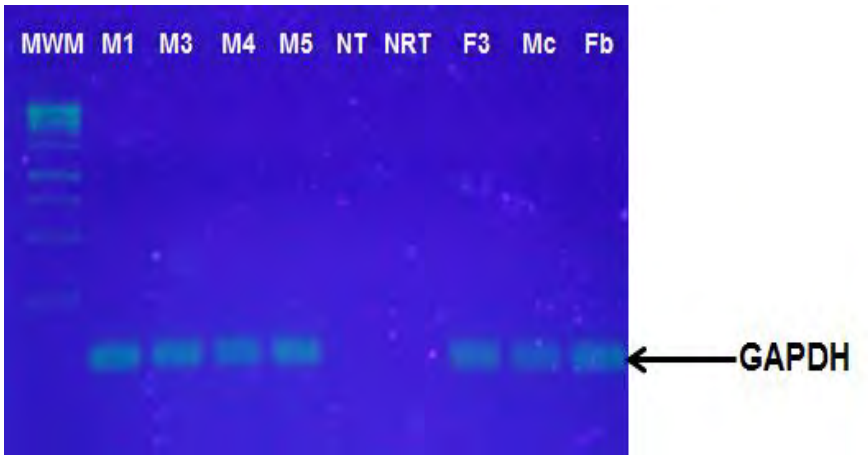

Figure 3.21. Reference gene PCR. Successful amplification of the *GAPDH* fragment in all patient and positive control samples. MWM = molecular weight marker. M1 = M151006A; M3 = M151013A; M4 = M151013B; M5 = M151020; NT = no template control; NRT = no reverse transcriptase control; F3= F151013A; Mc = M0712 p3; Fb = F150313 p3. PCR products were electrophoresed through a 2% agarose gel stained with 1X SYBR® Safe (Invitrogen) at 100V for 30min and visualised under UV light.

The nested-PCR protocol for amplification of the entire coding region of the *DMD* gene was optimised for skin cell cDNA, using material derived from control melanocytes (Fig. 3.22). The optimised protocol for cDNA synthesis and nested-PCR was then applied to RNA extracted from passage 3 of patient melanocytes.

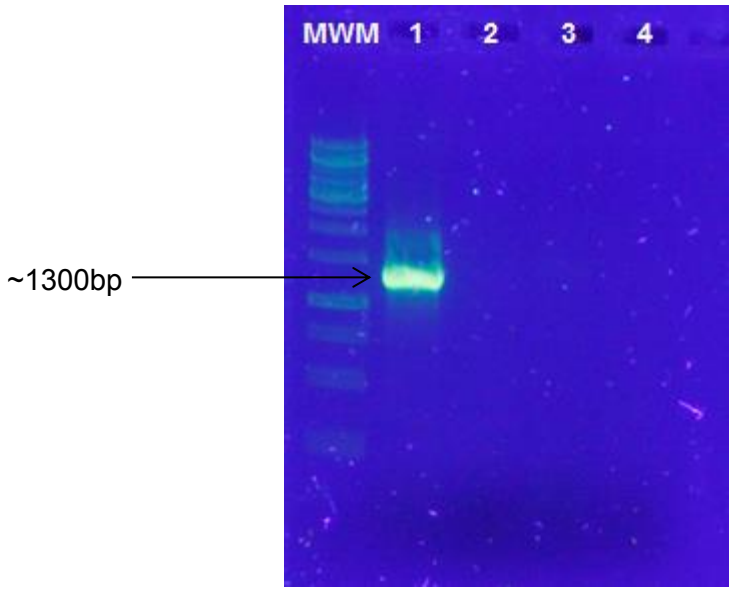

Figure 3.22. Optimisation of Nested-PCR. MWM = molecular weight marker. Numbers represent different PCR conditions: 1 = 40 cycles + $MgCl_2$; 2 = 20 cycles + $MgCl_2$; 3 = 40 cycles no $MgCl_2$ and 4 = 20 cycles no $MgCl_2$. PCR products were electrophoresed through a 1% agarose gel stained with 1X SYBR® Safe (Invitrogen) at 80V for 45min and visualised under UV light.

Amplification of all 79 exons of the *DMD* gene was observed for patient 151013A with a small deletion in exon 10 and 151013B, with a duplication of exon 19 (Fig. 3.23). As expected, no amplification was observed in patient 151020, in whom a deletion of the entire *DMD* gene was previously reported (Fig. 3.24 and Fig. 3.26).

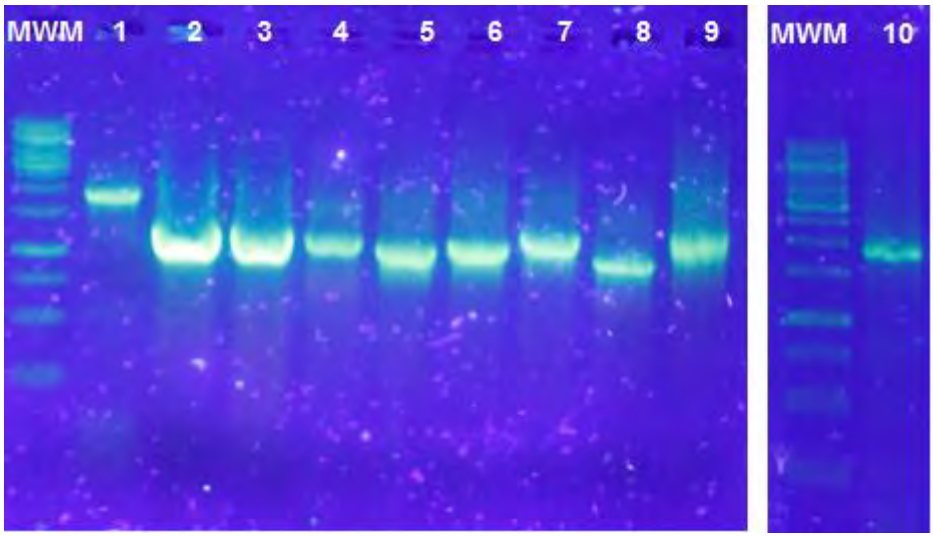

Figure 3.23. Representation of the secondary PCR products of M151013A and M151013B. Successful amplification of all primer sets. MWM = Molecular weight marker. Numbers 1-10 correspond to primer sets in appendix 4.2. PCR products were electrophoresed through a 1% agarose gel stained with 1X SYBR® Safe (Invitrogen) at 80V for 45min and visualised under UV light.

Figure 3.24. Representation of secondary PCR products of M151020 showing no amplification for all primer sets. MWM = Molecular weight marker. Numbers 1-10 correspond to primer sets in appendix 4.2. PCR products were electrophoresed through a 1% agarose gel stained with 1X SYBR® Safe (Invitrogen) at 80V for 45min and visualised under UV light.

In patient 151006A with a previously detected deletion of the Dp427M promoter region, amplification of exons 58 to 79 was observed (Fig. 3.25 and Fig. 3.26). This correlates with transcription from the Dp71 promoter of the *DMD* gene. The lack of amplification of the other exons is likely a result of the deletion of the Dp427M promoter.

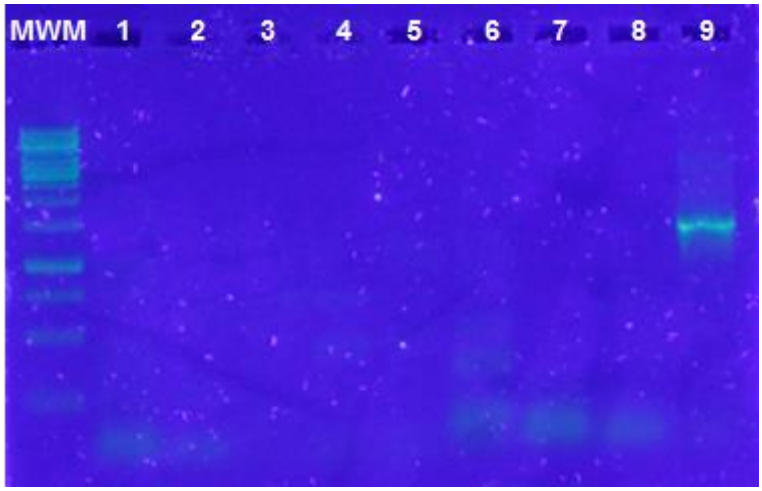

Figure 3.25. Representation of secondary PCR products of M151006A showing amplification of primer set 9. MWM = Molecular weight marker. Numbers 1-10 correspond to primer sets in appendix 4.2. PCR products were electrophoresed through a 1% agarose gel stained with 1X SYBR® Safe (Invitrogen) at 80V for 45min and visualised under UV light.

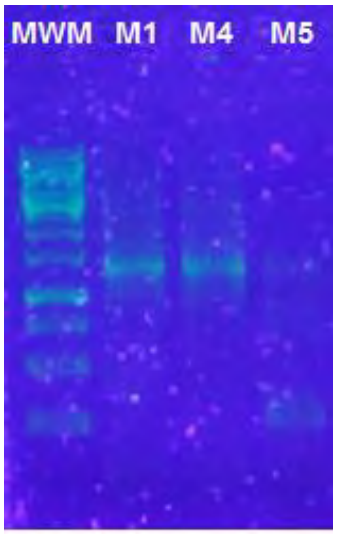

Figure 3.26. Representation of secondary PCR products of M151006A, M151013B and M151020 MWM = molecular weight marker. M1 = M151006A primer set 10; M4 = M151013B primer set 10 and M5 = M151020 primer set 10. PCR products were electrophoresed through a 1% agarose gel stained with 1X SYBR® Safe (Invitrogen) at 80V for 45min and visualised under UV light.

Interestingly a comparison between the primary PCR product yield of control melanocytes and fibroblasts showed a noticeable difference in the product yield for exons 2 to 11 of the *DMD* gene (Fig. 3.27). This correlates with the results obtained from qPCR analysis which showed that melanocytes had more robust expression of the longer dystrophin isoform (Dp427M).

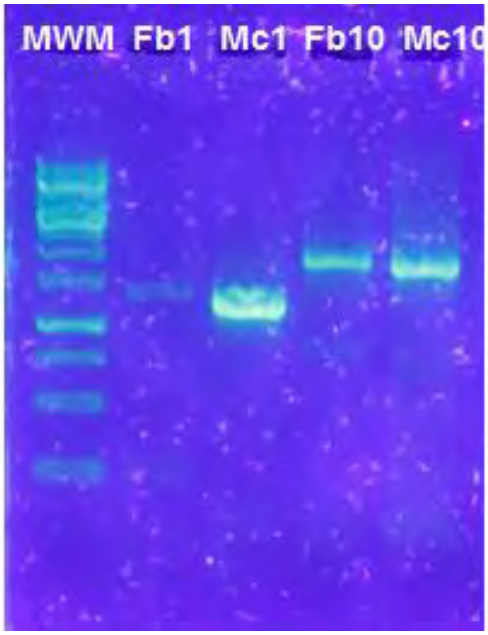

Figure 3.27. Comparison between the melanocyte and fibroblast PCR product yield after primary PCR reaction indicating differential product amplification. MWM = molecular weight marker. Fb1 = F150313 p3, primer set 1; Mc1 = M0712 p3, primer set 1; Fb10 = F150313 p3, primer set 10; Mc10 = M0712 p3, primer set 10. Ten microlitre of each PCR product was electrophoresed through a 1% agarose gel stained with 1X SYBR® Safe (Invitrogen) at 80V for 45min and visualised under UV light.

3.4.2. cDNA sequencing

To confirm the presence of the previously identified disease-causing mutations (see Methods section 2.2, table 2.1), in melanocytes, all PCR products for patients 151006A, 151013A and 151013B were sequenced.

Previous testing of genomic DNA in patient 151013A, revealed a small deletion in exon 10 in the *DMD* gene (c.968_981del; p.Glu323Fr). This deletion was also demonstrated on sequencing of the melanocyte cDNA from patient 151013A (Fig. 3.28A and B).

Figure 3.28. Sequencing results of patient 151013A indicating a deletion in exon 10 at nucleotide position 968-981. A – Alignment of a section of the sequencing results of patient 151013A to reference sequence. Red box indicates area that was deleted. The letter R represents A or G and dashes indicate gaps in the sequence. **B** – Section of reference sequence with red box indicating the position of the deletion in A. The number 10 above the sequence indicates exon 10, and the numbers at the end of each line of sequence indicates the position of the last nucleotide in that line. The letter M prior to the patient code (yy-mm-dd A/B) indicates cell type i.e. melanocyte. Ref = reference sequence (NM_004006.2). F seq = Forward primer sequence. R seq = Reverse primer sequence.

A duplication of exon 19 was previously reported on patient 151013B, by the NHLS (Fig. 3.29A and B). A contiguous duplication of exon 19 (c.2292_2380dup) was observed on sequencing the melanocyte cDNA, which correlates with the genetic diagnosis previously provided for this patient.

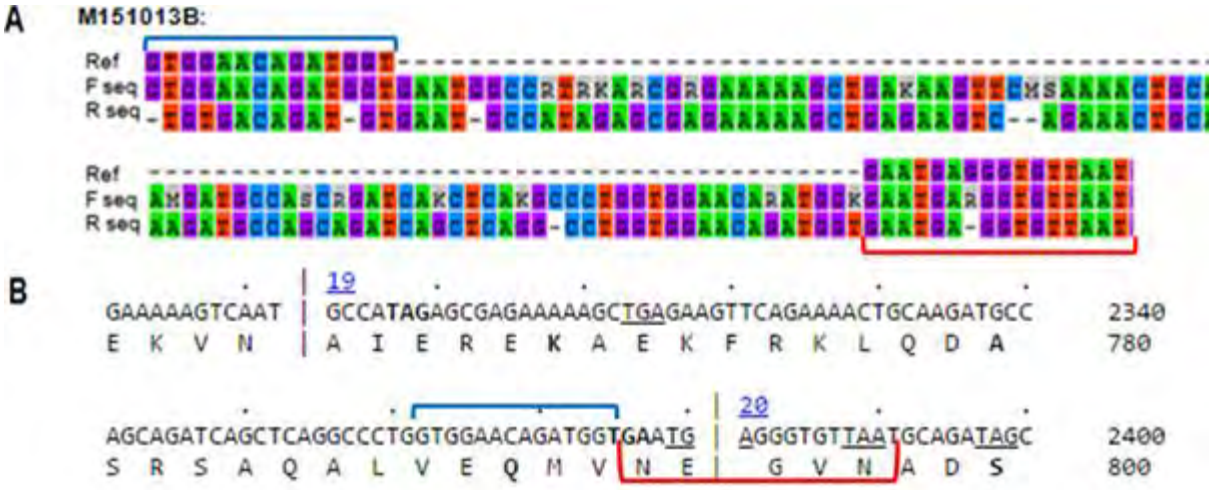

Figure 3.29. Sequencing results of patient 151013B showing a contiguous duplication of exon 19. A – Alignment of a section of the sequencing results of patient 151013B. The blue bracket at the start of the sequence correlates with the position of the blue bracket in B. The red bracket at the end of the sequence correlates with the position of the red bracket in B. The bottom sequence of M151013B continues from the top sequence. The letters R = A or G; K = G or T; M = A or C; S = C or G and dashes indicate gaps in the sequence. **B** – Section of reference sequence, the numbers 19 and 20 above the sequence indicate exons 19 and 20. The numbers at the end of each line of sequence indicate the position of the last nucleotide in that line. The letter M prior to the patient code (yy-mm-dd A/B) indicate cell type i.e. melanocyte. Ref = reference sequence (NM_004006.2). F seq = Forward primer sequence. R seq = Reverse primer sequence.

Additional sequence variants detected in all patients are listed in Table 3.2. All were listed in the Leiden Open Variation Database (LOVD)[36] as benign, with the exception of the exon 71 deletion. Within the context of cDNA from cultured melanocytes, this deletion was assumed to be a result of an alternative splicing event described by Richard et al. and as such was not associated with disease.

Table 3.2. Additional sequence variants identified in patients 151006A, 151013A and 151013B.

Patient	Variant	Exon	Function	Damaging or benign			Novel*	Translational effect
					SIFT°	PolyPhen[x]		
151006A	c.8729A>T	59	Missense	Benign	0.39	0.552	No	p.Glu291Val
	c.8734A>G	59	Missense	Benign	0.09	0.021	No	p.Asn2912Asp
	c.8810G>A	59	Missense	Benign	1	0	No	p.Arg2937Gln
151013A	c.7728T>C	53	Synonymous	Benign	1	0	No	p.(Asn2576=)/c.7728T>C
	c.8810G>A	59	Missense	Benign	1	0	No	p.Arg2937Gln
	+c.(10223+1_10224-1)_(10261+1_10262-1)del	71	In-frame deletion	Probably damaging+	N/A	N/A	Yes	p.Val3410_Pro3422del
151013B	c.2645A>G	21	Missense	Benign	0.48	0	No	p.Asp882Gly
	c.8810G>A	59	Missense	Benign	1	0	No	p.Arg2937Gln
	+c.(10223+1_10224-1)_(10261+1_10262-1)del	71	In-frame deletion	Probably damaging+	N/A	N/A	Yes	p.Val3410_Pro3422del

***According to Ensembl variant effect predictor[77], the single nucleotide polymorphism database (dbSNP), literature and Leiden Open Variation Database (LOVD), Leiden muscular dystrophy pages (http://www.dmd.nl)[36].**
°Score according to Sorting Intolerant from Tolerant (SIFT)[82]. Scores ≤0.05 are indicative of a possibly damaging variant, whereas scores >0.05 are indicative of a benign or tolerated variant.
[x]Score according to Polymorphism Phenotyping v2 (POLYPHEN-2)[83]. Scores closer to 0 are indicative of tolerated/benign variants while scores closer to 1 indicate potentially damaging variants.
+Alternative splicing of Dp71 isoform.

Chapter 5: Discussion

5.1. Dystrophin expression in skin

The skin and the cells comprising the skin have been of interest in the study of D/BMD since 1977, when Wyatt and Cox showed that fibroblasts derived from DMD patients could be distinguished from healthy fibroblasts based on the presence of inclusion bodies[84]. Subsequently, dystrophin staining in the arrector pili muscles of the skin was investigated by Marbini et al. (1995) as a less traumatic and cheaper alternative to the use of muscle biopsies[85,86]. This staining was found to be specific, sensitive and comparable to that performed on muscle biopsy tissue. It was however, not implemented in the clinic, possibly due to the uneven distribution of the arrector pili within the skin and the fact that myoepithelial cells are generally located deep within the dermis, necessitating deep skin biopsies[68].

A recent study by Pellegrini et al. demonstrated positive staining for dystrophin in skin sections and cultured melanocytes of healthy individuals, using fluorescence[68]. The study also incorporated immunohistochemical analysis on skin biopsies from five genetically characterised DMD patients and found dystrophin to be absent in the basal layer, despite the presence of melanocytes. The absence of dystrophin was also noted in the arrector pili muscles of the dermis of these patients[68].

In this study we attempted to demonstrate dystrophin expression in the skin by dystrophin staining of healthy adult foreskin tissue sections. The staining, however, only produced background signal. The initially supposed reason for this was the difference in the origin of the skin. Pellegrini and colleagues did not specify the site from which the skin biopsies were taken, but they were likely to be from the forearm or thigh of the patients, whereas the sections in our study were obtained from adult foreskin samples. Subsequently, however, it was decided that this is an unlikely reason, as our samples were obtained from healthy individuals and the cultured foreskin-derived melanocytes were shown to yield positive staining for dystrophin. A more plausible explanation is the difference in the antibodies used, as our antibody (NCL-DYS2; Leica Biosystems, Germany) was sourced from a different manufacturer and was specific to the C-terminus of dystrophin, as opposed to that used by Pellegrini et al. which was specific to the dystrophin rod domain (Dystrophin H-5 antibody; Santa Cruz, USA). There was also a difference in the sensitivity of the antibodies and our antibody may not have been sensitive enough to detect dystrophin in the skin sections. This is substantiated by the minimal dilution of the antibody (1:10 dilution) used in our study.

5.1.1. Dystrophin protein expression in fibroblast and melanocyte primary cultures

In order to investigate the utility of melanocytes and fibroblasts as a potential tool for genetic diagnosis of D/BMD., melanocytes and fibroblasts were cultured from shallow skin biopsy samples of both patients and healthy individuals.

Immunocytochemical analysis and fluorescent quantification of dystrophin expression in control fibroblasts and melanocytes indicated that dystrophin was indeed present within the cells. This is consistent with the results obtained in previous studies of dystrophin expression[62,68,69]. However, to our knowledge our study was the first to investigate the expression of dystrophin in fibroblasts and melanocytes across successive passages.

In fibroblasts, the expression of dystrophin appeared to be irregular, displaying an increase in fluorescence from p3 to p4, followed by a decrease at p5 and then by an increase at p6 and a decrease from p7 to p8. This irregular pattern of dystrophin protein expression could possibly be explained by fibroblast heterogeneity and the proposed 'leaky' or ectopic transcription of the full length muscle isoform of dystrophin in fibroblasts[54,62,63].

It has been shown that there are differences among fibroblasts from different parts of the body and that even within a single tissue type e.g. skin, fibroblasts do not exist as a homogenous population[54]. The dermal fibroblast populations can be separated into two distinguishable groups, namely the papillary dermal fibroblasts, located immediately below the epidermis, and the reticular dermal fibroblasts which are located below the papillary dermis and consist of dense connective tissue. The papillary dermis comprises of papillary dermal fibroblasts, dermal sheath fibroblasts and dermal papilla fibroblasts whereas the reticular dermis consists of reticular dermal fibroblasts and hypodermal fibroblasts[54]. There is also evidence that suggest papillary fibroblasts could differentiate to into reticular dermal fibroblasts upon aging[54].

It is therefore plausible that different fibroblasts express dystrophin at varying levels and depending on the composition of the culture at the time of analysis the expression of dystrophin may vary. This is supported by the findings by Hugnot and colleagues who showed variable dystrophin expression between cultures[62]. The low and inconsistent dystrophin expression observed in the fibroblasts in our study may therefore be a reflection of a natural high variability at early passages.

In melanocytes, fluorescent quantification of staining performed across successive passages revealed a passage-dependent increase in dystrophin expression from p3 to p5, followed by

a subsequent decrease in expression from p6 and beyond. These results correlate with the findings by Pellegrini and colleagues, that compared dystrophin protein expression in melanocytes at p3 and p6 and showed that p3 had higher expression of dystrophin than p6[68]. This expression pattern in melanocytes could be explained by the dedifferentiation of the cells in culture at higher passage numbers. Kormos et al. investigated *nestin* gene expression in melanocytes, across successive passages as a marker of dedifferentiation and found that *nestin* gene expression increased in melanocytes from p6 onwards[81].

To determine whether the staining signal observed with the ICC correlated with the expression of a full length dystrophin isoform in cells. Western blot analysis of dystrophin extracted from control fibroblasts and melanocytes was attempted. The large size of the full length dystrophin (427kDa) required the optimisation of the Western blot technique.

To improve on the results of the initial Western blot attempt, and despite high levels of background signal observed, a protein transfer time of 16h using a protein concentration of 100µg was chosen. To reduce the background staining, the blocking step was optimised by varying the concentrations of BSA and UHT milk blocking solutions. Although, the blocking solutions proved successful in reducing the background signal, the 427kDa isoform could not be detected in the C2C12 myoblast protein extract used for optimisation. Bands at 71kDa and 55kDa were observed with the BSA and the 5% milk blocking solutions, while a single band at 71kDa was observed with the100% milk blocking solution. It is likely that the 55kDa band represents residual background signal as there are no known dystrophin isoforms of that size, and the band at 71kDa represents the ubiquitous isoform of dystrophin (Dp71). No 427kDa band was observed and further optimisation with an increased transfer time (16h to 21h) and a decreased gel percentage (5%) was undertaken. This blot yielded a positive, albeit weak signal at 427kDa for the C2C12 myoblasts (positive control) and for control fibroblasts at p4. However, no signal was noted in for control fibroblasts at p6 or melanocytes at p5. This could potentially be due to human error, such as inaccurate loading of the protein sample. Additional work is required to confirm the Western blot results; but due to the limited time and financial constraints, was not performed as part of this study. This is addressed later in Section 5.4.

As an additional observation, during the culture process it was noted that patient melanocytes where morphologically different to the control cells, displaying multipolar and highly dendritic growth. We hypothesised that the absence of dystrophin in the patient cells may be responsible for the increased dendricity of the melanocytes, possibly through the functions of the DGC within the cell (see Section 5.4). No notable morphological differences were observed in patient fibroblasts during culture, although previous studies of D/BMD

patient derived fibroblasts indicated that dystrophin can influence the morphology, biochemistry and growth of the cells[60,61,84,87,88].

5.1.2. Molecular investigation of the *DMD* gene expression in control fibroblast and melanocyte primary cultures

DMD gene expression in control fibroblasts and melanocytes was investigated, using qPCR to determine which isoforms were expressed by each cell type, and whether a difference existed in expression across passages and between cell lines. Gene expression was represented as the relative expression of the individual gene normalised to *GAPDH* and *GUSB* reference genes.

We set out to determine whether the full length muscle isoform (Dp427M), the retinal isoform (Dp260) and the ubiquitous isoform (Dp71) of dystrophin was expressed in fibroblasts and melanocytes, as these isoforms provided broad coverage of the gene. *Tyrosinase* expression was also investigated in melanocytes, to assess the differentiation status of the cells across successive passages and how that related to *DMD* gene expression.

In fibroblasts only the Dp427M and Dp71 isoforms of dystrophin were found to be expressed. Low levels of the Dp427M transcript was present in fibroblasts in our study, similarly to the findings of Chelly et al. who attributed the expression of dystrophin in fibroblasts to illegitimate transcription[63]. Expectedly, the ubiquitous dystrophin isoform (Dp71) expression in fibroblasts appeared to be more robust than the Dp472M expression, with expression levels comparable to that of melanocytes.

Our findings in melanocytes revealed that the Dp427M, Dp71 and Dp260 dystrophin isoforms were robustly expressed across the passages analysed, which correlates with the findings by Pellegrini and colleagues who reported expression of Dp427M, Dp71 and Dp260 in melanocytes[68]. Expression of these isoforms in melanocytes is not particularly unexpected as melanocytes are closely associated with the retinal pigment epithelium and choroid of the eye, the heart, lungs and brain[64]. No significant differences were found in *tyrosinase* expression across the passages, inferring that the cells were not dedifferentiating in culture[81].

Amplification of *DMD* exons 9 to10, 25 to 26 and 34 to 35 was performed on control fibroblasts and melanocytes. These regions are a part of the full length dystrophin isoforms and were tested to demonstrate the presence of the full length transcript. The expression of these exons in fibroblasts and melanocytes, were similar to the expression profile of the Dp427M isoform in these cells, displaying low variable expression in fibroblasts and robust, consistent expression in melanocytes.

Nested-PCR for amplification and subsequent sequencing of the *DMD* transcript was optimised on cDNA from control melanocytes and fibroblasts. Interestingly a comparison between the PCR product yield of fibroblasts and melanocytes, after the primary PCR, revealed a noticeable difference between the two cell types. Amplification of exons 2-11, which is related to the full length isoform of the *DMD* gene, for fibroblasts was strikingly lower than that of melanocytes. This correlates with the results obtained from the qPCR analysis of the Dp427M isoform expression in fibroblasts and melanocytes, which indicated that the isoform had significantly decreased expression in fibroblasts. Almost no difference in expression was observed between fibroblasts and melanocytes for exons 67 to79, which is related to expression of the 71kDa isoform of dystrophin. This also associates with the qPCR results obtained for expression of Dp71, which showed similar levels of expression between the two cell lines. Similar findings were noted by Hugnot and colleagues indicating that fragments spanning exons 3 to 4, 48 to 49 and 62 to 79 amplified at different efficiencies[62].

It was therefore concluded that the full length dystrophin is expressed more robustly in skin melanocytes, as compared to fibroblasts, and appears to be a feasible source of RNA for genetic diagnosis of DMD.

5.2. *DMD* gene variant detection in cultured patient melanocytes.

In view of the dystrophin ICC, Western blot and qPCR results in our control cell lines, PCR and sequencing of the *DMD* gene was only performed on melanocyte cDNA of the four patients in our cohort. Amplification of all exons was observed in melanocyte cDNA from patients 151013A and 151013B. Sequencing revealed accurate identification of the disease-causing mutation for both patients, with a small deletion in exon 10 in 151013A and a duplication of exon 19 in 151013B. As expected, no cDNA amplification was seen in patient 151020, due to a deletion of the entire *DMD* gene.

A deletion of the Dp427M promoter reported in patient 151006A, based on a result of a deletion hot-spot multiplex PCR (mPCR), offered as a diagnostic test for D/BMD at the time. The full extent of the deletion was in fact not established. Our findings demonstrated amplification of exons 58 to 79 and no amplification of the preceding exons, which is consistent with the deletion of the Dp427M promoter and transcription from a promoter further downstream in the *DMD* gene for a smaller isoform of dystrophin (e.g. Dp71).

The disease-causing mutations were thus detected in all four patients studied. In addition, the cDNA sequencing analysis in patients 151006A, 151013A and 151013B revealed 5 benign small, previously published variants.

An interesting finding was an in-frame deletion of exon 71 identified in the cDNA of patients 151013A and 151013B, which was not previously detected in the genomic DNA of these patients. A previous study by Richard and colleagues of cultured human amniocytes revealed that the Dp71 isoform can be alternatively spliced to exclude exon 71 and/or exon 78, producing a non-pathogenic alternatively spliced variant of Dp71[89]. Analysis of the electropherograms for patients 151013A and 151013B showed presence of two different sequences. This was most likely due to the alternative splicing of Dp71 in some cells, resulting the exclusion of exon 71 in the transcript. It is therefore likely that the deletion of exon 71 detected in our patients is indeed a non-pathogenic, alternatively spliced variant of the Dp71 isoform.

The ability to determine the effects of a mutation on the mRNA level has become of increased importance, with the development of gene-based therapies for D/BMD. These therapies, which include exon-skipping and premature stop codon read through, require knowledge of the underlying gene defect in order to determine eligibility for the treatments. Although, genomic DNA from blood lymphocytes is the most commonly used template in the diagnostic protocols, RNA-based analysis can determine the downstream effects of a sequence alteration allowing for better determination of eligibility for therapy[13,36,37].

In 1991, a study was conducted exploring the utility of lymphoblastoid cells, peripheral blood lymphocytes and fibroblasts for the genetic diagnosis of D/BMD, specifically with regards to the mRNA analysis of the Dp427M isoform of dystrophin[63]. The results indicated that all of the cell types could be used to successfully determine mutations in the *dystrophin* gene, however, the expression of the Dp427M isoform was low and variable making diagnosis using these cells challenging[62,63,90]. Ito et al. also found that lymphocyte extracted mRNA could not be used to accurately determine D/BMD carrier status while muscle biopsy could[91]. For these reasons muscle biopsy remains useful for immunohistochemical diagnosis as well as RNA-based analysis[90]. However, the major limitation of muscle cDNA analysis is the requirement of a muscle biopsy which is invasive, traumatic, expensive and which usually requires the use of general anaesthesia, with its inherent risks for which D/BMD patients[86].

To our knowledge, our study is the first to investigate the use of melanocytes as a diagnostic tool for D/BMD. The possible use of melanocyte mRNA is appealing, as only a shallow skin biopsy is required, which is easy and cheap to obtain. The full length muscle isoform of dystrophin (Dp427M) is also better and more consistently expressed in melanocytes than in fibroblasts. There are, however, drawbacks to the use of melanocytes, such as the need for the technical expertise, staff and facilities required for cell culture, the risk of contamination and the increased turnaround time in diagnosis. The culture can, however, be further

optimised for a faster turnaround time, by using a slightly larger biopsy to increase the starting number of cells. The technical challenges notwithstanding, RNA-based mutation analysis using skin melanocytes may present an attractive option as an alternative diagnostic tool for genetic diagnosis of D/BMD.

5.3. Conclusion

This study sought to determine whether melanocytes and fibroblasts could be used as a tool to genetically diagnose D/BMD. This was achieved through the culture of primary cells, immunocytochemical analysis of both cell types across successive passages, analysis of gene expression across successive passages of both cell types, as well as sequencing of the cDNA synthesised from patient melanocytes. The study yielded significant results for the immunocytochemical analysis as well as for gene expression across successive passages, which indicated the presence of dystrophin in both melanocytes and fibroblasts, but at varying levels.

Fibroblast cultures in our study where shown to display variable and low expression of the Dp427M dystrophin isoform, making them a less reliable tool for genetic diagnosis of D/BMD. Melanocytes were, however, found to display more robust expression of Dp427M.The results obtained from the sequencing and point mutation analysis indicates that melanocytes can be used to accurately determine disease-causing mutations for the genetic diagnosis of D/BMD.

Overall, our study has shown that while there are additional technical challenges associated with melanocyte culture, RNA-based mutation analysis using melanocytes can be used as a potential alternative to muscle biopsy.

5.4. Additional findings and future work

As this work is on-going, future work will include further investigation into the immunohistochemical (IHC) staining of control skin sections, further optimisation and completion of the dystrophin Western blots and research into the function of dystrophin in melanocytes.

IHC staining with dystrophin antibodies of wildtype skin sections will be required, to determine whether dystrophin can be detected in skin sections. As this was not the primary focus of the thesis, an alternative antibody for dystrophin will need to be tested on the skin sections, to conclude whether the antibody used in this investigation was indeed not sensitive enough to detect dystrophin in the skin sections. Depending on the results obtained, future work could also include immunofluorescent staining of patient and wildtype skin sections in order to determine whether an accurate diagnosis of D/BMD status can be made using skin. If this proves successful, skin biopsies could potentially become a viable alternative to muscle biopsy for IHC diagnosis of D/BMD.

Due to time, quantification of the dystrophin protein expression in melanocytes and fibroblasts could not be completed in our study. Future work would therefore include the optimisation of the Western blot technique and the completion of the protein expression quantification. In our study a weak signal for the positive control was observed, which could indicate a decreased affinity of the antibody to the target protein. This would need to be tested either using newer antibodies or a different dystrophin antibody. The analysis will also need to be repeated with loading controls in order to determine whether the lack of signal in the melanocyte sample was due to human error. The use of a more sensitive detection reagent may also be necessary to improve the reproducibility of the Western blot as the melanocyte and fibroblast expression of dystrophin may be in low abundance. Furthermore transduction of the cells using a dystrophin plasmid, containing a micro-dystrophin tagged with enhanced green fluorescent protein (μDYS/eGFP) may be considered for future work[92]. This will allow for the use of pull-down or anti-GFP assays which could make the detection of the dystrophin protein more favourable.

Lastly, during the culture of patient and control melanocytes it was noted that patient melanocytes displayed multipolar and highly dendritic growth. This was hypothesised to be due to the absence of dystrophin in the patient cells.

This is supported by previous studies which have shown that the Rho family of small guanosine triphosphate (GTP)-binding proteins or GTPases, Ras-related C3 botulinum toxin substrate 1 (Rac1), cell division cycle 42 (Cdc42) and inhibition of Ras homolog gene family,

member A (RhoA) in particular, could be the potential master regulators of melanocyte dendrite formation[73,93]. This Rho family of GTPases is also critical for skeletal muscle differentiation and studies investigating the DGC as a signalling complex have linked the GTPases to the DGC[24,94–96]. An association between Rac1, Cdc42, H-Ras, laminin and β-dystroglycan, key component of the DGC, has been found[95].

The DGC protein syntrophin, which interacts with dystrophin and various members of the dystrophin family, was shown to recruit Rac1 through the growth factor receptor-bound protein 2 (Grb2) and son of sevenless homolog 1 (Sos1) protein complex[94]. Rac1 binds P21 activated kinase 1 (PAK1) and activates c-Jun N-terminal kinases (JNKs)[94]. Interestingly, the JNK pathway is known to play an important role in melanogenesis (the synthesis of melanin) and the activation of this pathway is known to cause downregulation of melanogenesis[97]. In the case of a D/BMD patient in which dystrophin is absent in the melanocytes, syntrophin would not be able to bind dystrophin and recruit Rac1 through the Grb2-Sos1 complex. This would possibly result in the JNK pathway not being activated through these proteins and could potentially prevent downregulation of melanogenesis through this specific pathway. Melanogenesis and thus melanocyte differentiation, is known to be related to dendrite formation, with decreased melanogenesis resulting in decreased dendricity[73]. Therefore, it is possible that the inability to down-regulate melanogenesis through the JNK pathway could result in the inability to down-regulate dendrite formation. This hypothesis, as far as we know, has not been extensively investigated in its relation to DMD and is certainly worth further investigation.

Grb2 is also capable of binding to β-dystroglycan in order to activate the Ras/MAPK signalling pathway[24,98]. The MAPK pathways have also been implicated in the regulation of various melanocyte biological activities, including the possible activation of Rho family GTPases which influence melanocyte dendricity[73]. Grb2 binding to β-dystroglycan has been found to be inhibited by dystrophin, which also binds to β-dystroglycan. It is speculated that the DGC has many functional states, some with low affinity and others with high affinity to Grb2 binding[24]. It is therefore plausible that without the competition of dystrophin for binding to the DGC, Grb2 is capable of binding more freely, activating the MAPK pathway and possibly increasing the dendricity of the cells.

The combined effects of dystrophin absence in these pathways could potentially explain the increased dendricity observed with our patients' melanocytes. The validity of this hypothesis would need to be determined experimentally, but was beyond the scope our current study. It therefore remains pertinent that future work explores the effects of dystrophin absence and its relationship to morphological and physiological functioning of melanocytes in the skin.

References

1. Durbeej, M., and Campbell, K.P. (2002). Muscular dystrophies involving the dystrophin – glycoprotein complex : an overview of current mouse models. Curr. Opin. Genet. Dev. *12*, 349–361.

2. Emery, A.E.H. (2002). The muscular dystrophies. Lancet *359*, 687–695.

3. Emery, A.E.H. (2008). Muscular Dystrophy: The Facts 3rd Edition (Oxford University Press).

4. Mercuri, E., and Muntoni, F. (2013). Muscular dystrophies. Lancet *381*, 845–860.

5. Dubowitz, V., Sewry, C.A., and Oldfors, A. (2013). Chapter 10 - Muscular Dystrophies and Allied Disorders I : Duchenne and Becker Muscular Dystrophy. In Muscle Biopsy: A Practical Approach Fourth Edition, pp. 250–275.

6. Aartsma-rus, A., Ginjaar, I.B., and Bushby, K. (2016). The importance of genetic diagnosis for Duchenne muscular dystrophy. J. Med. Genet. *53*, 1–7.

7. Dubowitz, V., Sewry, C.A., and Oldfors, A. (2013). Chapter 1 - The Procedure of Muscle Biopsy. In Muscle Biopsy: A Practical Approach Fourth Edition, pp. 1–15.

8. Jay, V., and Vajsar, J. (2001). The dystrophy of Duchenne. Lancet *357*, 550–552.

9. Bushby, K., Finkel, R., Birnkrant, D.J., Case, L.E., Clemens, P.R., Cripe, L., Kaul, A., Kinnett, K., McDonald, C., Pandya, S., et al. (2010). Diagnosis and management of Duchenne muscular dystrophy, part 1: diagnosis, and pharmacological and psychosocial management. Lancet Neurol. *9*, 77–93.

10. Baird, M.F., Graham, S.M., Baker, J.S., and Bickerstaff, G.F. (2012). Creatine-kinase- and exercise-related muscle damage implications for muscle performance and recovery. J. Nutr. Metab. *2012*,.

11. Sejerson, T., and Bushby, K. (2009). Standards of care for duchenne muscular dystrophy: Brief treat-NMD recommendations. Adv. Exp. Med. Biol. *652*, 13–21.

12. Abbs, S., Tuffery-Giraud, S., Bakker, E., Ferlini, A., Sejersen, T., and Mueller, C.R. (2010). Best practice guidelines on molecular diagnostics in Duchenne/Becker muscular dystrophies. Neuromuscul. Disord. *20*, 422–427.

13. Laing, N.G., Davis, M.R., Bayley, K., Fletcher, S., and Wilton, S.D. (2011). Molecular diagnosis of duchenne muscular dystrophy: Past, present and future in relation to

implementing therapies. Clin. Biochem. Rev. *32*, 129–134.

14. Hoffman, E.P., Brown, R.H., and Kunkel, L.M. (1987). Dystrophin: the protein product of the Duchenne muscular dystrophy locus. Cell *51*, 919–928.

15. Eagle, M., Bourke, J., Bullock, R., Gibson, M., Mehta, J., Giddings, D., Straub, V., and Bushby, K. (2007). Managing Duchenne muscular dystrophy - The additive effect of spinal surgery and home nocturnal ventilation in improving survival. Neuromuscul. Disord. *17*, 470–475.

16. Davies, K., Pearson, P., Harper, P., Murray, J., O'Brien, T., Sarfarazi, M., and Williamson, R. (1983). Linkage analysis of two cloned DNA sequences flanking the Duchenne muscular dystrophy locus on the short arm of the human X chromosome. Nucleic Acids Res. *11*, 2303–2312.

17. Monaco, A.P., Neve, R.L., Colletti-Feener, C., Bertelson, C.J., Kurnit, D.M., and Kunkel, L.M. (1986). Isolation of candidate cDNAs for portions of the Duchenne muscular dystrophy gene. Nature *323*, 646–650.

18. Kunkel, L., Monaco, A., Middlesworth, W., Ochs, H., and Latt, S. (1985). Specific cloning of DNA fragments absent from the DNA of a male patient with an X chromosome deletion. Proc. Natl. Acad. Sci. U. S. A. *82*, 4778–4782.

19. Scherer, S. (2010). Guide to the Human Genome (Cold Spring Harbor Laboratory Press).

20. Muntoni, F., Torelli, S., and Ferlini, A. (2003). Dystrophin and mutations: One gene, several proteins, multiple phenotypes. Lancet Neurol. *2*, 731–740.

21. Koenig, M., Hoffman, E.P., Bertelson, C.J., Monaco, A.P., Feener, C., and Kunkel, L.M. (1987). Complete cloning of the Duchenne muscular dystrophy (DMD) cDNA and preliminary genomic organization of the DMD gene in normal and affected individuals. Cell *50*, 509–517.

22. Nishio, H., Takeshima, Y., Narita, N., Yanagawa, H., Suzuki, Y., Ishikawa, Y., Ishikawa, Y., Minami, R., Nakamura, H., and Matsuo, M. (1994). Identification of a novel first exon in the human dystrophin gene and of a new promoter located more than 500 kb upstream of the nearest known promoter. J. Clin. Invest. *94*, 1037–1042.

23. Wheway, J.M., and Roberts, R.G. (2003). The dystrophin lymphocyte promoter revisited: 4.5-Megabase intron, or artefact? Neuromuscul. Disord. *13*, 17–20.

24. Rando, T. (2001). The dystrophin-glycoprotein complex, cellular signaling, and the regulation of cell survival in the muscular dystrophies. Muscle Nerve *24*, 1575–1594.

25. Ehmsen, J., Poon, E., and Davies, K. (2002). The Dystrophin-Associated Protein Complex. J. Cell Sci. *115*, 2801–2803.

26. Moser, H. (1984). Duchenne muscular dystrophy: pathogenetic aspects and genetic prevention. Hum. Genet. *66*, 17–40.

27. Sironi, M., Pozzoli, U., Comi, G.P., Riva, S., Bordoni, A., Bresolin, N., and Nag, D.K. (2006). A region in the dystrophin gene major hot spot harbors a cluster of deletion breakpoints and generates double-strand breaks in yeast. FASEB J. *20*, 1910–1912.

28. Beggs, A., Koenig, M., Boyce, F., and Kunkel, L. (1990). Detection of 98% of DMD/BMD gene deletions by polymerase chain reaction. Hum. Genet. *86*, 45–48.

29. Bladen, C.L., Salgado, D., Monges, S., Foncuberta, M.E., Kekou, K., Kosma, K., Dawkins, H., Lamont, L., Roy, A.J., Chamova, T., et al. (2015). The TREAT-NMD DMD Global Database: analysis of more than 7,000 Duchenne muscular dystrophy mutations. Hum. Mutat. *36*, 395–402.

30. Costa, M.F., Oliveira, A.G.F., Feitosa-Santana, C., Zatz, M., and Ventura, D.F. (2007). Red-green color vision impairment in Duchenne muscular dystrophy. Am. J. Hum. Genet. *80*, 1064–1075.

31. Costa, M.F., Barboni, M.T.S., and Ventura, D.F. (2011). Psychophysical measurements of luminance and chromatic spatial and temporal contrast sensitivity in Duchenne muscular dystrophy. Psychol. Neurosci. *4*,.

32. Daoud, F., Angeard, N., Demerre, B., Martie, I., Benyaou, R., Leturcq, F., Cossée, M., Deburgrave, N., Saillour, Y., Tuffery, S., et al. (2009). Analysis of Dp71 contribution in the severity of mental retardation through comparison of Duchenne and Becker patients differing by mutation consequences on Dp71 expression. Hum. Mol. Genet. *18*, 3779–3794.

33. Taylor, P.J., Betts, G.A., Maroulis, S., Gilissen, C., Pedersen, R.L., Mowat, D.R., Johnston, H.M., and Buckley, M.F. (2010). Dystrophin gene mutation location and the risk of cognitive impairment in duchenne muscular dystrophy. PLoS One *5*,.

34. Monaco, A.A.P., Bertelson, C.J.C., Liechti-Gallati, S., Moser, H., and Kunkel, L.M. (1988). An explanation for the phenotypic differences between patients bearing partial deletions of the DMD locus. Genomics *2*, 90–95.

35. Tuffery-Giraud, S., Béroud, C., Leturcq, F., Yaou, R. Ben, Hamroun, D., Michel-Calemard, L., Moizard, M.P., Bernard, R., Cossée, M., Boisseau, P., et al. (2009). Genotype-

phenotype analysis in 2,405 patients with a dystrophinopathy using the UMD-DMD database: A model of nationwide knowledgebase. Hum. Mutat. *30*, 934–945.

36. Aartsma-Rus, A., Van Deutekom, J.C.T., Fokkema, I.F., Van Ommen, G.J.B., and Den Dunnen, J.T. (2006). Entries in the Leiden Duchenne muscular dystrophy mutation database: An overview of mutation types and paradoxical cases that confirm the reading-frame rule. Muscle and Nerve *34*, 135–144.

37. Kesari, A., Pirra, L.N., Bremadesam, L., McIntyre, O., Gordon, E., Dubrovsky, A.L., Viswanathan, V., and Hoffman, E.P. (2008). Integrated DNA, cDNA and protein studies in Becker muscular dystrophy show high exception to the reading frame rule. Hum. Mutat. *29*, 728–737.

38. Ginjaar, I.B., Kneppers, a L., v d Meulen, J.D., Anderson, L. V, Bremmer-Bout, M., van Deutekom, J.C., Weegenaar, J., den Dunnen, J.T., and Bakker, E. (2000). Dystrophin nonsense mutation induces different levels of exon 29 skipping and leads to variable phenotypes within one BMD family. Eur. J. Hum. Genet. *8*, 793–796.

39. Lim, L.E., and Rando, T.A. (2008). Technology insight: therapy for Duchenne muscular dystrophy-an opportunity for personalized medicine? Nat. Clin. Pract. Neurol. *4*, 149–158.

40. Fairclough, R.J., Wood, M.J., and Davies, K.E. (2013). Therapy for Duchenne muscular dystrophy: renewed optimism from genetic approaches. Nat. Rev. Genet. *14*, 373–378.

41. Farini, A., Razini, P., Erratico, S., Torrente, Y., and Meregalli, M. (2009). Cell based therapy for duchenne muscular dystrophy. J. Cell. Physiol. *221*, 526–534.

42. Zatti, S., Martewicz, S., Serena, E., Uno, N., Giobbe, G., Kazuki, Y., Oshimura, M., and Elvassore, N. (2014). Complete restoration of multiple dystrophin isoforms in genetically corrected Duchenne muscular dystrophy patient-derived cardiomyocytes. Mol. Ther. Methods Clin. Dev. *1*, 1.

43. TREAT-NMD (2016). TREAT-NMD Neuromuscular Network.

44. Goyenvalle, A., Griffith, G., Babbs, A., Andaloussi, S. El, Ezzat, K., Avril, A., Dugovic, B., Chaussenot, R., Ferry, A., Voit, T., et al. (2015). Functional correction in mouse models of muscular dystrophy using exon-skipping tricyclo-DNA oligomers. Nat. Med.

45. Bidou, L., Allamand, V., Rousset, J.P., and Namy, O. (2012). Sense from nonsense: Therapies for premature stop codon diseases. Trends Mol. Med. *18*, 679–688.

46. Mendell, J.R., Rodino-Klapac, L.R., Sahenk, Z., Roush, K., Bird, L., Lowes, L.P., Alfano,

L., Gomez, A.M., Lewis, S., Kota, J., et al. (2013). Eteplirsen for the treatment of Duchenne muscular dystrophy. Ann. Neurol. *74*, 637–647.

47. Muntoni, F., and Wood, M.J.A. (2011). Targeting RNA to treat neuromuscular disease. Nat. Rev. Drug Discov. *10*, 621–637.

48. Guiraud, S., Chen, H., Burns, D.T., and Davies, K.E. (2015). Advances in genetic therapeutic strategies for Duchenne muscular dystrophy. Exp. Physiol. *12*, 1458–1467.

49. Goyenvalle, A., Babbs, A., Wright, J., Wilkins, V., Powell, D., Garcia, L., and Davies, K.E. (2012). Rescue of severely affected dystrophin/utrophin-deficient mice through scAAV-U7snRNA-mediated exon skipping. Hum. Mol. Genet. *21*, 2559–2571.

50. Esterhuizen, A.I., Greenberg, L.J., Ballo, R., Goliath, R.G., and Wilmshurst, J.M. (2016). Duchenne muscular dystrophy in the Western Cape, South Africa: Where do we come from and where are we going? South African Med. J. *106*, 67.

51. Tobin, D.J. (2006). Biochemistry of human skin--our brain on the outside. Chem. Soc. Rev. *35*, 52–67.

52. Venus, M., Waterman, J., and McNab, I. (2011). Basic physiology of the skin. Surgery *29*, 471–474.

53. Powell, J. (2007). Skin physiology. Found. Years *3*, 193–196.

54. Sriram, G., Bigliardi, P.L., and Bigliardi-Qi, M. (2015). Fibroblast heterogeneity and its implications for engineering organotypic skin models in vitro. Eur. J. Cell Biol. *94*, 483–512.

55. Mortiboys, H., Thomas, K.J., Koopman, W.J.H., Klaffke, S., Abou-Sleiman, P., Olpin, S., Wood, N.W., Willems, P.H.G.M., Smeitink, J.A.M., Cookson, M.R., et al. (2008). Mitochondrial function and morphology are impaired in parkin-mutant fibroblasts. Ann. Neurol. *64*, 555–565.

56. Auburger, G., Klinkenberg, M., Drost, J., Marcus, K., Morales-Gordo, B., Kunz, W.S., Brandt, U., Broccoli, V., Reichmann, H., Gispert, S., et al. (2012). Primary skin fibroblasts as a model of Parkinson's disease. Mol. Neurobiol. *46*, 20–27.

57. Marianthi, L., Olga, P., Aristotelis, C., Nikolaos, V., and Fragiskos, K. (2016). Gene Expression Analysis of Fibroblasts from Patients with Bipolar Disorder. J. Neuropsychopharmacol. Ment. Heal. *1*,.

58. Hernandez, M.A., Schulz, R., Chaplin, T., Young, B.D., Perrett, D., Champion, M.P.,

Taanman, J.-W., Fensom, A., and Marinaki, A.M. (2010). The diagnosis of inherited metabolic diseases by microarray gene expression profiling. Orphanet J. Rare Dis. *5*, 34.

59. Zanotti, S., Gibertini, S., Bragato, C., Mantegazza, R., Morandi, L., and Mora, M. (2011). Fibroblasts from the muscles of Duchenne muscular dystrophy patients are resistant to cell detachment apoptosis. Exp. Cell Res. *317*, 2536–2547.

60. Jones, G.E., and Witkowski, J.A. (1979). Reduced adhesiveness between skin fibroblasts from patients with Duchenne muscular dystrophy. J. Neurol. Sci. *43*, 465–470.

61. Rodemann, H.P., and Bayreuther, K. (1984). Abnormal collagen metabolism in cultured skin fibroblasts from patients with Duchenne muscular dystrophy. Proc. Natl. Acad. Sci. U. S. A. *81*, 5130–5134.

62. Hugnot, J.P., Gilgenkrantz, H., Chafey, P., Lambert, M., Eveno, E., Kaplan, J.C., and Kahn, A. (1993). Expression of the dystrophin gene in cultured fibroblasts. Biochem Biophys Res Commun *192*, 69–74.

63. Chelly, J., Gilgenkrantz, H., Hugnot, J.P., Hamard, G., Lambert, M., R??can, D., Akli, S., Cometto, M., Kahn, A., and Kaplan, J.C. (1991). Illegitimate transcription: Application to the analysis of truncated transcripts of the dystrophin gene in nonmuscle cultured cells from duchenne and becker patients. J. Clin. Invest. *88*, 1161–1166.

64. Brenner, M., and Hearing, V. (2009). What are melanocytes really doing all day long…? : from the ViewPoint of a keratinocyte: Melanocytes – cells with a secret identity and incomparable abilities. Exp. Dermatol. *18*, 799–819.

65. Yamaguchi, Y., Brenner, M., and Hearing, V.J. (2007). The regulation of skin pigmentation. J. Biol. Chem. *282*, 27557–27561.

66. Herzog, C., Has, C., Franzke, C.W., Echtermeyer, F.G., Schlötzer-Schrehardt, U., Kröger, S., Gustafsson, E., Fässler, R., and Bruckner-Tuderman, L. (2004). Dystroglycan in skin and cutaneous cells: β-Subunit is from the cell surface. J. Invest. Dermatol. *122*, 1372–1380.

67. Pinon, P., and Wehrle-Haller, B. (2011). Integrins: Versatile receptors controlling melanocyte adhesion, migration and proliferation. Pigment Cell Melanoma Res. *24*, 282–294.

68. Pellegrini, C., Zulian, A., Gualandi, F., Manzati, E., Merlini, L., Michelini, M.E., Benassi, L., Marmiroli, S., Ferlini, A., Sabatelli, P., et al. (2013). Melanocytes-A novel tool to study mitochondrial dysfunction in Duchenne muscular dystrophy. J. Cell. Physiol. *228*, 1323–1331.

69. Körner, H., Epanchintsev, A., Berking, C., Schuler-Thurner, B., Speicher, M.R., Menssen, A., and Hermeking, H. (2007). Digital karyotyping reveals frequent inactivation of the Dystrophin/DMD gene in malignant melanoma. Cell Cycle *6*, 189–198.

70. Ballo, R., Viljoen, D., and Beighton, P. (1994). Duchenne and Becker muscular dystrophy prevalence in South Africa and molecular findings in 128 persons affected. South African Med. J. *84*, 494–497.

71. Aasen, T., and Belmonte, J.C.I. (2010). Isolation and cultivation of human keratinocytes from skin or plucked hair for the generation of induced pluripotent stem cells. Nat. Protoc. *5*, 371–382.

72. Schneider, C. a, Rasband, W.S., and Eliceiri, K.W. (2012). NIH Image to ImageJ: 25 years of image analysis. Nat. Methods *9*, 671–675.

73. Kim, M.Y., Choi, T.Y., Kim, J.H., Lee, J.H., Kim, J.G., Sohn, K.C., Yoon, K.S., Kim, C.D., Lee, J.H., and Yoon, T.J. (2010). MKK6 increases the melanocyte dendricity through the regulation of Rho family GTPases. J. Dermatol. Sci. *60*, 114–119.

74. Pfaffl, M.W., Tichopad, A., Prgomet, C., and Neuvians, T.P. (2004). Determination of stable housekeeping genes, differentially regulated target genes and sample integrity: BestKeeper--Excel-based tool using pair-wise correlations. Biotechnol. Lett. *26*, 509–515.

75. Tamura, K., Peterson, D., Peterson, N., Stecher, G., Nei, M., and Kumar, S. (2011). MEGA5: Molecular evolutionary genetics analysis using maximum likelihood, evolutionary distance, and maximum parsimony methods. Mol. Biol. Evol. *28*, 2731–2739.

76. Weckx, S., Del-Favero, J., Rademakers Rosa, Claes, L., Cruts, M., De Jonghe, P., Van Broeckhoven, C., and De Rijk, P. (2005). novoSNP, a novel computational tool for sequence variation discovery. Genome Res. *15*, 436–442.

77. McLaren, W., Gil, L., Hunt, S.E., Riat, H.S., Ritchie, G.R.S., Thormann, A., Flicek, P., and Cunningham, F. (2016). The Ensembl Variant Effect Predictor. Genome Biol. *17*,.

78. Schwarz, J.M., Rödelsperger, C., Schuelke, M., and Seelow, D. (2010). MutationTaster evaluates disease-causing potential of sequence alterations. Nat. Methods *7*, 575–576.

79. Choi, Y., Sims, G.E., Murphy, S., Miller, J.R., and Chan, A.P. (2012). Predicting the Functional Effect of Amino Acid Substitutions and Indels. PLoS One *7*,.

80. Vogel, C., and Marcotte, E.M. (2013). Insights into regulation of protein abundance from proteomics and transcriptomis analyses. Nat. Rev. Genet. *13*, 227–232.

81. Kormos, B., Belső, N., Bebes, A., Szabad, G., Bacsa, S., Széll, M., Kemény, L., and Bata-Csörgő1, Z. (2011). In Vitro Dedifferentiation of Melanocytes from Adult Epidermis. PLoS One *6*,.

82. Kumar, P., Henikoff, S., and Ng, P.C. (2009). Predicting the effects of coding non-synonymous variants on protein function using the SIFT algorithm. Nat. Protoc. *4*, 1073–1081.

83. Adzhubei, I.A., Schmidt, S., Peshkin, L., Ramensky, V.E., Gerasimova, A., Bork, P., Kondrashov, A.S., and Sunyaev, S.R. (2010). A method and server for predicting damaging missense mutations. Nat. Methods *7*, 248–249.

84. Wyatt, P.R., and Cox, D.M. (1977). Duchenne's Muscular Dystrophy : Studies in Cultured Fibroblasts. Lancet *309*, 172–174.

85. Marbini, A., Marcello, N., Bellanova, M.F., Guidetti, D., Ferrari, A., and Gemignani, F. (1995). Dystrophin expression in skin biopsy immunohistochemical. Localisation of striated muscle type dystrophin. J. Neurol. Sci. *129*, 29–33.

86. Tanveer, N., Sharma, M.C., Sarkar, C., Gulati, S., Kalra, V., Singh, S., and Bhatia, R. (2009). Diagnostic utility of skin biopsy in dystrophinopathies. Clin. Neurol. Neurosurg. *111*, 496–502.

87. Hillier, J., Jones, G.E., Statham, H.E., Witkowski, J. a, and Dubowitz, V. (1985). Cell surface abnormality in clones of skin fibroblasts from a carrier of Duchenne muscular dystrophy. J. Med. Genet. *22*, 100–103.

88. Gelman, B.B., Davis, M.H., Morris, R.E., and Gruenstein, E. (1981). Structural Changes in Lysosomes from Cultured Human Fibroblasts in Duchenne ' s Muscular Dystrophy. J. Cell Biol. *88*,.

89. Richard, C.A., Howard, P.L., D'souza, V.N., Klamut, H.J., and Ray, P.N. (1995). Cloning and characterization of alternatively spliced isoforms of Dp71. Hum. Mol. Genet. *4*, 1475–1483.

90. Tuffery-Giraud, S., Saquet, C., Chambert, S., Echenne, B., Marie Cuisset, J., Rivier, F., Cossée, M., Philippe, C., Monnier, N., Bieth, E., et al. (2004). The role of muscle biopsy in analysis of the dystrophin gene in Duchenne muscular dystrophy: Experience of a national referral centre. Neuromuscul. Disord. *14*, 650–658.

91. Ito, T., Takeshima, Y., Yagi, M., Kamei, S., Wada, H., Nakamura, H., and Matsuo, M.

(2003). Analysis of dystrophin mRNA from skeletal muscle but not from lymphocytes led to identification of a novel nonsense mutation in a carrier of Duchenne muscular dystrophy. J. Neurol. *250*, 581–587.

92. Kimura, E., Han, J.J., Li, S., Fall, B., Ra, J., Haraguchi, M., Tapscott, S.J., and Chamberlain, J.S. (2008). Cell-lineage regulated myogenesis for dystrophin replacement: a novel therapeutic approach for treatment of muscular dystrophy. Hum. Mol. Genet. *17*, 2507–2517.

93. Scott, G. (2002). Rac and rho: the story behind melanocyte dendrite formation. Pigment Cell Res. *15*, 322–330.

94. Oak, S.A., Zhou, Y.W., and Jarrett, H.W. (2003). Skeletal muscle signaling pathway through the dystrophin glycoprotein complex and Rac1. J. Biol. Chem. *278*, 39287–39295.

95. Chockalingam, P.S., Cholera, R., Oak, S. a, Zheng, Y., Jarrett, H.W., and Thomason, D.B. (2002). Dystrophin-glycoprotein complex and Ras and Rho GTPase signaling are altered in muscle atrophy. Am. J. Physiol. Cell Physiol. *283*, C500–C511.

96. Constantin, B. (2014). Dystrophin complex functions as a scaffold for signalling proteins. Biochim. Biophys. Acta - Biomembr. *1838*, 635–642.

97. Chan, C.F., Huang, C.C., Lee, M.Y., and Lin, Y.S. (2014). Fermented broth in tyrosinase- and melanogenesis inhibition. Molecules *19*, 13122–13135.

98. Yang, B., Jung, D., Motto, D., Meyer, J., Koretzky, G., and Campbell, K.P. (1995). SH3 domain-mediated interaction of dystroglycan and Grb2. J. Biol. Chem. *270*, 11711–11714.

UNIVERSITY OF CAPE TOWN

Faculty of Health Sciences

Human Research Ethics Committee

Room E52-24 Old Main Building
Groote Schuur Hospital
Observatory 7925
Telephone (021) 404 7682 • Facsimile (021) 406 6411
Email: ms.hrec@uct.ac.za
Website: www.health.uct.ac.za/fhs/research/humanethics/forms

27 August 2014

HREC REF: 311/2014

Ms A Esterhuizen
Human Genetics
CLS
IIDMM

Dear Ms Esterhuizen

PROJECT TITLEMELANOCYTES AS A NOVEL TOOL IN GENETIC DIAGNOSIS OF DUCHENNE MUSCULAR DYSTROPHY (Sub-study linked to 141/2011)

Thank you for submitting your study to the Faculty of Health Sciences Human Research Ethics Committee for review.

It is a pleasure to inform you that the HREC has **formally approved** the above-mentioned study.

Approval is granted for one year until the 30th August 2015

Please submit a progress form, using the standardised Annual Report Form if the study continues beyond the approval period. Please submit a Standard Closure form if the study is completed within the approval period.

Forms can be found on our website: www.health.uct.ac.za/fhs/research/humanethics/forms)

Please use the correct name for the Faculty of Health Sciences Human Research Ethics Committee in the parental consent and healthy control consent forms (currently "Research Committee").

Please note that the ongoing ethical conduct of the study remains the responsibility of the principal investigator.

Please quote the HREC REF in all your correspondence.

Yours sincerely

PROFESSOR MARC BLOCKMAN
CHAIRPERSON, FHS HUMAN RESEARCH ETHICS COMMITTEE

FHS016: Annual Progress Report / Renewal

HREC office use only (FWA00001832; IRB00001938)			
This serves as notification of annual approval, including any documentation described below.			
☑ Approved	Annual progress report	Approved until/next renewal date	30.8.2016
☐ Not approved	See attached comments		
Signature Chairperson of the HREC		Date Signed	3/11/2015

Comments to PI from the HREC

Principal Investigator to complete the following:

1. Protocol information

Date (when submitting this form)	26/11/2015		
HREC REF Number	311/2014	Current Ethics Approval was granted until	August 2015
Protocol title	Melanocytes as a novel tool in genetic diagnosis of Duchenne Muscular Dystrophy		
Protocol number (if applicable)	N/A		
Are there any sub-studies linked to this study?	☑ Yes ☐ No		
If yes, could you please provide the HREC Ref's for all sub-studies? **Note:** A separate FHS016 must be submitted for each sub-study.	HREC REF 141/2011		
Principal Investigator	Ms Alina Esterhuizen		
Department / Office Internal Mail Address	Division of Human Genetics, Institute of Infectious Diseases and Molecular Medicine (IDMM), Wernher Beit North, UCT Medical School, Anzio Rd. Observatory 7925		

1.1 Does this protocol receive US Federal funding?	☐ Yes	☑ No
1.2 If the study receives US Federal Funding, does the annual report require full committee approval?	N/A	
1.3 Has sponsorship of this study changed? If yes, please attach a revised summary of the budget.	☐ Yes	☑ No

(Note: Please complete the Closure form (FHS010) if the study is completed within the approval period)

1.2. Example of the parental consent form

INFORMATION SHEET AND PARENTAL CONSENT FORM FOR PARTICIPATION IN A RESEARCH PROJECT

Study Investigators:
Dr. Lester Davids:
Dept. Human Biology UCT, tel: 021 406 6787, e-mail: lesterdavids@uct.ac.za
Mrs. Alina Esterhuizen:
Div. of Human Genetics UCT/NHLS, tel: +27 21 404 4680, e-mail: A.Esterhuizen@uct.ac.za
Prof. Jo Wilmshurst:
Paediatric Neurology, Red Cross Children's Hospital, tel: 021 658 5111 ext 5434, e-mail: JoWilmshurst@uct.ac.za

Project title: *Melanocytes as a novel tool in genetic diagnosis of Duchenne muscular dystrophy.*

Project Background

Duchenne/Becker Muscular Dystrophy (D/BMD) is a severe, muscle wasting disease, caused by mutations in the *DMD* gene. Genes are part of DNA, which is a very long molecule present in most cells of the body. Genes carry the codes for all human characteristics (traits). An error in a particular code (a mutation) can cause a disease, as is the case in D/BMD. Such errors can be passed on (inherited) from one generation to the next (parent to child).

D/BMD is passed on in an X-linked recessive fashion. This means that if a woman carries a *DMD* gene mutation, she *will not* develop D/BMD (in most cases), but a boy who inherits the mutation from his mother will become ill. There is a 50% chance that a D/BMD female carrier will pass her *DMD* mutation onto her child each time she is pregnant, and if the child is a boy, he will have D/BMD. There is no cure or treatment available to date but genetic testing can often reveal which mutation runs in the family. This knowledge is useful, because it confirms the diagnosis (there are other types of muscular dystrophies) and allows the family to make informed decisions for future family planning. In their search to find treatment, scientists are working hard at developing what is termed "gene-based therapy" for D/BMD, which could "fix" genetic mutations. Since D/BMD can be caused by different types of mutations in the *DMD* gene, this therapy would be tailor-made for each patient. It is therefore very important that laboratory tests are capable of detecting *all* types of *DMD* mutations.

The problem lies in the fact that that the *DMD* gene is extremely large and finding the mutation can be really difficult. At present, medical laboratories offer testing for only certain types of mutations, giving answers to some, but *not all* D/BMD patients. Also, testing for D/BMD is currently done on DNA from blood, as it is an easy specimen to obtain. Ideally however, one should test RNA, which is another type of a genetic code, from muscle tissue. RNA testing can give the best results in terms of the type of mutation present and the best potential genetic therapy for that patient in the future. The problem here though, is that taking a muscle biopsy is more complicated than taking blood, and has to be done in theater. Also, RNA is very fragile and easily degraded, so the specimen transport and processing must be done as quickly as possible.

Scientists have shown that the *DMD* gene in melanocytes behaves in a similar way to that in muscle tissue and may be a useful to study D/BMD. Melanocytes are the pigment-producing cells found in skin and are easily available through skin biopsies. In this study, we hope to show that melanocytes can be successfully cultured in our local laboratories, and that RNA extracted from these cells can provide D/BMD patients and their families with better information about "their" mutations.

This research protocol has been approved by the Department of Clinical Laboratory Sciences Research Committee as well as the Research Ethics Committee of the Faculty of Health Sciences of UCT (HREC REF: 311/2014).

SELECTION AND RECRUITMENT

Muscle biopsies

Your child will be having a muscle biopsy procedure, to help the doctors find the cause of his illness. We request that a small section of the biopsy be donated to this project. It is important to understand that we only make this request of parents and children who are already scheduled for a muscle biopsy procedures as part of their medical care. No child will be asked to have a muscle biopsy taken purely for use in this research.

Skin biopsies

We will be asking for skin biopsy samples from:

- DMD patients as research subjects
- healthy volunteers for inclusion as healthy controls.

Skin Biopsy Procedure

The skin sample will be obtained by a process called a "punch biopsy". Since your child will already be undergoing a muscle biopsy procedure under anaesthetic, the skin sample will be taken at the same time from the muscle biopsy insertion site. This should not cause him any additional discomfort. A small round blade of four millimeters in diameter will be pressed into the skin, creating a circular cut about four millimeters deep. The sample will then be removed and the area closed and dressed appropriately. The whole procedure should take about 15 minutes to perform, including the time for cleaning and preperation. The consultation and biopsy procedure should not take more than an hour. Sampling of the skin biopsy for this study should not place your child at any additional risk, as he is already undergoing an anaesthetic procedure for a muscle biopsy sample. If you have any concerns afterwards, the contact details of the doctor performing the biopsy will be made available to you. We will only request a punch biopsy once.

What will happen to my child's sample?

The biopsies will be used to grow cells and create cell lines. These cell lines (multiple copies of the cells) can only survive in a laboratory culture medium, though they can be kept alive for an extended period of time. After the completion of the study, the cell lines as well as the genetic material (RNA/DNA) extracted from the cell lines will be stored in the DMD Repository for Biological Material at the Division of Human Genetics, for an unspecified period of time, based on the ethical approval for the repository (HREC REF 234/2010).

Voluntary Participation and Confidentiality

- Participation as a subject or control is completely voluntary.
- You reserve the right to refuse to participate in the study.
- A decision to refuse will not effect your child's treatment now or in the future.
- You are free to withdraw consent at any time.
- All information given will remain strictly confidential. Each specimen will be stored in a secure location and assigned an anonymous code known only to the investigators working on the project.
- You may request to have your child's samples removed from the DMD Repository and discarded after completion of the study.
- This study is being conducted according to the principles of the Declaration of Helsinki (Brazil 2013), which looks after the interest of the participants.

This research protocol has been approved by the Department of Clinical Laboratory Sciences Research Committee as well as the Research Ethics Committee of the Faculty of Health Sciences of UCT (HREC REF: 311/2014).

WHAT IF SOMETHING GOES WRONG?

The University of Cape Town (UCT) undertakes that in the event of your child suffering any significant deterioration in health or well-being, or from any unexpected sensitivity or toxicity, that is caused by his participation in the study, it will provide immediate medical care. UCT has appropriate insurance cover to provide prompt payment of compensation for any trial-related injury according to the guidelines outlined by the Association of the British Pharmaceutical Industry, ABPI 1991. Broadly-speaking, the ABPI guidelines recommend that the insured company (UCT), without legal commitment, should compensate you without you having to prove that UCT is at fault. An injury is considered trial-related if, and to the extent that, it is caused by study activities. You must notify the study doctor immediately of any side effects and/or injuries during the trial, whether they are research-related or other related complications.

UCT reserves the right not to provide compensation if, and to the extent that, your injury came about because you chose not to follow the instructions that you were given while you were taking part in the study. Your right in law to claim compensation for injury where you prove negligence is not affected. Copies of these guidelines are available on request.

Participants may contact the Human Research Ethics Committee at the UCT with any questions or concerns about their rights or welfare as research participants: tel: +27 21 406 6338; fax: +27 21 406 6411; Email: nosi.tsama@uct.ac.za or shuretta.thomas@uct.ac.za

Benefits of the Study

The study offers no direct benefit to the participants or their families. The research is however conducted with the long term view of improving diagnostic genetic testing for DMD. Participation may therefore have a long term benefit in helping to develop and improve the genetic diagnostic service for DMD in South Africa.

This research protocol has been approved by the Department of Clinical Laboratory Sciences Research Committee as well as the Research Ethics Committee of the Faculty of Health Sciences of UCT (HREC REF: 311/2014).

PARENTAL CONSENT

PLEASE TICK WHERE RELEVANT:

1. I agree to the use of my child's muscle biopsy in this study. ☐ Yes ☐ No
   I agree to the sampling and use of my child's skin biopsy in this study. ☐ Yes ☐ No

2. I have been informed that my child's sample, the cell lines and DNA/RNA will be assigned a unique identification code. This code and the link between the code and my child's name will be known only to the investigators in the study. ☐ Yes ☐ No

   I agree to the storage of the cell culture lines from my child's biopsy/s. ☐ Yes ☐ No

   I agree to the use of my child's cell culture lines in future research project/s approved by the Research Committee of the Faculty of Health Sciences at UCT. ☐ Yes ☐ No

   I agree to the storage my child's DNA/RNA. ☐ Yes ☐ No

   I agree to the use of my child's DNA/RNA in future research project/s, approved by the Research Committee of the Faculty of Health Sciences at UCT. ☐ Yes ☐ No

3. I understand that the results of this project may be used as theses material for higher degrees, and publication in scientific journal/s. ☐ Yes ☐ No

4. I understand that the results of this research project may provide information about the genetic background of my child's illness (D/BMD). These results will not provide information about my child's complete genetic makeup. ☐ Yes ☐ No

6. ALL OF THE ABOVE HAS BEEN EXPLAINED TO ME IN A LANGUAGE THAT I UNDERSTAND AND MY QUESTIONS ANSWERED BY: _____

   _____

Child's Name (print): _____

Parent/Legal Guardian's Name (Print): _____

Parent/Guardian Signature: _____

Date: _____

This research protocol has been approved by the Department of Clinical Laboratory Sciences Research Committee as well as the Research Ethics Committee of the Faculty of Health Sciences of UCT (HREC REF: 311/2014).

Appendix 2: Reagents

2.1. Cell Culture Reagents

Dulbecco's Modified Eagle's Medium (DMEM; pH7.4, 1L)

27.06g	DMEM Powder (Sigma-Aldrich)
7.4g	$NaHCO_3$ (Merck, USA)
1.8L	autoclaved double distilled H_2O (addH_2O)

pH to 7.4

Fill up to 1L with addH_2O.

Sterilise through a 0.2µm filter and store at 4°C.

100x Penicillin/Streptomycin (100x pen/strep; 1L)

6g	1662U/mg Penicillin (Sigma-Aldrich)
10g	750U/mg Streptomycin (Sigma-Aldrich)

Dissolve in 1L distilled H_2O.

Sterilise through a 0.2µm filter.

DMEM supplemented with FCS and pen/strep (DMEM ++, 500mL)

10%	100% Foetal Calf Serum (FCS, Gibco)
1x	100x pen/strep

Fill up to 500mL with DMEM.

Filter sterilise through a 0.2µm filter.

1x Phosphate Buffered Saline (PBS; pH7.4, 2L)

16g	NaCl (KIMIX)
2.52g	Na_2HPO_4 anhydrous (Merck)
0.4g	KCl (KIMIX)
0.4g	KH_2PO_4 (Merck)

Dissolve in 1.6L addH_2O

pH to 7.4

Fill up to 2L and autoclave to sterilise.

Trypsin/EDTA (TE, 500mL)

0.25g	Trypsin (Sigma-Aldrich)
0.1g	EDTA (Sigma-Aldrich)

Dissolve trypsin in 500mL PBS.

Add and dissolve the EDTA.

Filter sterilise through a 0.2µm filter.

Hoechst Nuclear Stain (2µg/mL, 1mL)

100µL	1000ug/mL Hoechst 33342 (Invitrogen)
900µL	addH_2O

2.2. Immunohistochemistry and Immunocytochemistry Reagents

10x Tris Buffered Saline (TBS; pH7.5, 1L)

60.5g	Tris (Merck)
87,6g	NaCl (KIMIX)

Dissolve in 700mL double distilled H_2O (ddH_2O).

pH to 7.5.

Fill up to 1L with ddH_2O.

4% Paraformaldehyde (PFA; 100mL)

4g	PFA (Merck)

Add 80mL 1x PBS.

Heat to 50°C and stir until dissolved.

Fill up to 100mL with 1x PBS.

2.3. Western Blotting Reagents

Radioimmunoprecipitation Assay Buffer (RIPA Buffer; 50mL, pH 7.4)

150mM	NaCl (KIMIX)
1%	Triton-X (Sigma-Aldrich)
0.1%	10% Sodium Dodecyl Sulphate (SDS)
20mM	1M Tris; pH7.5
1%	Deoxycholic acid (Sigma-Aldrich)

Fill up to 50mL with distilled H_2O (dH_2O).

RIPA Complete Extraction Buffer (500µL)

1x	25x Complete protease inhibitor cocktail (25xCPIC; Sigma-Aldrich)
1µg/mL	Aprotinin (Roche)
0.5mM	100mM Phenylmethylsulfonylfluoride (PMSF; Sigma-Aldrich)
1µg/mL	Pepstatin (Sigma-Aldrich)

Fill up to 500µL with RIPA buffer.

Resolving Gel Buffer (pH 8.9, 200mL)

36.2g	Tris (Merck)
0.8g	SDS (Sigma-Aldrich)

pH to 8.9.

Make up to 200mL with ddH_2O.

Store at 4°C.

Stacking Gel Buffer (pH 6.8, 100mL)

5.9g	Tris (Merck)
0.4g	SDS (Sigma-Aldrich)

pH to 6.8.

Make up to 100mL with ddH_2O.

Store at 4°C.

10x Running Buffer (1L)

30.2g	Tris (Merck)
144g	Glycine (KIMIX)
10g	SDS (Sigma-Aldrich)

Make up to 1L with ddH_2O.

1x TBST

100mL	10x TBS, pH 7.5
900mL	ddH_2O
1mL	Tween-20 (Sigma-Aldrich)

5x Loading Buffer (50mL)

1.75g	Tris (Merck)
30mL	Glycerine/Glycerol (Merck)

Make up to 40mL with ddH_2O.

pH to 6.8.

Add 5g SDS.

Make up to a final volume of 50mL

5x Loading Dye

Heat up loading buffer to allow SDS precipitate to dissolve.

Mix 2:1:1 (Loading Buffer: β-Mercaptoethanol: 0.025% Bromophenol Blue)

Use at 1x.

10x Transfer Buffer (1L)

144g	Glycine (KIMIX)

38g	Tris (Merck)

Make up to 1L with ddH_2O.

1x Transfer Buffer

100mL	10x Transfer Buffer
700mL	ddH_2O
200mL	Isopropanol (KIMIX)

Resolving Gel (1.5mm gel)

For 6% gel

3mL	Resolving gel buffer, pH 8.9
1.84mL	30% Acrylamide (Sigma-Aldrich)
4.16mL	ddH_2O
180µL	10% Ammonium Persulphate (APS, Promega)
18µL	Tetramethylethylenediamine (TEMED)

For 10% gel

3mL	Resolving gel buffer, pH 8.9
3mL	30% Acrylamide (Sigma-Aldrich)
3mL	ddH_2O
180µL	10% APS
18µL	TEMED

Stacking Gel (1.5mm gel)

1.5mL	Stacking gel buffer, pH 6.8
1mL	30% Acrylamide (Sigma-Aldrich)
3.5mL	ddH_2O
60µL	10% APS

6µL	TEMED

2.4. Agarose gel Reagents

RNA loading dye

18mL	Formamide (ACE Chemicals, RSA)
198mg	Sucrose (Univar, USA)
10µg	Bromophenol Blue (Sigma)
10µL	Xylene cyanol (Thermo Fisher Scientific)

10x Tris/Borate/EDTA (TBE) buffer

216g	Tris (Merck)
110g	Boric acid (Sigma-Aldrich)
14.8g	EDTA (Sigma-Aldrich)

Made up to 2L with Diethylpyrocarbonate-treated (DEPC-treated) autoclaved distilled water.

Agarose gels

For 50mL gel

0.5g agarose (Life Technologies, USA) per percentage required

50mL 1x TBE buffer

1X SYBR® Safe (Invitrogen)

Microwave until the agarose is completely dissolved. Cool before adding stain and pouring.

Appendix 3: Protocols

3.1. Immunocytochemistry Protocol

ICC – Dystrophin

Mouse monoclonal antibody to Dystrophin Rod Domain (NCL-DYS1) – Novocastra (use undiluted)

Mouse monoclonal antibody to Dystrophin C-terminus (NCL-DYS2) – Novocastra (use undiluted)

Mouse monoclonal antibody to Dystrophin N-terminus (NCL-DYS3) – Novocastra (use undiluted)

Block solution (10mL):

5% Bovine Serum Albumin (BSA)	0.5g
0.01% Triton-X	1µL

Fill up to 10mL with Phosphate Buffered Saline (PBS)

ICC protocol

1.	Wash with PBS (3x5min)	15min
2.	Add 4% PFA in PBS (5min)	5min
3.	Remove PFA	
4.	Add 100% ice cold methanol	5min
5.	Remove methanol	
6.	Wash with PBS (3x5min)	15min
7.	Add block solution for one hour.	1h
8.	Remove block (no PBS wash) – don't remove from secondary only wells (no-primary wells).	
9.	Add 20µL primary antibody to parafilm in humidity chamber and place coverslips face down on primary antibody.	
10.	Incubate at room temperature for 1h.	1h
11.	Wash with PBS (3x5min)	15min
12.	Secondary antibody added.	
13.	Incubate 2 hours in dark at room temp	2h
14.	Wash with PBS (3x5min)	15min
15.	Add Hoechst (@2µg/mL), incubate for 5 min.	5min
16.	Aspirate to remove Hoechst. Rinse 3x with PBS.	10min
17.	Mount onto slide with mounting fluid containing n-propyl galate (anti-fade; Sigma-Aldrich)	
18.	Incubate at room temp overnight.	
19.	Visualize with fluorescent microscope.	

3.2. RIPA Buffer Extraction Protocol

1. Wash cells with cold PBS twice.
2. Place dish on ice and add 100µL RIPA complete extraction buffer to a 10cm dish.
3. Extract protein from cells by scraping the dish using a rubber policeman or syringe plunger.
4. Collect the cell lysate into a 1.5mL tube.
5. Centrifuge at 10000rpm at 4°C for 10min to pellet debris.
6. Transfer supernatant to a new 1.5mL tube.
7. Quantify and store at -80°C.

3.3. Roche High Pure RNA Extraction Protocol

1. Trypsinise cells in dish and pellet at 2000rpm in a 15mL tube containing medium supplemented with FCS, to deactivate trypsin.
2. Aspirate off medium and resuspend pellet in 200µL room temperature PBS.
3. Add 400µL of lysis buffer to tube and vortex for 15s.
4. Transfer cell lysate to a High Pure filter tube, which has been inserted into a collection tube.
5. Centrifuge at 9200rpm for 15s.
6. Discard flowthrough and reuse the collection tube.
7. Add 10µL DNase I to the filter tube along with 90µL DNase incubation buffer and incubate for 15min.
8. Add 500µL wash buffer I to filter tube and centrifuge at 9200rpm for 15s.
9. Discard flowthrough and reuse the collection tube.
10. Add 500µL wash buffer II to filter tube and centrifuge for 15s at 9200rpm.
11. Discard flowthrough and reuse the collection tube.
12. Add 200µL wash buffer II to filter tube and centrifuge at maximum speed for 2min.
13. Discard collection tube.
14. Place filter tube into a sterile 1.5mL.
15. Add 30µL elution buffer to the filter tube.
16. Centrifuge for 1min at 9200rpm.
17. Store RNA at -80°C for later analysis.

3.4. cDNA Synthesis Protocol (Promega)

1. Add 1µg RNA; 1µL random oligonucleotide (61µM) and RNase-free H_2O to a PCR tube up to a volume of 10.5µL.
2. Incubate samples for 5min at 70°C and transfer to ice.

Master mix	Final concentration	Volume per reaction
10mM dNTP	1mM	2µL
25nM $MgCl_2$	2.5mM	2µL
5x RT Buffer	1x	4µL
RNase inhibitor (40u/µL)	1U/µL	0.5µL

3. Mix the cocktail well and add 8.5µL to each of the samples.
4. Add 1µL MMLV reverse transcriptase to f the mast mix each of the samples except the no reverse transcriptase control (NRT), to which 1µL of RNase-free H_2O is added. Tube will contain a total volume of 20µL.
5. Incubate at 42°C for 1h.
6. Store cDNA at -20°C

Appendix 4: Standard Operating Procedure for RNA-based D/BMD mutation analysis using skin melanocytes

RNA-based analysis using melanocytes showed accurate determination of the expected causative mutations within our patient cohort. A standard operating procedure (SOP) was designed for the purpose of potential translation of RNA-based mutation analysis using skin melanocytes for the diagnosis of D/BMD.

RNA-based D/BMD mutation analysis using skin melanocytes

Molecular Genetics of Duchenne/Becker Muscular Dystrophy		
Gene Symbol	**Chromosomal Locus**	**Protein Name**
DMD	Xp21.2-p21.1	Dystrophin

Data are compiled from the following references: Gene symbol from HUGO, chromosomal locus, chromosomal locus from OMIM and protein name from UniProtKB.

OMIM Entries for Duchenne Muscular Dystrophy	
310200	MUSCULAR DYSTROPHY, DUCHENNE TYPE; DMD
300376	MUSCULAR DYSTROPHY, BECKER TYPE; BMD
300377	DYSTROPHIN; DMD

BACKGROUND

Expression of dystrophin in melanocytes was first noted in 2007 by Körner et al., who performed digital karyotyping analysis of malignant melanoma and *DMD* expression analysis in cultured melanocytes[69]. Pellegrini et al. later confirmed the expression of the Dp427M, Dp260, Dp116 and Dp71 isoforms of dystrophin in primary cultured melanocytes in 2013[68].

This SOP relates to the use of cultured skin melanocytes for use in RNA-based mutation analysis, as a diagnostic or gene-based therapy eligibility test for D/BMD patients.

SAMPLING INSTRUCTIONS

A shave biopsy at least 4mm in diameter/ 4mm x 4mm in size will be taken from the patient, by the appropriate medical personal and stored according to the sample storage/transport procedure. The biopsy should be shallow to ideally not obtain too much of the underlying tissue.

SAMPLE STORAGE/TRANSPORT

Skin biopsies will be placed into a 50mL centrifuge tube containing 5mL DMEM with 1% penicillin/streptomycin added. Samples must be stored and transported at 4°C. Samples can be stored for up to 3 days prior to culture. Phosphate buffered saline can be used for short-term transport and storage of no more than 24h.

TEST PRINCIPLE AND STRATEGY

Sanger sequencing analysis of the *DMD* gene using cDNA synthesised from RNA extracted from cultured melanocytes. The investigation consists of three steps:

Step1

Melanocytes will be isolated and cultured from a patient skin biopsy. This is primarily aimed at generating a sufficient number of cells for RNA extraction. The cells will be cultured confluency in a 10cm culture dish, until a pure melanocyte culture is obtained. The passage number of the cells must be kept between p3 and p8.

Step 2

Extraction of total RNA from the melanocytes, followed by the synthesis of cDNA using extracted RNA.

Step 3

Amplification of the dystrophin gene from the cDNA using nested-PCR and the Leiden PTT primer sets (http://www.dmd.nl/). Sanger sequencing of the PCR products and bioinformatic analysis of the sequencing for disease-causing mutations.

SCOPE OF TESTING

The test is offered as a diagnostic test or eligibility test for gene-based therapies.

FREQUENCY AND TURNAROUND TIME

The turnaround time for culture and mutation analysis is estimated to be from 6 to10 weeks.

RESPONSIBILITY

A medical technician, technologist, scientist or registrar trained in cell culture and molecular biology techniques will perform the test.

SPECIMENS

RNA is extracted from cultured melanocytes by the following procedure:

High Pure RNA Isolation Kit (Roche)

See SOPs and reagent manuals for the procedures.

QUALITY CONTROL

- The integrity and purity of RNA samples are confirmed via agarose gel electrophoresis and spectrophotometric analysis using the NanoDrop ND-100 Spectrophotometer, prior to cDNA synthesis.
- A no reverse transcriptase (reaction contains no polymerase enzyme) control is included for cDNA synthesis to detect whether genomic DNA may be present in sample.
- A reference gene PCR is performed using cDNA to ensure that synthesis was successful.
- A no DNA (distilled water) control is included in every PCR run.
- If DNA contamination is suspected (i.e. PCR products detected in the no DNA control), all the working dilutions and aliquots of reagents must be discarded and the assay repeated using fresh reagents.

MATERIALS AND REAGENTS

Tissue Culture

- **Dulbecco's Modified Eagle Medium (DMEM)**
- **50mL tubes** (nuclease and pyrogen free)
- **15mL tubes** (nuclease and pyrogen free)
- **Sterile blade holder**
- **Disposable rounded blades to fit holder**
- **Sterile petri dishes**
- **Hank's Balanced Salt solution (HBSS)** (Thermo Fisher Scientific)
- **Dispase** (Thermo Fisher Scientific)
- **0.25% Trypsin in 0.05% EDTA (JC/TE)**
- **Foetal calf serum (FCS),** heat inactivated (Thermo Fisher Scientific)
- **FETI**
    - **Hams F10** (Sigma-Aldrich)
    - **Endothelin 1** (Sigma-Aldrich)

    - **12-O-tetradecanoylphorbol-13-acetate (TPA)** (Sigma-Aldrich)
    - **3-isobutyl-1-methyl xanthine (IBMX)** (Sigma-Aldrich)
    - **Ultoser G** (PALL Life Sciences)
    - **Basic fibroblast growth factor (bFGF)** (Miltenyi Biotech)
- **Sterile 70µm mesh sieves**
- **Fine sterile forceps**
- **Phosphate buffered saline (PBS),** sterile
- **Penicillin-Streptomycin (100x Pen/Strep)** (Sigma-Aldrich)
- **Water bath**
- **Centrifuge** for 15mL tubes
- **Culture dishes** (35mm, 6cm and 10cm)
- **Trypsin-EDTA** (Thermo Fisher Scientific)
- **Automatic pipettes and sterile pipette tips:** P2, P10, P20, P200 and P1000
- **CO_2 Incubator**
- **Tissue Culture Hood**
- **Geneticin®/G418** (Thermo Fisher Scientific)
- **70% Ethanol**

RNA extraction, cDNA synthesis, Nested-PCR and Sequencing

- **High Pure RNA isolation kit** (Roche)
- **NanoDrop ND-1000 Spectrophotometer**
- **M-MLV reverse transcriptase (M-MLV RT)** (Promega)
- **dNTP mix** (Promega)
- **$MgCl_2$** (Promega)
- **Reverse Transcriptase buffer** (Promega)
- **RNase-free water**
- **RNase inhibitor** (Promega)
- **Random oligonucleotides** (SYNTHETIC DNA LABORATORY, Dept. of Molecular & Cell Biology, University of Cape Town)
- **A Thermocycler**
- **A gel electrophoresis tank**
- **Agarose powder** (molecular grade)
- **SYBR®Safe DNA gel stain** (Thermo Fisher Scientific)
- **RNA loading dye**
- **DNA Loading dye** (Thermo Fisher Scientific)

- **TBE Buffer**
- **O'GeneRuler^{TM} 100bp Plus DNA Ladder** (Thermo Fisher Scientific)
- **Filter pipette tips:** P2, P10, P20, P200 and P1000
- **1.5 ml microfuge tubes** (nuclease and pyrogen free)
- **0.2 ml PCR tubes** (nuclease and pyrogen free)
- **A UV transilluminator**
- **GoTaq Buffer** (Promega)
- **GoTaq Hotstart polymerase** (Promega)
- **Nucleofast® 96 PCR clean-up kit** (Machery-Nagel)
- **Sephadex columns** (Princeton Scientific)
- **Sodium dodecyl sulphate (SDS)**
- **Sterile distilled water**
- **BigDye Terminator v3.1 cycle sequencing kit** (Thermo Fisher Scientific)
- **96-well plates and septa** (supplied by the analytical facility)
- **An ABI 3130*xl* Genetic Analyser** (Thermo Fisher Scientific)

  Product resolution and sizing done by **capillary electrophoresis (CE)** at the Genome Facility, Div. of Human Genetics, UCT Medical School, Institute of Infectious Diseases and Molecular Medicine (IIDMM) (tel: 021 406 6456) OR by the Central Sequencing Facility at the University of Stellenbosch (tel: 021 808 5887).
- **HiDye Formamide and GS500 -250** size standard (ROX500-250) for capillary electrophoresis (provided by the analytical facility).
- **GeneMapper v.4.1 fragment analysis software** (Thermo Fisher Scientific)

- **Leiden PTT Primers and GAPDH primers:**

  Red names represent outer primers. Green names represent nested primers

Primer	Sequence 5'-3'	Fragment size (bp)	Exon
DMD1h	CAAAAGAAAACATTCACAAAATGG	1345	2-11
DMD1a	TTAGCCAGTCATTCAACTCTTTCA		
DMD1d	GCGGATCCTAATACGACTCACTATAGGAACAGACCACC ATGTCTAAGTTTGGGAAGCAGCA	1258	
DMD1c	TGAGGCATTCCCATCTTGA		
DMD1b	CGATTCAAGAGCTATGCCTAC	1350	10-18
DMD1g	ACTCTGCAACACAGCTTCTGAG		
DMD1f	GGATCCTAATACGACTCACTATAGGAACAGACCACCAT GTTGCAAGCACAAGGAGAGATT	1174	
DMD1e	CTTCTGAGCGAGTAATCCAGCT		
DMD2h	CGGATCCACAAGGGAACAGATCCTGGTAA	1327	17-25
DMD2a	GTCTCAAGTCTCGAAGCAAACTCT		
DMD2d	GCGGATCCTAATACGACTCACTATAGGAACAGACCACC ATGAGGCAGATTACTGTGGATTCTGA	1244	
DMD2c	CCCACCTTCATTGACACTGTT		
DMD2b	ATTGAGGGACGCTGGAAGA	1538	23-32
DMD2g	CGGGATCCTGCTTTTTCTGTACAATCTGACG		
DMD2f	GCGGATCCTAATACGACTCACTATAGGAACAGACCACC ATGGAGCATTGTCAAAAGCTAGAGGA	1411	
DMD2e	TCCACACTCTTTGTTTCCAATG		
DMD3h	TCACATTCATTGACAAGCAGTTGG	1533	31-38
DMD3a	CAATGTCATCCAAGCATTTCAG		
DMD3d	GCGGATCCTAATACGACTCACTATAGGAACAGACCACC ATGGCCCAAAGAGTCCTGTCTCA	1093	
DMD3c	TTAAACTGCTCCAATTCCTTCAA		
DMD3b	CACAAAGTGGATCATTCAGGC	1473	36-45
DMD3g	GCGAATTCACTGGCATCTGTTTTTGAGGAT		
DMD3f	GGATCCTAATACGACTCACTATAGGAACAGACCACCAT GGCTGACACACTTTTGGATG	1450	
DMD3e	CTTCCCCAGTTGCATTCAAT		
DMD4h	GCAACGCCTGTGGAAAGGGTG	1463	44-52
DMD4a	CGATCCGTAATGATTGTTCTAGC		
DMD4d	GGATCCTAATACGACTCACTATAGGAACAGACCACCAT GGCTGAACAGTTTCTCAGAAAGACACAA	1308	
DMD4c	CTCTTGATTGCTGGTCTTGTTTT		
DMD4b	AGCTCCTGGACTGACCACTATT	1543	51-59
DMD4g	CTCTTGAAGTTCCTGGAGTCTTTC		
DMD4f	GGATCCTAATACGACTCACTATAGGAACAGACCACCAT GTGGACAGAACTTACCGACTGG	1351	
DMD4e	CCCACTCAGTATTGACCTCCTC		
DMD5h	AAAAGTCTCTCAACATTAGGTCCC	1886	58-68
DMD5a	ATCCATTGCTGTTTTCCATTTC		
DMD5d	GCGGATCCTAATACGACTCACTATAGGAACAGACCACC ATGACAGAGCAGCCTTTGGAAG	1383	
DMD5c	TGGACACTCTTTGCAGATGTTAC		
DMD5b	ACGAGACTCAAACAACTTGCTG	1926	67-79
DMD5g	GCGAATTCTATTCTGCTCCTTCTTCATCTGTC		

DMD5f	GCGGATCCTAATACGACTCACTATAGGAACAGACCACC ATGGGTGAAGTTGCATCCTTTGG	1381	67-79
DMD5e	ATCATCTGCCATGTGGAAAAG		
GAPDH (Forward)	GAAGGCTGGGGCTCATTT	138	-
GAPDH (Reverse)	CAGGAGGCATTGCTGATGAT		

Primers are manufactured by Integrated DNA Technologies (IDT), Whitehead Scientific.

MELANOCYTE PRIMARY CULTURE

ALL THESE PROCEDURES REQUIRE A STERILE ENVIRONMENT.

If the dermis is present and visible on the skin biopsy sample:

Day 1:

- Pour DMEM collection fluid into a discard tube, careful not to pour out the sample.
- Rinse the sample twice with PBS containing 1x Pen/Strep.
- Pour the sample into a sterile petri dish.
- Cut the skin into 2mm^2 pieces and place in 35mm^2 culture dish, containing 2mL of 0.5mg/mL Dispase in HBSS.
- Place at 4°C overnight.

Day 2:

- Place one large drop of PBS containing 1x Pen/Strep into a petri dish and a small drop of JC/TE in another area of the petri dish.
- Transfer the skin pieces into the drop of PBS + Pen/Strep, using the fine forceps strip the epidermis off of the dermis.
- Place the pieces of epidermis into the drop of JC/TE.
- Wet the scalpel blade and chop the piece of epidermis finely using a rocking motion.
- Place 5mL of JC/TE into a 50mL tube, invert the tube to ensure the tube is wet.
- Place finely cut epidermal pieces into the tube and place the tube at 37°C for 15min. Shake gently every 5 min.
- Triturate gently using a pre-wet p1000 pipette tip, until pieces of skin is broken up (approximately 10 times).
- Add 500µL FCS and triturate further.
- Filter the cell suspension through a 70µm mesh sieve into another 50mL tube (pre-wet the filter with melanocyte culture medium FETI).
- Transfer the filtrate to a 15mL tube and centrifuge slowly (500rpm) for 10 min.

- Aspirate the supernatant and resuspend the pellet of cells in 1mL FETI. And plate into a 35mm dish. 35mm dish should contain a maximum of 2mL medium.
- Leave cells in incubator to adhere overnight.
- Change medium of the cells the next day, if many floating cells are present in the culture (continue from expansion of melanocyte primary culture).

No dermis present on the skin biopsy sample:

- Pour DMEM collection fluid into a discard tube, careful not to pour out the sample.
- Rinse the sample twice with PBS containing 1x Pen/Strep.
- Place a small drop of JC/TE into a petri dish.
- Transfer the skin into the drop of JC/TE
- Wet the scalpel blade and chop the piece of epidermis finely using a rocking motion.
- Place 5mL of JC/TE into a 50mL tube, invert the tube to ensure the tube is wet.
- Place finely cut epidermal pieces into the tube and place the tube at 37°C for 15min. Shake gently every 5 min.
- Triturate gently using a pre-wet p1000 pipette tip, until pieces of skin is broken up (approximately 10 times).
- Add 500µL FCS and triturate further.
- Filter the cell suspension through a 70µm mesh sieve into another 50mL tube (pre-wet the filter with melanocyte culture medium FETI).
- Transfer the filtrate to a 15mL tube and centrifuge slowly (500rpm) for 10 min.
- Aspirate the supernatant and resuspend the pellet of cells in 1mL FETI. And plate into a 35mm dish. 35mm dish should contain a maximum of 2mL medium.
- Leave cells in incubator to adhere overnight.
- Change medium of the cells the next day, if many floating cells are present in the culture (continue from expansion of melanocyte primary culture).

Expansion of melanocyte primary culture:

- **If the culture consists completely of melanocytes,** change medium once every 3 to 4 days (twice a week) and expand culture until the 35mm^2 dish is 80% confluent.
- Trypsinise the cells and transfer to a 6cm^2 dish (max 4mL medium in dish).
- Once the 6cm dish is approximately 80% confluent transfer the cells to a 10cm^2 dish (max 8mL medium in dish).
- Continue to expand until a 90% confluent 10cm^2 dish is obtained.
- **If the culture is mixed,** perform a partial trypsinisation of the cells on the third or fourth day of culture.

- Transfer the cells to a new 35mm^2 dish and allow the cells to adhere overnight.
- Repeat the process until a pure culture of melanocytes is obtained.

OR

- Add 100µg/mL Geneticin® to culture and leave for two days (**NB** Geneticin® kills the fastest proliferating cells in the culture and will therefore target fibroblasts first, prolonged exposure will, however, kill the melanocytes as well).
- Change medium on the third day, wash cells with sterile PBS before adding the fresh medium.
- If fibroblast contamination is still present after 1 week, treat cells again.
- Once a pure culture is obtained expand the culture until a 90% confluent 10cm^2 dish is obtained.

RNA EXTRACTION

- Isolate RNA using the High Pure RNA isolation kit, according manufacturer's instructions.
- Quantify the RNA using the Nanodrop ND1000 spectrophotometer and test RNA integrity using agarose electrophoresis.

Agarose gel electrophoresis (RNA)

Mix 0.5-1µg RNA with RNA loading dye and electrophorese through a 2% agarose gel containing 2.5µL SYBR® Safe DNA gel stain for 30 min. Visualise using a UV transilluminator.

cDNA SYNTHESIS

7. Add 1µg RNA; 1µL random oligonucleotide (61µM) and RNase-free H_2O to a PCR tube up to a volume of 10.5µL.
8. Incubate samples for 5 min at 70°C and transfer to ice.

Mastermix	Final concentration	Volume per reaction
10mM dNTP	1mM	2µL
25nM $MgCl_2$	2.5mM	2µL
5x RT Buffer	1x	4µL
RNase inhibitor (40u/µL)	1U/µL	0.5µL

9. Mix the cocktail well and add 8.5µL of the mastermix to each of the samples.

10. Add 1µL MMLV reverse transcriptase to each of the samples except the no reverse transcriptase control (noRT), to which 1µL of RNase-free H_2O is added. Tube will contain a total volume of 20µL.
11. Incubate at 42°C for 1h.
12. Store cDNA at -20°C

NESTED-PCR

Method per reaction in a 0.2mL PCR tube:

Component	Manufacturer	Final Concentration	Primary PCR reaction volume	Secondary PCR reaction volume
5x GoTaq Buffer	Promega	1x	5µL	5µL
10mM dNTP mix	Promega	0.2mM	0.5µL	0.5µL
GoTaq Hotstart polymerase (5U/µL)	Promega	0.04U/ µL	0.2µL	0.2µL
25mM $MgCl_2$	Promega	1.9mM	2µL	2µL
Forward Primer (10µM)	IDT	0.4µM	1µL	1µL
Reverse Primer (10µM)	IDT	0.4µM	1µL	1µL
dH_2O	-	-	14.5µL	15.3µL
Template	-	-	1.8µL [a]	1µL [b]
Total volume			26µL	26µL

[a] Template used in primary PCR is total cDNA(50ng/µL). [b] Template used in secondary PCR is PCR product of the primary PCR reaction.

The mastermix is made in a 1.5mL microfuge tube for all samples in the batch. After mixing well, the reaction volume is aliquoted into the individual PCR tubes and the template is added.

PCR cycling parameters:

1 cycle:	95ºC	5 min
1 cycle:	94ºC	5 min
40 cycles:	94ºC	40s
	60ºC	40s
	72ºC	2 min
1 cycle:	72ºC	5 min

Agarose gel electrophoresis (Nested-PCR products)

Mix 3µL of the secondary PCR product with DNA loading dye and electrophorese through a 1% agarose gel containing 2.5µL SYBR® Safe DNA gel stain for 45min. Add 5µL of the O'GeneRuler^{TM} 100bp plus DNA ladder in a well adjacent to samples to estimate the approximate size of the PCR products. Visualise using a UV transilluminator.

SEQUENCING AND CAPILLARY ELECROPHORESIS

Perform post-PCR clean-up using the NucleoFast® 96 PCR clean-up kit (Macherey-Nagel) according to manufacturer's instructions. Perform cycle sequencing using the BigDye Terminator v3.1 cycle sequencing kit (Thermo Fisher Scientific) according to standard methodologies. Treat sequencing products with SDS and transfer onto Sephadex columns (Princeton Scientific), centrifuge and allow the cleaned sequencing products to dry.

Once the samples are completely dried resuspend in Hi-Di formamide (Thermo Fisher Scientific) and transfer to a 96-well plate with septa. Denature the samples at 95°C for 2 min and cool to 4°C, prior to electrophoresis using the 3101xl Genetic analyser (Thermo Fisher Scientific).

ANALYSIS AND INTERPRETATION

Compare the sequencing output files to the coding sequence reference file of Dp427M isoform of dystrophin (GenBank reference file NM_004006.2). Align to form one contiguous sequence using the MEGA5 sequence alignment software version 5.02 (www.megasoftware.net)[75], in order to detect possible disease-causing mutations.

Identify point/small mutations using novoSNP (www.molgen.ua.ac.be/bioinfo/novosnp)[76], by creating a new project inserting the reference sequence in FASTA format (NM_004006.2). Add the sequencing output files to the program and adjust the quality cut-off setting to 10 (default 20), in order to reduce the chance of detecting false negatives. Analyse the mutations found, to determine whether the point/small mutation identified was a false positive or not. Refer to the Leiden Open Variation database (LOVD, http://www.dmd.nl)[36], literature and other published databases to determine whether the small/point mutations identified are novel or not. Determine the possible disease association of the point/small mutations using *in silico* analysis, published databases and literature.

Appendix 5: Primer Sequences

5.1. qPCR Primers

Primer	Forward Primer	Reverse Primer	Product size (bp)
Dp427M	TCGCTGCCTTGATATACACTTTTCA	GGTTCTCAATATGCTGCTTCCCA	145
Dp260	AGGAAGCTGCGAAATCTGTCTTAC	GGCAGACTGGATGCTCTGTTCA	75
Dp71	CATGAGGGAACAGCTCAAAGGC	CAGTCTTCGGAGTTTCATGGCA	142
Exon Junction 9-10	CGGAGCCCATTTCCTTCACAGCATT	CCGGCCCTGATGGGCTGTCA	246
Exon Junction 25-26	GGCCTGCCCTTGGGGATTCA	TCTGGCATAGACCTGTTGGCACA	221
Exon Junction 34-35	TGCCTGGGGAAAGGCTACTCA	GCAGTGGTCACCGCGGTTTG	415
Tyrosinase	AGGAGCATTCCCTAGGTAGT	AAAGGGATCCGTGAAAACAC	1003
GAPDH	GAAGGCTGGGGCTCATTT	CAGGAGGCATTGCTGATGAT	138

HS_GUSB_1_SG QuantiTect Primer assay primers were used for determining *GUSB* expression. Primers are proprietary of Qiagen.

5.2. Leiden PTT Primers (Nested-PCR)

Red names represent outer primers. Green names represent nested primers.

Primer	Sequence 5'-3'	Fragment size (bp)	Exon
DMD1h	CAAAAGAAAACATTCACAAAATGG	1345	2-11
DMD1a	TTAGCCAGTCATTCAACTCTTTCA		
DMD1d	GCGGATCCTAATACGACTCACTATAGGAACAGACCACCATGTCTA AGTTTGGGAAGCAGCA	1258	
DMD1c	TGAGGCATTCCCATCTTGA		
DMD1b	CGATTCAAGAGCTATGCCTAC	1350	10-18
DMD1g	ACTCTGCAACACAGCTTCTGAG		
DMD1f	GGATCCTAATACGACTCACTATAGGAACAGACCACCATGTTGCAA GCACAAGGAGAGATT	1174	
DMD1e	CTTCTGAGCGAGTAATCCAGCT		
DMD2h	CGGATCCACAAGGGAACAGATCCTGGTAA	1327	17-25
DMD2a	GTCTCAAGTCTCGAAGCAAACTCT		
DMD2d	GCGGATCCTAATACGACTCACTATAGGAACAGACCACCATGAGG CAGATTACTGTGGATTCTGA	1244	
DMD2c	CCCACCTTCATTGACACTGTT		
DMD2b	ATTGAGGGACGCTGGAAGA	1538	23-32
DMD2g	CGGGATCCTGCTTTTTCTGTACAATCTGACG		
DMD2f	GCGGATCCTAATACGACTCACTATAGGAACAGACCACCATGGAG CATTGTCAAAAGCTAGAGGA	1411	
DMD2e	TCCACACTCTTTGTTTCCAATG		
DMD3h	TCACATTCATTGACAAGCAGTTGG	1533	31-38
DMD3a	CAATGTCATCCAAGCATTTCAG		
DMD3d	GCGGATCCTAATACGACTCACTATAGGAACAGACCACCATGGCC CAAAGAGTCCTGTCTCA	1093	
DMD3c	TTAAACTGCTCCAATTCCTTCAA		
DMD3b	CACAAAGTGGATCATTCAGGC	1473	36-45
DMD3g	GCGAATTCACTGGCATCTGTTTTTGAGGAT		
DMD3f	GGATCCTAATACGACTCACTATAGGAACAGACCACCATGGCTGA CACACTTTTGGATG	1450	
DMD3e	CTTCCCCAGTTGCATTCAAT		
DMD4h	GCAACGCCTGTGGAAAGGGTG	1463	44-52
DMD4a	CGATCCGTAATGATTGTTCTAGC		
DMD4d	GGATCCTAATACGACTCACTATAGGAACAGACCACCATGGCTGAA CAGTTTCTCAGAAAGACACAA	1308	
DMD4c	CTCTTGATTGCTGGTCTTGTTTT		
DMD4b	AGCTCCTGGACTGACCACTATT	1543	51-59
DMD4g	CTCTTGAAGTTCCTGGAGTCTTTC		
DMD4f	GGATCCTAATACGACTCACTATAGGAACAGACCACCATGTGGACA GAACTTACCGACTGG	1351	
DMD4e	CCCACTCAGTATTGACCTCCTC		
DMD5h	AAAAGTCTCTCAACATTAGGTCCC	1886	58-68
DMD5a	ATCCATTGCTGTTTTCCATTTC		
DMD5d	GCGGATCCTAATACGACTCACTATAGGAACAGACCACCATGACA GAGCAGCCTTTGGAAG	1383	
DMD5c	TGGACACTCTTTGCAGATGTTAC		
DMD5b	ACGAGACTCAAACAACTTGCTG	1926	67-79
DMD5g	GCGAATTCTATTCTGCTCCTTCTTCATCTGTC		
DMD5f	GCGGATCCTAATACGACTCACTATAGGAACAGACCACCATGGGT GAAGTTGCATCCTTTGG	1381	
DMD5e	ATCATCTGCCATGTGGAAAAG		

Appendix 6: DNA and Protein Ladders

6.1. O'GeneRuler™ 100bp Plus DNA Ladder, ready to use (Thermo Fisher Scientific)

The size of the bands in base pairs as well as the amount of DNA present within 0.5µg of marker is represented below.

(Image obtained from: https://www.fishersci.ca/productDetails_4073114)

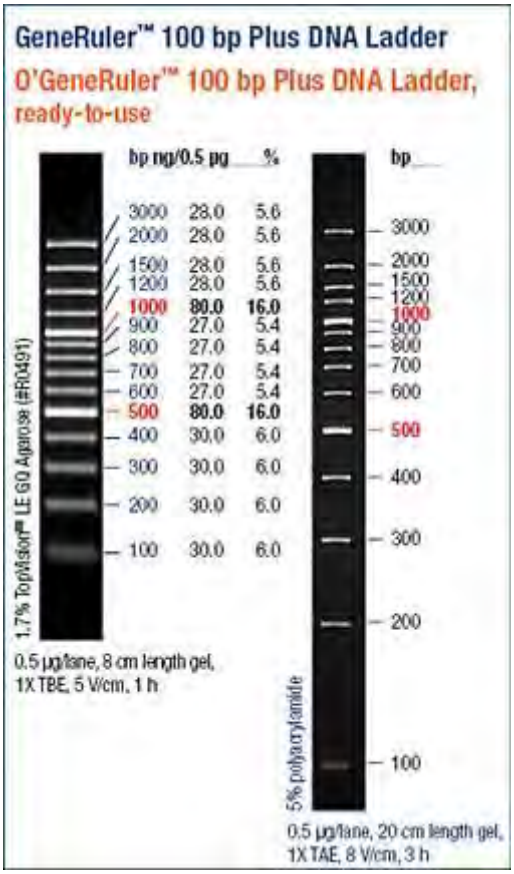

6.2. HiMark Pre-stained Protein Standard (Thermo Fisher Scientific)

The size of the the bands in kDa is represented bellow as well as the appearance of the protein standard (A) on a gel and (B) on a nitrocellulose membrane. (Image obtained from: https://www.thermofisher.com/order/catalog/product/LC5699)

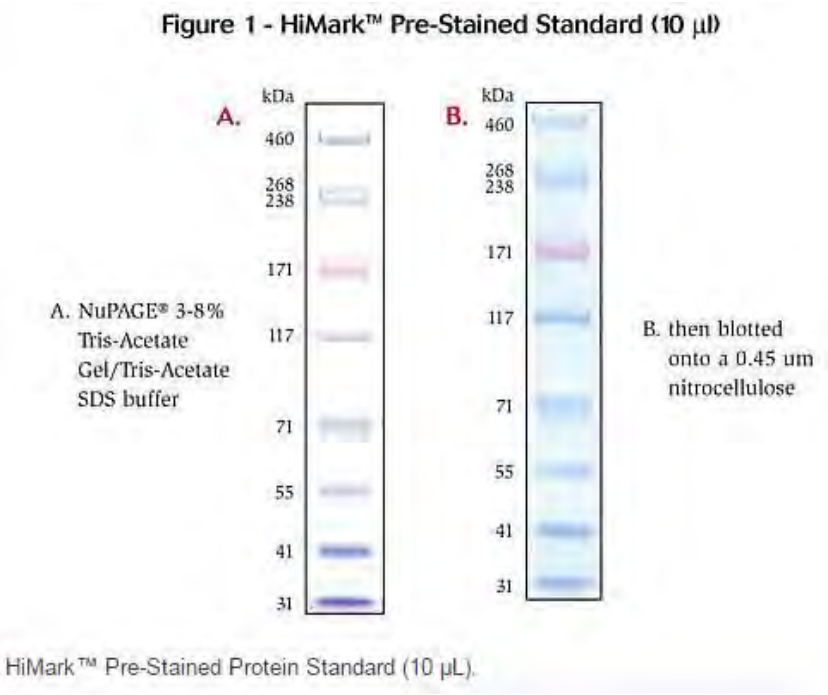

6.3. PageRuler Pre-stained Protein Ladder

The size of the the bands in kDa is represented bellow as well as the appearance of the protein standard (Gel) on a gel and (Blot) on a nitrocellulose membrane. (Image obtained from: https://www.thermofisher.com/order/catalog/product/26616)